UNIVERSITY OF TRENTO - Italy

PhD Program in Biomolecular Sciences

Centre for Integrative Biology

33nd Cycle

Engineered heart tissues to investigate the role of mechanical loading and injury in cardiomyocyte proliferation

Tutor:

Prof. Serena Zacchigna, M.D., Ph.D.

Advisor:

Prof. Francesco Loffredo, M.D., Ph.D.

Ph.D. Thesis of

Giulio Ciucci

ICGEB, Trieste.

Academic Year 2020-2021

ABSTRACT

Myocardial infarction is one of the most severe acute pathologies of the cardiovascular system. The adult mammalian heart is indeed unable to regenerate most of the lost cardiomyocytes (CMs) after cardiac injury. The loss of cardiomyocytes and the myocardial scarring after myocardial infarction eventually compromise contractility of the remaining myocardium, leading to heart failure. Therefore, promoting heart regeneration is one of the most crucial therapeutic targets in cardiovascular medicine. The lack of regenerative response is due to the loss of proliferative capacity of adult CMs which in mice occurs seven days after birth. One of the events which occur at birth in neonatal hearts is a sudden increase in mechanical loading that may contribute to switching mammal CMs phenotype from neonatal proliferative to adult postmitotic. Therefore, understanding the role of mechanotransduction in regulating the balance between CM proliferation and maturation may bring us to the identification of unknown mediators and new potential strategies to induce cardiac regeneration. Regulation of mechanical load in bi-dimensional cultures of CMs can be achieved in different ways, however, the poor degree of CM maturation that can be reached in a culture dish together with the lack of a tridimensional structure represent a major limitation to performing mechanotransduction studies. In our work we developed a novel system to study mechanotransduction of CMs based on 3D culture of cardiac cells, called engineered heart tissues (EHTs), that allow us to reduce or increase mechanical loading easily. We show that the three-dimensional setting of the culture leads to an improvement of CM maturation that may be reversed by mechanical unloading inducing cell proliferation. On the other hand, a persisting overload stimulus eventually induces CM switch to a more mature phenotype with a low degree of proliferation.

Also, we have focused our work on developing an EHT-based model able to recapitulate the adult infarct injury in order to investigate the biology of cardiac regeneration in this setting. Specifically, we set up a cryoinjury protocol that is relatively easy and reproducible. Cryoinjury produces a localized injury without

compromising EHT's structural integrity. Indeed, all the EHTs subjected to cryoinjury preserved their contractile activity and did not show any significant change in shape. Considering that EHTs are unpurified cardiac culture rich in fibroblast and endothelial cells, we observed that cryoinjury induce fibroblast proliferation and activation together with a lack of proliferative response of the cardiomyocytes which is, on the other hand, present in the early phase of EHT's development, similarly to what has been shown in mice and rats after myocardial infarction, highlighting the robustness of our cryoinjury approach as a model to investigate cardiac regeneration.

INDEX

1. INTRODUCTION 1

1.1. Cardiovascular diseases (CVDs) 1

1.1.1. Epidemiology of CVDs 1

1.2. Myocardial infarction 3

1.2.1. Cardiomyocyte response to MI 4

1.2.2. ECM remodeling 5

1.2.3. Fibrosis after MI and ECM remodeling 5

1.3. Tissue Regeneration 7

1.3.1. Heart regeneration 8

1.3.2. Heart regeneration in lower vertebrates 8

1.3.3. Regeneration in urodele amphibians 8

1.3.4. Regeneration in zebrafish 9

1.3.5. Heart regeneration in mammals 11

1.4. Postnatal factors implicated in cardiomyocytes loss of the proliferative potential 13

1.4.1. Mechanotransduction in the heart 16

1.4.2. Mechanotransduction in cardiomyocytes development and maturation 19

1.4.3. Mechanotransduction in cardiomyocyte proliferation 21

1.5. Cardiac tissue engineering 23

1.5.1. Prefabricated matrix 26

1.5.2. Decellularized tissue 26

1.5.3. Cell sheets 26

1.5.4. Hydrogel-based Technique 27

1.5.5. Fibrin-based engineered heart tissue (EHT) 28

1.6. Recent advances in engineered cardiac tissues 29

1.7. The importance of 3D in investigating cardiomyocytes proliferation and differentiation 30

2. AIMS OF THE THESIS 32

3. MATERIALS AND METHODS 33

3.1. Neonatal rat cardiomyocytes isolation 33

3.2. Generation of fibrin-based EHTs 33

3.3. Immunohistochemistry and Immunofluorescent Analysis 34

3.4. Gene expression analysis 35
3.5. Video optical recording and analysis 36
3.6. Mechanical unloading and increased afterload in EHTs 37
3.7. Adjustable mechanical loading system 37
3.8. Cryoinjury 38
3.9. MuDy video analysis 39
3.10. Statistical analysis 40
4. RESULTS 42
4.1. Cardiomyocyte DNA synthesis decreases during EHT development and is associated with an increase of binucleated cells 42
4.2. Mechanical unloading in EHTs induces an increase in EdU^+ Cardiomyocytes 45
4.3. EHT unloading reduces the expression of genes associated with mature cardiomyocyte phenotype 46
4.4. Increasing afterload in EHTs leads to a trend toward reduced CMs DNA synthesis and a more organized sarcomeric structure. 49
4.5. Mechanical loading in EHTs regulates CM proliferation and maturation. 50
4.6. Cryoinjury interrupts EHTs functional syncytium leading to loss of synchronous contraction 56
4.7. Cryoinjury leads to a reproducible 50% loss of force of contraction that does not recover over time 58
4.8. Cryoinjury-induced DNA synthesis in mature EHT CMs does not translate into an increase of proliferation 62
4.9. Cryoinjury in immature EHTs induced CMs proliferation 64
4.10. Cryoinjury induces focal collagen deposition which decreases over time. ..66
4.11. Cryoinjury stimulates a gene expression profile which resembles the activation of cardiac fibroblast after myocardial infarction 68
4.12. Cryoinjury induces proliferation of fibroblasts localized at the injury border zone 71
5. DISCUSSION 73
6. BIBLIOGRAPHY 80

1. INTRODUCTION

1.1. Cardiovascular diseases (CVDs)

1.1.1. Epidemiology of CVDs

CVDs represent almost 50% of total deaths from non-communicable diseases worldwide, with a projected 30% increase in the number of people with CVD over the next 20 years (Khavjou, Phelps, and Leib 2016). According to the 10th revision of the International Classification of Diseases (ICD-10), mortality data show that approximately 17.7 million people, the majority of which (63%) were aged 70 years and above, died from CVDs, underlying CVDs as the world's biggest killer (Roger et al. 2011). In Europe, CVDs account for 45% of total deaths and 29% of deaths before the age of 65 (Townsend et al. 2015). Aging plays a remarkable effect on lowering the threshold for the manifestation of these diseases. (Thomas and Rich 2007) (Lloyd-Jones et al. 2010) (De Luca d'Alessandro, Bonacci, and Giraldi 2012). Moreover, as predicted by the World Health Organization, the proportion of aged people will double between 2000 and 2050 therefore this poses an incremental need for healthcare for chronic diseases worldwide (Kirkwood 2005) (Organization 2018). By 2030 indeed, approximately 20% of the population will be aged 65 or older and, in this age group, cardiovascular diseases will result as the leading cause of death, producing a tremendous impact in terms of healthcare costs. (Roger 2013) (Mahmood and Wang 2013).

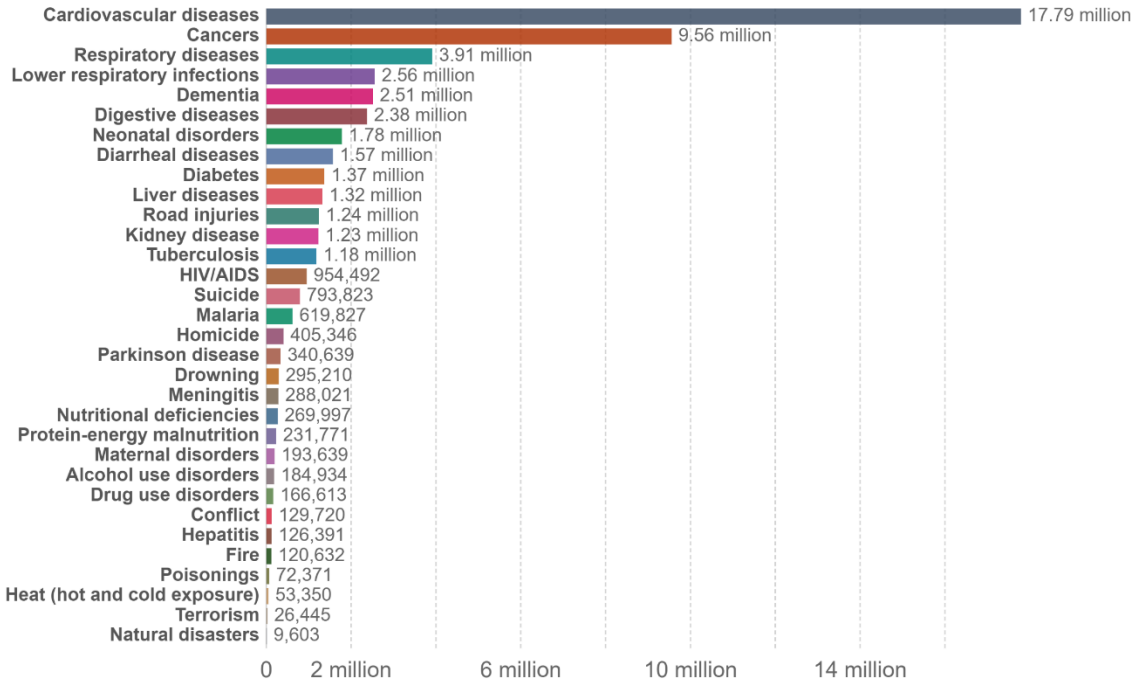

Figure 1. Number of deaths worldwide by cause in 2017. Source: IHME, Global Burden of Disease (Collaborators 2018).

Cardiovascular diseases include a collection of diseases that affect the cardiovascular system, which comprises the heart and blood vessels. These include: coronary heart disease (CHD), stroke, rheumatic heart disease, congenital heart disease, peripheral arterial disease, aortic aneurysm and dissection, deep vein thrombosis, and other, less common, cardiovascular conditions. Among all the CVDs, CHD is the overall leading cause of death in developed countries and one of the leading causes of death in developing countries. Coronary heart disease, also known as Coronary Artery Disease (CAD) and Ischemic Heart Disease (IHD), is characterized by the narrowing or occlusion of the coronary arteries mainly secondary to atherosclerotic disease (Thomas, Diamond et al. 2018). Atherosclerotic plaque formation starts from a lesion in the arterial wall allowing the accumulation of low-density lipoproteins (LDL) in the intima of the coronary vessels, which undergo oxidation (Ibanez, Vilahur et al. 2007). Oxidized LDLs act as a chemoattractant for leukocytes and may be ingested by macrophages which become proliferating foamy cells forming, together with the lipids, the fatty streak.

The process continues with the recruitment in the lesion of smooth muscle cells (SMCs), which start proliferating, producing extracellular matrix that eventually leads to the formation of a fibrous plaque. As a result of the formation of the atherosclerotic plaque in the coronary artery, narrowing or obstruction of the vessel occurs reducing blood flow and leading to an imbalance between myocardial oxygen demand and supply (Cassar, Holmes et al. 2009).

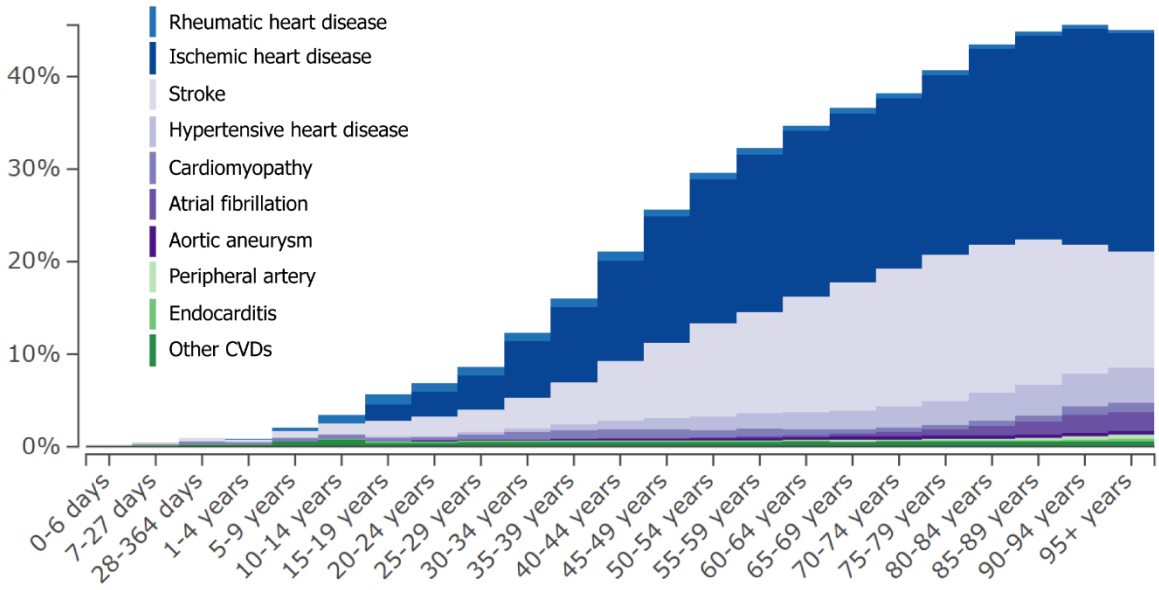

Figure 2. Percentage of total deaths for cardiovascular diseases. Source: IHME, Global Burden of Disease. (Collaborators 2018)

1.2. Myocardial infarction

CAD may clinically occur as stable angina, unstable angina, myocardial infarction (MI), or sudden cardiac death. MI can be defined as a manifestation of CAD, in which the reduced O_2 supply leads to the necrosis of cardiac cells and consequently, to the loss of contractile myocardium (Brooks G.A., Fahey TD, White TP 2000) (Ventura-Clapier et al. 2011).

Myocardial infarction is the most severe and sudden pathology of the cardiovascular system. Annually, it leads to more than a third of total deaths in developed nations

(Yeh et al. 2010), just more than 2-4 million deaths in the USA and more than 4 million in Europe and northern Asia (Townsend et al. 2015). Depending on the size of the infarct, the prognosis and the outcomes are different (McKay et al. 1986). Cardiac infarction triggers a remodeling process in which a wound healing response creates an inflammatory bed for scar tissue formation, followed by proliferation and maturation. (Dobaczewski, Chen, and Frangogiannis 2011) (Frangogiannis 2008). Cardiac remodeling is a multi-factorial, multi-level and progressive process in which the function and structure of the heart undergo numerous genetic, molecular, cellular and intercellular changes (Pfeffer et al. 1991) (Hochman and Bulkley 1982) (Weisman et al. 1985) (Korup et al. 1997) (Giannuzzi et al. 2001). Initially, an adaptive response occurs in order to compensate and maintain cardiac output. The main mechanisms involved in the adaptive response are the Frank–Starling's mechanisms, which restore failed cardiac pumping through the maintenance of cardiac contractility (Ertl et al. 1991), and the hyper-activation of the neurohumoral system, both the sympathetic nervous system (SNS) and the renin-angiotensin-aldosterone system (RAAS), which act through the regulation of posttranslational mechanisms (Curran et al. 2007). Chronic activation of these responses might lead to a maladaptive environment and, consequently, to a worsening of the disease (Cohn, Ferrari, and Sharpe 2000).

1.2.1. Cardiomyocyte response to MI

Following myocardial infarction (MI), up to 1 billion cardiac cells die in response to ischemia (Laflamme and Murry 2005), within the first days, the necrotic tissue is replaced with a fibrotic scar. Thickening (hypertrophy) and stiffening (fibrosis) of the left ventricular wall occur during the remodeling process (Sutton and Sharpe 2000). Consequently, overstretching of the ventricular wall induces elongation and compensatory hypertrophy of CMs through the disruption of the sarcomeres and further impairment of the contractility (Harding et al. 1989), (Opie et al. 2006). Subsequently, the remodeling and expansion of the scar occur because CM loss continues after MI as the result of both necrosis (Tan et al. 1991) and apoptosis (Olivetti et al. 1997) (Zhao et al. 2003) (Holmes et al. 1994). Senyo and collaborators

using pulse-chase approaches—genetic fate-mapping with stable isotope labelling have shown how CMs may go through DNA synthesis in the borderzone of infarcted myocardium leading to polyploidy and multinucleation but not cell division (Senyo, Steinhauser et al. 2013).

1.2.2. ECM remodeling

Myocardial infarction triggers an early inflammatory response. The invasion of inflammatory cells, the increasing activity of collagenases and proteinases, the release of cytokines by the necrotic tissue and the mechanical stretch induce cardiac resident fibroblast to proliferate and transdifferentiate into myofibroblasts, which are the collagen-producing cells in the infarct and the contributors to the development of fibrosis and a stable collagen structure (Beltrami et al. 2003) (Anderson, Sutton, and Lie 1979) (Weber et al. 1990)(Sadoshima and Izumo 1993) (Shamhart and Meszaros 2010).

1.2.3. Fibrosis after MI and ECM remodeling

Cardiac fibroblasts (CFs) are implicated in a wide range of functions after myocardial infarction, characterized by proliferation and phenotypic changes. The death of cardiomyocytes leads to the release of Damage-Associated Molecular Patterns (DAMPs), activating a pro-inflammatory phenotype in CFs. Soon after MI, cardiac fibroblasts start secreting cytokines (such as IL-1, TNF-a, and GM-CSF) and chemokines (such as CCL2), contributing to the recruitment and activation of leukocytes. Subsequently, cytokine-stimulated fibroblasts secrete matrix metalloproteinases (MMPs), promoting extracellular matrix degradation and release of pro-inflammatory matrix fragments.

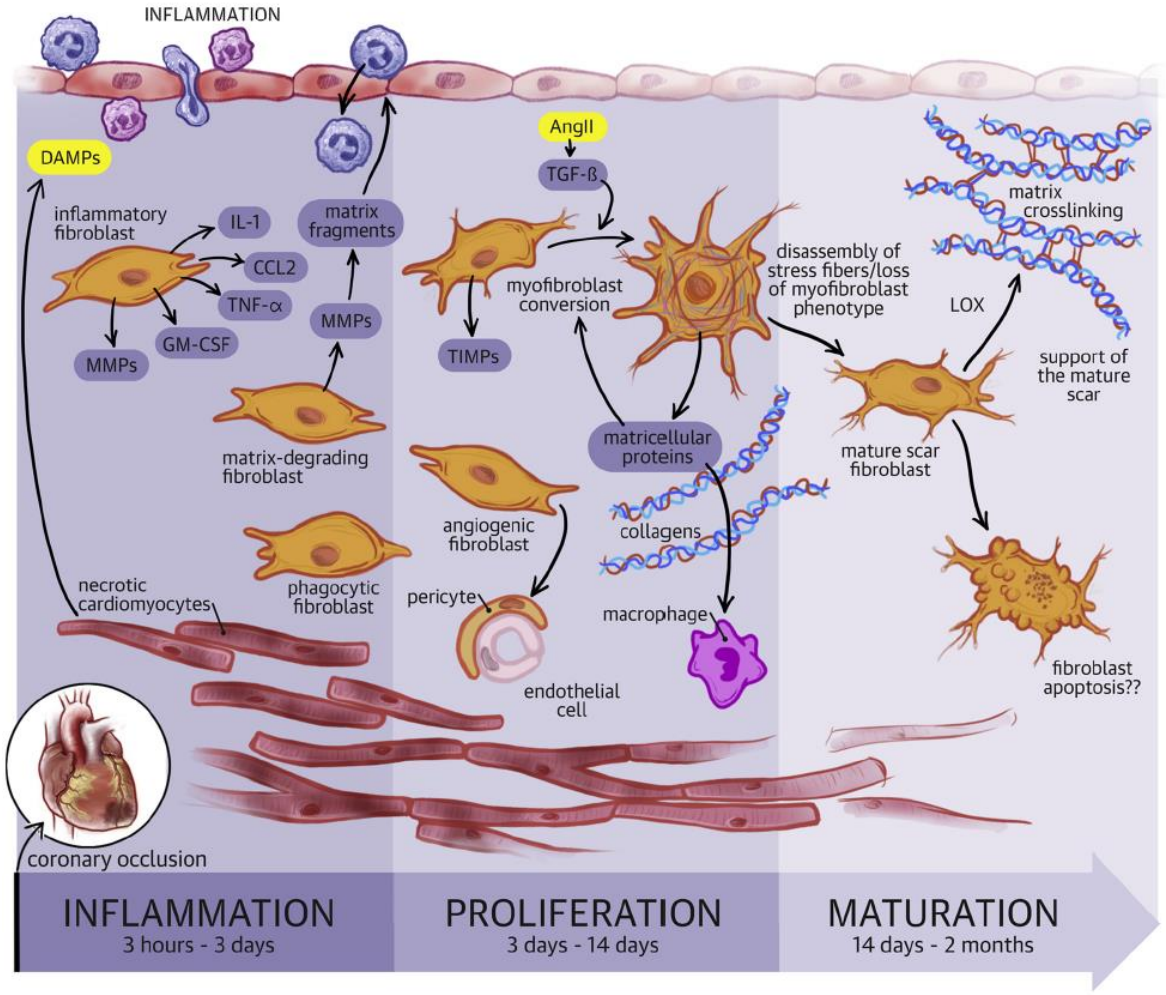

Figure 3. Phases of fibroblast activation and maturation after myocardial infarction. [Illustration credit (Humeres and Frangogiannis 2019)]

The second phase is represented by the clearance of the infarcted heart from dead cells whit the releasing of anti-inflammatory signals, fibrogenic growth factors and neurohumoral mediators which stimulate fibroblast proliferation, migration, and differentiation into myofibroblasts, the key players for the formation of a mature scar (Van Den Borne et al. 2010). After migrating in the healing infarct borderzone, fibroblasts proliferate and become myofibroblasts by incorporating Alpha-SMA into cytoskeletal stress fibers. Myofibroblasts are the primary matrix-synthesizing cells in the infarcted heart and produce both structural extracellular matrix proteins and matricellular macromolecules. Fibroblasts exhibit disassembly of a-SMA-decorated stress fibers during scar maturation and may produce matrix-crosslinking enzymes such as lysyl-oxidases (LOX).

Although the initial fibrosis is crucial to maintain the integrity of the ventricular wall, an exaggerated fibrotic response may induce cardiac dysfunction both in the injured and uninjured area contributing to heart failure (Francis Stuart et al. 2016) (Jugdutt 2003) (Gulati et al. 2013)(Lakatta 2003).

1.3. Tissue Regeneration

Regeneration is an intricate sequential orchestration of events that implies the regeneration or replacement of human cells, tissue or organs, to restore or establish normal function (Mason and Dunnill 2008). According to the book “Regeneration” written during the ‘90s by Thomas Hunt Morgan, an American evolutionary biologist and winner of the Nobel Prize in Medicine in 1933 for discoveries linking chromosomes and heredity, the first systematic studies on regeneration was performed by the French scientist René-Antoine Ferchault de Réaumur (1683-1757) in 1712, based on the observations of crayfish limb regeneration. Later on, during the 18th century Abraham Trembley, considered the founder of modern regeneration, described the regenerating capacity of Hydras. Lazzaro Spallanzani (1729-1799), an Italian Catholic priest, biologist and physiologist, was the first to carry out detailed studies on regeneration in vertebrates. However, it was only in 1930 that the idea of creating an artificial organ became a reality, thanks to the work of Alexis Carrel (Nobel Price for the study of vascular anastomosis) and Charles Lindbergh (a professional aviator), who collaborated on the development of an artificial perfusion pump, the groundwork for the modern artificial heart (Aida 2014). To mention some of the achievements in the regenerative medicine field, the first organ to be replaced in a human being was the kidney in 1954 (Guild et al. 1955), the first heart transplant was performed in 1967 (Brink and Hassoulas 2009), the first successful bone marrow transplantation in humans was obtained in 1968 (Starzl 2000) and the first engineered tissue transplantation dates back to 1981 with engineered skin engraftment (Constant and Burke 1982). Despite a rich background of regeneration researches, including studies on hydra, crustaceans, worms, fruit

flies, frogs, salamanders, zebrafish and mammals (Poss 2010), many studies are still required for a clear knowledge of the mechanisms involved in the regenerative progress and for the development of targeted therapies that can clinically impact the field.

1.3.1. Heart regeneration

Heart regeneration is a key and multifaceted challenge worldwide. As heart diseases are the leading cause of death of the 21st century, it is essential to understand the molecular and cellular mechanisms that govern cardiac regenerative capacity to develop therapies for the replacement or restoration of the damaged myocardium.

The cardiac regenerative capacity in response to damage varies widely across species and the development of comparative studies is of particular interest to display differences and homologies among them.

During vertebrate embryogenesis, the heart is the first organ to form and function, supporting blood circulation through rhythmic contractions, controlled by electric stimuli. Among all vertebrates, the heart is characterized by a muscular wall, comprised of contractile cardiac myocytes supplemented with connective tissue, and typically vascularized and innervated (Uygur and Lee 2016). Despite a similar embryonic development, cardiac injury triggers different responses in vertebrates. In the following paragraphs, an overview of the regenerative mechanisms, both in lower vertebrates and mammals, will be described.

1.3.2. Heart regeneration in lower vertebrates

The first descriptions of cardiac regeneration in lower vertebrates were only reported within the last few decades (J. O. Oberpriller and Oberpriller 1974) (Rumyantsev 1966) (Rumyantsev 1961). The best-known models to possess unsurpassed ability to replace cardiac tissue are urodele amphibians, including salamanders, newts, and axolotls (*Ambystoma mexicanum)*, and Zebrafish (*Danio Rerio)*, (Gamba, Harrison, and Lien 2014) (Poss, Wilson, and Keating 2002) (Witman et al. 2011).

1.3.3. Regeneration in urodele amphibians

Urodeles are the only vertebrates able to completely restore an embryonic environment via formation of a wound epidermis, followed by proliferation of undifferentiated cells to form a structure called blastema and a consequent differentiation of the blastema cells to replace the lost tissue. This phenomenon is called, to cite the scientist T.H. Morgan, *epimorphic regeneration* or perfect regeneration (Dinsmore and American Society of Zoologists 1991), (Echeverri, Clarke, and Tanaka 2001) (Echeverri and Tanaka 2002).

Historically, urodele's regeneration ability was described in 1769 by Spallanzani and during the 1930s many studies were conducted regarding its capacity to reform the limb and the tail (Weiss and Walker 1934). The evidence of cardiac regeneration on amphibian was first speculated in the 1960s (Rumyantsev 1966) (Rumyantsev 1961) (Sulima 1968). The results were not significantly impressive: although the presence of mitotic figures after complete removal of the ventricular apex occurs, the regenerative response was followed by the development of a scar. Curiously, in 2011, Whitman and colleagues proved the presence of a better regeneration with less scarring tissue after a minor resection at the base of the cardiac ventricles on newts (Witman et al. 2011).

As highlighted from the results, depending on the type of damage, multiple restoring responses are triggered. However, in all the studies there was a strong presence of mitotic figures as a consequence of cardiomyocytes proliferation. (J. Oberpriller and Oberpriller 1971) (J. O. Oberpriller and Oberpriller 1974) (Rumyantsev 1973) (Witman et al. 2011) (Flink 2002).

1.3.4. Regeneration in zebrafish

In contrast to the regenerative heart variability in urodeles, the teleost zebrafish (*Danio Rerio*) and the giant danio (*Devario aequipinnatus)* display a more robust and well-characterized ability to regenerate injured cardiac tissues. Furthermore, this ability can be achieved through different injury approaches, including ventricular resection, cryoinjury and genetic cardiomyocyte ablation (Gonzalez-Rosa et al. 2011) (Poss, Wilson, and Keating 2002) (Jinhu Wang et al. 2011).

Regarding the apical resection technique, Poss and colleagues have demonstrated that seconds after resection, the hemorrhage is stopped by a fibrin-rich milieu deposition which is almost instantly replaced by proliferating cardiomyocytes and by 60 days post-resection, the majority of the lost myocardium is replaced with contractile cells (Kikuchi and Poss 2012) (Poss, Wilson, and Keating 2002).

The cryoinjury approach instead is believed to be an efficient alternative to coronary artery ligation (van den Bos et al. 2005). It is characterized by a thin filament or needle cooled by liquid nitrogen and delivered to the apex's surface, resulting in necrosis and the disassembly of the functional syncytium. After 130 days post-injury, the necrotic tissue was completely recovered with contractile cells. These results were obtained both in zebrafish (Chablais et al. 2011) (González-Rosa et al 2011) (Schnabel et al. 2011) and giant danio (Lafontant et al. 2012).

Another approach to injure the zebrafish heart is genetic ablation, based on the development of a transgenic system. Briefly, two transgenes were employed, the 4-hydroxytamoxifen (4-HT)-inducible Cre recombinase (CreER) specific for cardiomyocytes and the cytotoxic DTA (diphtheria toxin A chain) gene that can be induced to target CreER-expressing cells. After a single injection of 4-HT, a 60% depletion of cardiomyocytes was obtained. As seen in the previous technique, following cell-specific depletion a plethora of responses rapidly regenerate the myocardium (Jinhu Wang et al. 2011).

Interestingly, while most of the initial findings indicated a population of stem or progenitor cells as the source of newly formed cardiomyocytes (Poss, Wilson, and Keating 2002), cardiomyocytes regeneration is depending on pre-existing cardiomyocytes, which are able to reduce the organization of their sarcomeric structures and dedifferentiate to a more embryonic form, followed by proliferation (Jopling et al. 2010). Additionally, further investigations revealed that this subpopulation of pre-existing cardiomyocytes expressed the GATA4 gene, which is known to be a critical transcription factor for cardiac development, generally expressed during the embryonic life (Kikuchi et al. 2010).

1.3.5. Heart regeneration in mammals

The magnitude of heart regeneration in mammals is still a matter of debate, offering many challenges in the regenerative medicine field.

While it is well known and proved that lower vertebrates have an extraordinary ability to prompt cardiac regeneration (Gamba, Harrison, and Lien 2014) (Poss, Wilson, and Keating 2002) (Witman et al. 2011), a multitude of controversies is reported in the mammalian heart counterpart. In response to cardiac injury, adult mammals—of major interest, mice and humans—fail to regenerate the majority of the lost cardiomyocytes, developing scar tissue, which in turn, determines a contractile demise of the heart. Depending on the extension of the lesion, the progression towards heart failure or even death is almost inevitable (Enzo R. Porrello and Olson 2014).

A key concept in regenerative medicine is that there is a strong correlation between regeneration and development. As Spallanzani demonstrated already in 1768, limb regeneration in salamanders is an age-dependent process (Spallanzani 1768). Many processes that were initially characterized in urodele limb and tail regeneration, such as wound healing and innervation, have now been shown to play a role in heart regeneration across multiple species (Uygur and Lee 2016). Axolotl or newt heart after an injury can replace lost tissue and function within 90 days without evidence of scarring (Becker, Chapin et al. 1974). In mice instead, this regenerative ability is preserved exclusively in a time-window, from the fetal stage to 7 days post-natal life (Enzo R. Porrello, Mahmoud, et al. 2011) (Enzo R. Porrello and Olson 2014).

Traditionally, the heart has been indeed viewed as a refractory and post-mitotic organ in which cardiomyocyte proliferation ceases soon after birth (Enzo R. Porrello, Mahmoud, et al. 2011)(Ahuja, Sdek, and MacLellan 2007) (Bicknell, Coxon, and Brooks 2007). However, a growing number of evidences have revealed the potential for cardiogenesis occurring at a low rate in mammals, including humans (Foglia and

Poss 2016) (Enzo R. Porrello, Mahmoud, et al. 2011) (Bergmann et al. 2009) (Bergmann et al. 2015) (Mollova et al. 2013) (Senyo et al. 2013).

Several studies have provided evidence for a potential compensatory growth of healthy cardiac cells in diseased embryonic mouse hearts. Drenckhahn and colleagues proved that pre-existing cardiomyocytes were the regenerating source of proliferation, as seen in zebrafish (Drenckhahn, Schwarz et al. 2008). Furthermore, Porrello et al. developed a surgical model of cardiac injury in 1-day-old neonatal mice through the permanent ligation of the left anterior descending coronary artery, inducing myocardial infarction associated with a loss of CMs viability. Almost 95% of the infarcted tissue was restored within three weeks post-injury (E. R. Porrello et al. 2013). In the adult heart, despite the ability to maintain a regenerative profile following injury, the degree of cell turnover, which is the ability to replace lost cardiomyocytes by new ones, is not sufficient to overcome the loss of almost 1 billion out of 2-6 billion cardiomyocytes after injury (Enzo R. Porrello, Mahmoud, et al. 2011) (E. R. Porrello et al. 2013).

The first reports of human cardiac regeneration were conducted on children with cardiac hypertrophy and myocarditis, in which the presence of mitotic figures and splitting of myocardial fibers were considered as a regenerative reaction (Macmahon 1937) (Warthin 1924). Another case of cardiac regeneration in humans was reported by Fratz and colleagues where children with anomalous left coronary artery from the pulmonary artery (ALCAPA), a rare congenital heart disease, recover their cardiac function without evidences of myocardial scarring after cardiac corrective surgery (Fratz et al., 2011). Interestingly, a case report of a newborn infant with a large anterior myocardial infarction displayed healing by regeneration, with full functional recovery seven weeks after ischemia, suggesting, similar to neonatal rodents, newborn humans might have the intrinsic capacity to repair myocardial damage and completely recover cardiac function (Haubner et al., 2016).

One major evidence in the loss of the regenerative ability is a phenotypic switch of the mammal CMs from the neonatal state to the adult state (Bersell et al. 2009)

(Chen et al. 2013) (Eulalio et al. 2012) (Enzo R. Porrello, Mahmoud, et al. 2011) (Mahmoud et al. 2013) (Sdek et al. 2011) (Xin et al. 2013) (Puente et al. 2014).

During embryogenesis, the heart is characterized by great plasticity and subjected to rapid growth, facing different environmental and molecular changes (Enzo R. Porrello, Widdop, and Delbridge 2008). Among all the factors involved in cardiac differentiation during embryonic heart development, it stands the transcription factor Meis1 (Paige et al. 2012) (Wamstad et al. 2012). Meis1 belongs to the TALE (three amino acid loop extension) family of homeodomain transcription factors (Hisa et al. 2004) (Stankunas et al. 2008). Mahmoud et al. demonstrated that the genetic deletion of Meis1, both in the postnatal mouse heart and in the neonatal mouse heart, was associated with an increase of CMs proliferation rate and a limited proliferative response, respectively (Mahmoud et al. 2013).

Soon after birth such plasticity is, however, lost. A switch from a mononucleate to a binucleate phenotype occurs in cardiomyocytes. Binucleation is a feature of terminally differentiated cells, whereas mononucleate cells still retain the potential to undergo the normal cycle and thus proliferate. After a final round of acytokinetic mitosis (karyokinesis without cytokinesis), the majority of the cardiomyocytes become terminally binucleated (Ahuja, Sdek, and MacLellan 2007) (M. H. Soonpaa et al. 1996) (Mark H. Soonpaa and Field 1998) (Walsh et al. 2010).

1.4. Postnatal factors implicated in cardiomyocytes loss of the proliferative potential

The withdrawal of cardiomyocytes from the cell cycle after birth is accompanied by various changes, both at the molecular and structural level (Mollova et al. 2013). Recent studies have demonstrated a plausible role of the chromatin remodeling with the maintenance of a differentiated phenotype in CMs, in particular through DNA methylation, ATP-dependent chromatin remodeling, and covalent histone acetylation and methylation (Sdek et al. 2011) (Montgomery et al. 2007) (Trivedi et

al. 2010) (Toyoda et al. 2003) (Park et al. 2010) (Hang et al. 2010). Several postnatal regulatory events have been shown as putative causes for the phenotype switch of mammal CMs from the neonatal proliferative state to the adult post-mitotic state. In particular, the shifting from the embryonic to the postnatal life is associated with an increasing oxygenation state as a consequence of breathing, reaching an oxygen tension of 100 mmHg compared to the 30 mmHg in the embryo (Webster and Abela 2007). Simultaneously to the hyperoxia state, the development of oxygen free radicals (reactive oxygen species, ROS) occurs and leads to cellular damages, resulting in cell-cycle arrest (Gao and Raj 2010) (Hoeijmakers 2009). In addition, marked metabolic adaptations in postnatal cardiomyocytes occur in response to high-energy demands (Pohjoismäki et al. 2012). Indeed, while the hypoxic embryonic heart utilizes anaerobic glycolysis as the primary source of energy (Lopaschuk, Collins-Nakai, and Itoi 1992) (Lopaschuk et al. 1994), adult cardiomyocytes utilize the oxygen-dependent mitochondrial oxidative phosphorylation (Wisneski et al. 1985), a high energy source way which, on the other hand, produces mitochondrial ROS, thus contributing to cellular toxicity (Miquel et al. 1980).

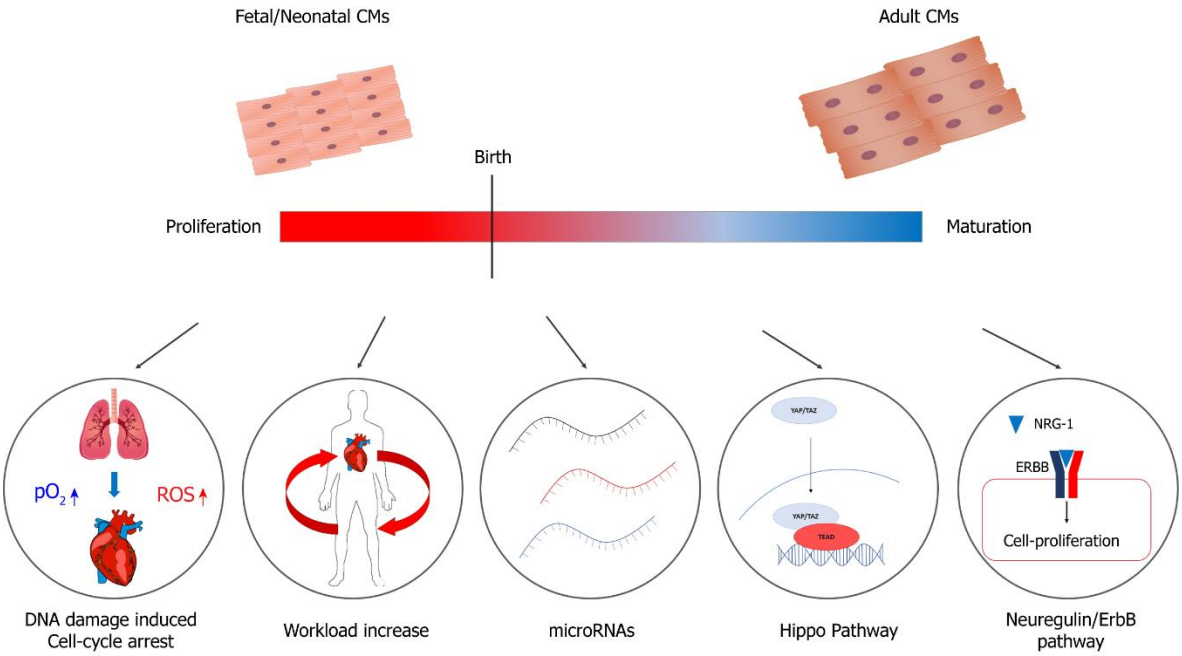

Figure 4. Schematic summary of some known pre- and postnatal regulators of cardiomyocyte proliferation. The proliferative potential of CMs gradually decrease after birth (Red bar). On the other hand, the maturation of the CMs increase inducing a post-mitotic phenotype (Blue bar).

Another major post-natal event is the massive workload that the heart has to face in response to an increasing body weight. The consequences for this physiological event leads to an improvement of the contractile capacities of the cardiomyocytes, initially by hyperplasic growth and then by hypertrophic growth (Li et al. 1996), while on the other hand leads to an increasing mechanical stress and energetic demand for the sustainment of age-related physiological events (Enzo R. Porrello, Mahmoud, et al. 2011) (Lopaschuk and Jaswal 2010). Therefore, the interconnection between these events is detrimental for the maintenance of a proliferative state, thus promoting cardiomyocyte cell cycle arrest (Schmelter et al. 2006).

The microRNAs network has emerged as one of the most essential post-transcriptional gene regulators. MicroRNAs are small, highly conserved RNA molecules that act by binding a complementary mRNA and consequently orchestrate the expression of genes, both in an up-regulation and down-regulation fashion. (Bartel 2009) (Van Wynsberghe et al. 2011) (Mallory and Vaucheret 2004). miRNAs play a pivotal role in both physiological and pathological cardiac development. Recent evidence highlighted that specific miRNAs are involved in postnatal cardiomyocyte mitotic arrest (Mahmoud et al. 2013) (Enzo R. Porrello, Johnson, et al. 2011) (E. R. Porrello et al. 2013). Overexpression of miR-195, a member of the miR-15 family, during development induced premature cardiomyocyte cell-cycle arrest. Another group of miRNAs playing an important function on cardiomyocyte proliferation during embryogenesis and postnatal life is represented by the miR-17~92 cluster. (Jun Wang et al. 2010) (Chen et al. 2013). Eulalio et al., by performing a high throughput screening of a library of 875 miRNA, have identified two specific miRNAs associated with CMs proliferation, miR-199a and miR-590. (Eulalio et al. 2012). The effects of the overexpression of the two candidates were linked to increased cardiomyocyte proliferation, reduced fibrotic scarring and improved cardiac function following myocardial infarction (Eulalio et al. 2012).

Another key regulator of cardiomyocyte proliferation and fetal heart growth throughout development and after birth is the evolutionarily conserved Hippo pathway (Todd Heallen et al. 2011) (T. Heallen et al. 2013) (von Gise et al. 2012) (Xin et al. 2013). Mechanical stress, cell polarity, cell adhesion and cell junction proteins promote the activation of the pathway through the inhibition of the core signaling components Yes-associated protein (YAP) and the transcriptional co-activator PDZ-binding motif (TAZ). When YAP is inactivated in the fetal heart, a decrease rate of CMs proliferation occurs. When YAP is activated, it induces a pro-proliferative response in the fetal and postnatal heart (von Gise et al. 2012) (Xin et al. 2011). Interestingly, the Hippo pathway interacts with other signaling pathways, such as the canonical Wnt/b-catenin signaling. Heallen et al. showed that the cardiac-specific repression of Salvador homolog1 (Sav1) in mice facilitates the regenerating process, decreasing the scar tissue formation after adult myocardial injury (Todd Heallen et al. 2011) (T. Heallen et al. 2013), reinforcing the concept that YAP activation plays an important role for heart regeneration.

Neuregulin/ErbB/ERK pathway also plays a primary role in cardiac development, structural maintenance, and functional integrity of the heart (Dugaucquier, Feyen et al. 2020)(Bersell et al. 2009). Neuregulin (NRG-1) is a member of the epidermal growth factor family and acts through the association with the ErbB family of tyrosine kinase receptors (Wadugu and Kuhn 2012).

NRG-1 promotes cardiac regeneration targeting mononucleated cardiomyocytes that are induced to divide, producing an hyperplastic rather than a hypertrophic response after injury (Chien et al. 1991) (Bersell et al. 2009). In addition, NRG1 contributes to the regulation of sarcomere disassembly through the downstream activation of the cardiac myosin regulatory light chain kinase, cMLCK (Sawyer et al. 2002) (Bersell et al. 2009) (Chan et al. 2008) (Seguchi et al. 2007).

1.4.1. Mechanotransduction in the heart

Mechanotransduction is a multistep process through which cells sense and respond to mechanical stimuli. It includes mechanical forces that are converted into signals

sensed by sensor cells, a biochemical coupling which consists in the conversion of mechanical signal into a biochemical signal to elicit a cellular response such as gene activation, transfer of a signal from sensor to effector cells, and the effector cell response. The heart is a dynamic organ characterized by a continuous contractile activity which needs to be adjustable in relation to different condition, such as physiological variation of blood supply from the body or due to pathological impairments of cardiac function. For this purpose, cardiomyocytes are mechanically durable and capable of sensing a variety of environmental signals including mechanical cues. As an example, during physiological growth, myocytes undergo to an adaptively remodeling to the initial mechanical load. On the other hand, maladaptive remodeling may be induced by pathological stimuli. Mechanotransduction plays a pivotal role in the biology of cardiomyocytes, including their development, maturation and determination of the hypertrophic or atrophic phenotypes.

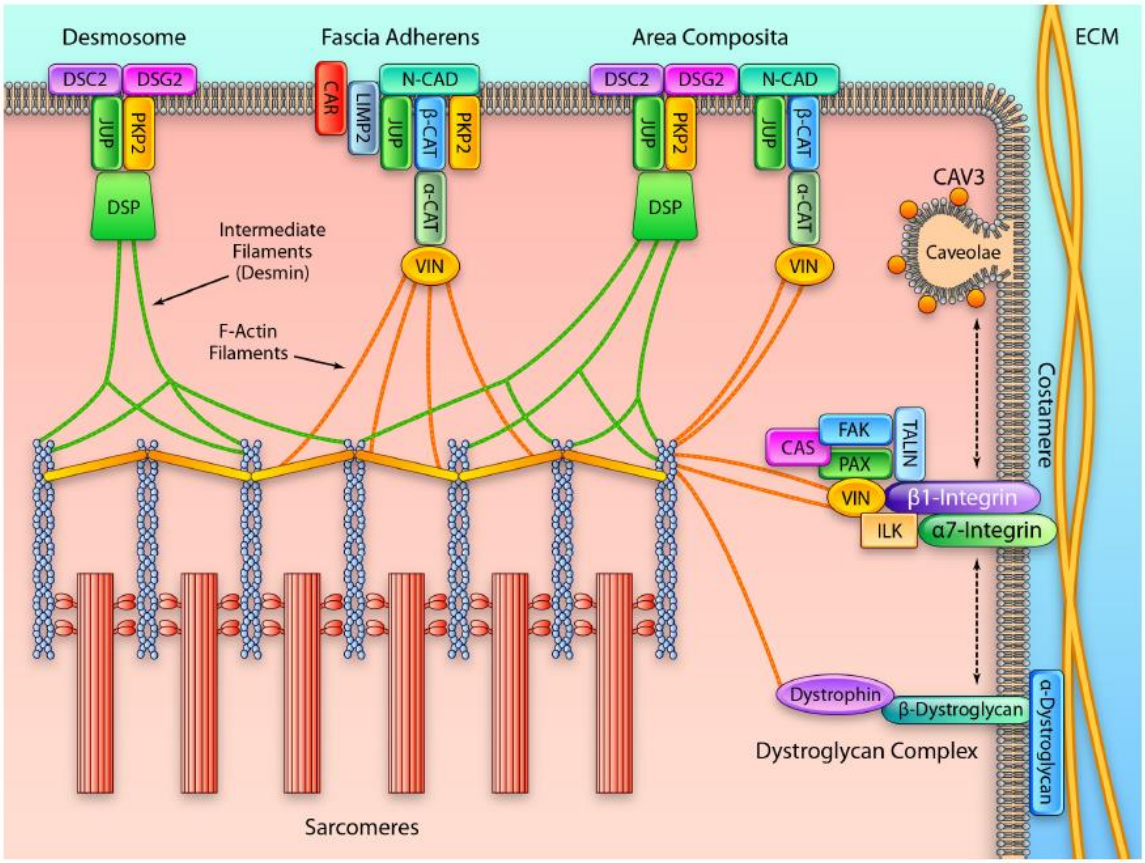

Figure 5. A schematic representation of the specific protein complexes linked to cell–cell junction and sarcolemma-mediated mechanotransduction and mechanotransmission in cardiac muscle. [Illustration credit: (Lyon, Zanella et al. 2015)]

Several evidences have highlighted the key role of sarcomere in mediating the mechanical sensing of CM. The sarcomere represents the basic contractile unit of cardiac muscle and is characterized by a complex assembly of myofilament proteins (Gautel 2011). The interaction between myosin heads (thick filament) and actin thin filament proteins is the driving event able to generate force in cardiac muscle (Spudich 2001). Besides the main role in the contraction, the sarcomere is directly connected to the cytoskeleton via Z-disc and myosin is stabilized by titin and other structural proteins, corroborating the idea that sarcomeric proteins play a role in mechanotransduction (Frank and Frey 2011, Buyandelger, Mansfield et al. 2014). Indeed, one of the primary mediators of mechanical cues in the cell is the cytoskeleton which is implicated in regulating cell shape (Singhvi, Kumar et al. 1994) and influencing migration, cellular function and homeostasis (Chen, Mrksich et al. 1997, Bray, Adams et al. 2010).

The sarcomere is connected to the sarcolemma by cytoskeletal components, such as F-actin and desmin, which link the Z-disc to costameres. Costameres are complex networks of proteins and glycoproteins, and they consist of two major protein complexes: the dystrophin-glycoprotein complex (DGC) and the integrin-vinculin-talin complex which bind to components of the ECM.9 The intermediate filament desmin also links the Z-disc to the nucleus connecting the cytoskeleton with the nucleoskeleton through a linker (Linker of Nucleoskeleton and Cytoskeleton - LINC complex) (Lazarides 1980). Furthermore, sarcomere is linked by the cytoskeletal actin and desmin to the components of the specialized cardiac muscle cell-cell junction, the intercalated disc (ICD) (Sheikh, Ross et al. 2009). Intercalated discs play a crucial role in maintaining mechanical and electric coupling between cardiomyocytes allowing transmission of the force generated by the sarcomere from adjacent cells. The three main complexes located in the intercalated discs are adherens junction, desmosome and gap junction. Gap junctions are composed of intercellular channels of connexin proteins that permit direct cell–cell transfer of ions

and small molecules allowing the diffusion of action potential in the cardiomyocytes (Goodenough and Paul 2009). On the other hand, Adherens junctions and desmosomes are inter membrane protein complexes able to anchor different cells together which determinates their putative role in mechanotransduction. Adherens junctions anchor together different cells by the extracellular domain of cadherins which are connected in the plasmatic space with cytoskeletal actin (Wang, Li et al. 1999). In the heart, the proteins bound to the adherens junctions junctional complex include transmembrane proteins that are mainly composed of N-cadherin (N-CAD), which are calcium-dependent.

Desmosomes are cell-to-cell adhesion types that serve to mechanically couple cells in tissues that experience constant mechanical stress, such as the heart (Sheikh, Ross et al. 2009). They are responsible for the anchoring of the cytoskeletal intermediate filament network between cardiomyocytes (Sheikh, Ross et al. 2009). In cardiac muscle, desmosomes are composed of extracellular transmembrane-based cadherins, desmocollin-2 and desmoglein-2, which with their cytoplasmatic tails provide a binding site to members of the armadillo family, JUP and plakophilin-2, that are then in turn bound to the plakin family member, desmoplakin, which is the central cytoplasmic link to the intermediate filament network composed of desmin.

Mechanical forces generated by the sarcomere are transmitted both longitudinally and laterally to the sarcolemma of the cardiac muscle cell (Tangney, Chuang et al. 2013). Since there is evidence for directional-dependence of myocyte stress sensing (Simpson, Majeski et al. 1999, Gopalan, Flaim et al. 2003) there may be directional dependence of mechanotransduction within a myocyte.

1.4.2. Mechanotransduction in cardiomyocytes development and maturation

Mechanical forces are epigenetic factors that are fundamental in the regulation of organ development (Ingber 2006). Both contractile activity of the cells and the physical features of the environment surrounding them affect the embryogenesis process (Wozniak and Chen 2009). The recognition of the external mechanical cues

is mediated by the interaction with the ECM via integrin binding and by intercellular junctions (Chen, Tan et al. 2004). Mechanical forces are implicated in the morphological changes of the heart during its development. For example, the looping of the embryonic heart tube is conditioned by the alteration of the cardiomyocyte shape and spatial organization (Taber, Lin et al. 1995, Latacha, Remond et al. 2005) (Itasaki, Nakamura et al. 1991).

Mechanotransduction plays a key role also in the growth and development of the post-natal cardiomyocytes which are constantly exposed to physical stretching as a result of the contractile activity of the heart. Contraction activates mechano-sensitive signaling pathways that influence cardiac cell phenotype such as the increased cardiomyocyte size that occurs soon after birth due to the increase of the hemodynamic load (Frey and Olson 2003, Sheehy, Huang et al. 2009).

Transmembrane integrin receptors allow the communication between the ECM and the cytoskeleton, in this way, external physical forces may influence intra-cellular processes (Schwartz, Schaller et al. 1995). Over the course of heart development, ECM composition and expression of α- and β-integrin isoforms that recognize various ECM components change (Terracio, Rubin et al. 1991, Price, Nakagawa et al. 1992, Ross and Borg 2001). The expression levels of fibronectin and α5β1 integrin receptors in the fetal stage are elevated compared to expression levels detected in the adult myocardium (Samuel, Farhadian et al. 1994, Farhadian, Contard et al. 1995). This variation in the expression of fibronectin and β1 integrins present in pre-natal cardiomyocytes has been associated with the proliferation and spreading, features that are lost post-partum (Hilenski, Ma et al. 1992, Hornberger, Singhroy et al. 2000). Furthermore, embryonic and adult cardiomyocytes are characterized by different expressions of β1 integrin. Embryonic myocardium has been shown to mainly expresses the β1A isoform, while in the adult heart, cardiomyocytes express primarily the β1D variant (Belkin, Zhidkova et al. 1996, van der Flier, Gaspar et al. 1997, de Melker and Sonnenberg 1999).

Despite the fact that they lack intrinsic kinase activity, transmembrane integrin receptors are able to transmit mechanical forces to the cytoskeleton, where they

activate mechanosensitive signal transducers, such as focal adhesion kinase (FAK), that are able to translate the mechanical cue into a biochemical response (Burridge and Chrzanowska-Wodnicka 1996, Schwartz and Ginsberg 2002, Samarel 2005).

Several chemical signaling pathways are activated through this mode of information transmission, including the Rho kinase, PI3K, ILK, Src, ERK, and MAP kinase pathways that modulate transcriptional activity and direct important cellular activities, such as cell cycle entry and the induction of apoptosis (Schwartz, Schaller et al. 1995, Chen, Mrksich et al. 1997, Ingber 2006, Discher, Mooney et al. 2009, Fletcher and Mullins 2010) . Many of these signaling intermediates are immobilized on the cytoskeleton, particularly at the Z-discs in cardiomyocytes, such as Melusin, muscle LIM protein (MLP) and Titin. They have been shown to be subjected to mechanical perturbations that may modulate their activity and translocation to cellular compartments(Knoll, Hoshijima et al. 2002, Brancaccio, Fratta et al. 2003, Heineke, Ruetten et al. 2005, Puchner, Alexandrovich et al. 2008).

Cardiomyocytes may also perceive biomechanical cues from their neighbor cells via intercellular junctions and through direct transmembrane ligand–receptor interactions (Simpson, Decker et al. 1993, Kresh and Chopra 2011). During heart development, actomyosin cross-bridges generate tension on cytoskeleton that plays a key role in forming and maintaining of intercellular junctions (Peters, Severs et al. 1994, Niessen, Leckband et al. 2011). Notch receptors and the Wnt signaling intermediates localize to adherens junctions, playing an important role in regulating the organization of nascent cells during tissue formation that demands a hierarchical organization of gene expression and precise interactions between neighboring cells (Nelson and Nusse 2004, Gessert and Kuhl 2010).

1.4.3. Mechanotransduction in cardiomyocyte proliferation

Given the well-established role of mechanotransduction in cardiac development and maturation, even though its mechanism remains unclear, there is a growing interest in the putative role of mechanotransduction in cardiomyocyte proliferation. Indeed,

emerging evidences show that alteration of cytoskeleton and sarcomere may induce cardiomyocyte-cell cycle activation.

For instance, it has been shown that structural and functional integrity of the DGC plays a specific role in the regulation of CM proliferation. DGC is a complex that binds ECM to dystrophin, while dystrophin anchors DGC to the F-actin cytoskeleton (Rybakova, Amann et al. 1996). Dystroglycan 1 (Dag1) is a component of this complex that has been reported to bind YAP directly and inhibits its pro-proliferative function (Morikawa, Heallen et al. 2017). Moreover, Dag1 and DGC are also the targets of the ECM proteoglycan agrin, which promotes cardiac regeneration in neonatal mouse hearts (Bassat, Mutlak et al. 2017).

During the early post-natal phase of cardiac maturation, ICD components go through a redistribution among cell membrane moving to the longitudinal ends of rod-shaped CM. These changes in the distribution of ICD components correlate with the exit of CMs from the cell cycle soon after birth (Li, Wang et al. 1996, Soonpaa, Kim et al. 1996), suggesting a possible function of ICD components in the regulation of CM proliferation. αE-catenin anchors cadherin-catenin complex to the cytoskeletal actin and it plays a key role in the proliferation of different cell types (Lien, Klezovitch et al. 2006, Schlegelmilch, Mohseni et al. 2011). Furthermore, inhibition of α-catenin expression in mice induces CM proliferation by releasing YAP from cadherin-catenin complexes after MI (Lin, von Gise et al. 2014). Consistently, inhibition of expression of αE-catenin and αT-catenin induces CM proliferation in the adult heart (Li, Gao et al. 2015).

On the intracellular side, it is well established that there is a robust functional correlation between cytoskeleton and cell-cycle machinery. In particular, cytoskeletal actin organization regulates cell cycle progression in several cell types (Spector, Shochet et al. 1983, Thery and Bornens 2006). Perturbation of proper cytoskeleton reorganization leads to cell cycle arrest due to the activation of checkpoints in both the G1 (Reshetnikova, Barkan et al. 2000) and G2/M (Gachet, Tournier et al. 2001) phases of the cell cycle. For instance, an actin-depolymerizing factor (ADF), Cofilin 1, overexpression may arrest the cells in G1 (Lee and Keng

2005), although increased F-actin polymerization leads to delayed mitosis and defective cytokinesis, which eventually determines cell multinucleation in cardiomyocytes.

Finally, Canseco and collaborators in 2015 reported the pro-proliferative effect of prolonged mechanical unloading in human left ventricle. They evaluated the effect of human ventricular unloading after implantation of left ventricular assist devices (LVADs) on cardiomyocyte proliferation in 10 patients before LVAD implantation and after the explant of the device, observing a significant increase in both phosphorylated histone H3–positive and Aurora B–positive cardiomyocytes in the post-LVAD hearts (Canseco, Kimura et al. 2015).

1.5. Cardiac tissue engineering

Generating three-dimensional (3D) cardiac cultures is considered to be relatively easy because immature cardiac cells beat spontaneously and also have an intrinsic capacity to form 3D functional syncytia. In the late 1950s, Moscona et al. induced the formation of spontaneously beating spheroids by simple rotatory shaking of Erlenmeyer flask with embryonic chicken cardiac myocytes (Moscona 1959). These spheroids showed improved functionality when compared with standard 2D-cultured myocytes. This self-assembly is still used with variations to generate cardiac microspheres (Kelm, Ehler et al. 2004). Over the years, several in vitro models of engineered cardiac tissues have been proposed as tools to investigate all the aspects of myocardial biology. In the last decade, a vast number of platforms of 2D and 3D cardiac cell culture have been developed taking advantage of diverse cell sources, such as neonatal CM of rodents and human induced pluripotent stem cells (hiPSCs) and supports for tissue organization.

One of the main sources of cardiac cell for tissue engineering is rat neonatal cardiomyocytes due to their availability and the ease isolation (Hansen, Eder et al. 2010). On the other hand, other animal sources of primary cells have been successfully utilized for the generation of in vitro cardiac model such as mouse and

guinea pig neonatal CM (Stoehr, Neuber et al. 2014, Weinberger, Breckwoldt et al. 2016).

Given the advantage of hiPSCs derived from patients which can be used to easily produce different cell types of the heart (Giacomelli, Mummery et al. 2017) (Passier, Orlova et al. 2016), many researchers have developed human engineered cardiac tissues based on hiPSCs-derived cardiomyocytes (hiPSC-CMs). Among these engineered tissues, emerging models include cardiac microtissues (Giacomelli, Meraviglia et al. 2020), engineered myocardium (Eder, Vollert et al. 2016), heart-on-a-chip (HoC) devices (Zhang, Aleman et al. 2015), and hEHT (Eder, Vollert et al. 2016) in many cases with relevant sensors and environmental stimuli, such as mechanical and electrical stressors. Despite growing evidence of their utility, one of the major issues of the hiPSC-CMs remained the relative immaturity of the cells that can be in part resolved when subjected to cyclic stress or are in contact with non-CM cells of the heart (Abilez, Tzatzalos et al. 2018, Ronaldson-Bouchard, Ma et al. 2018, Giacomelli, Meraviglia et al. 2020).

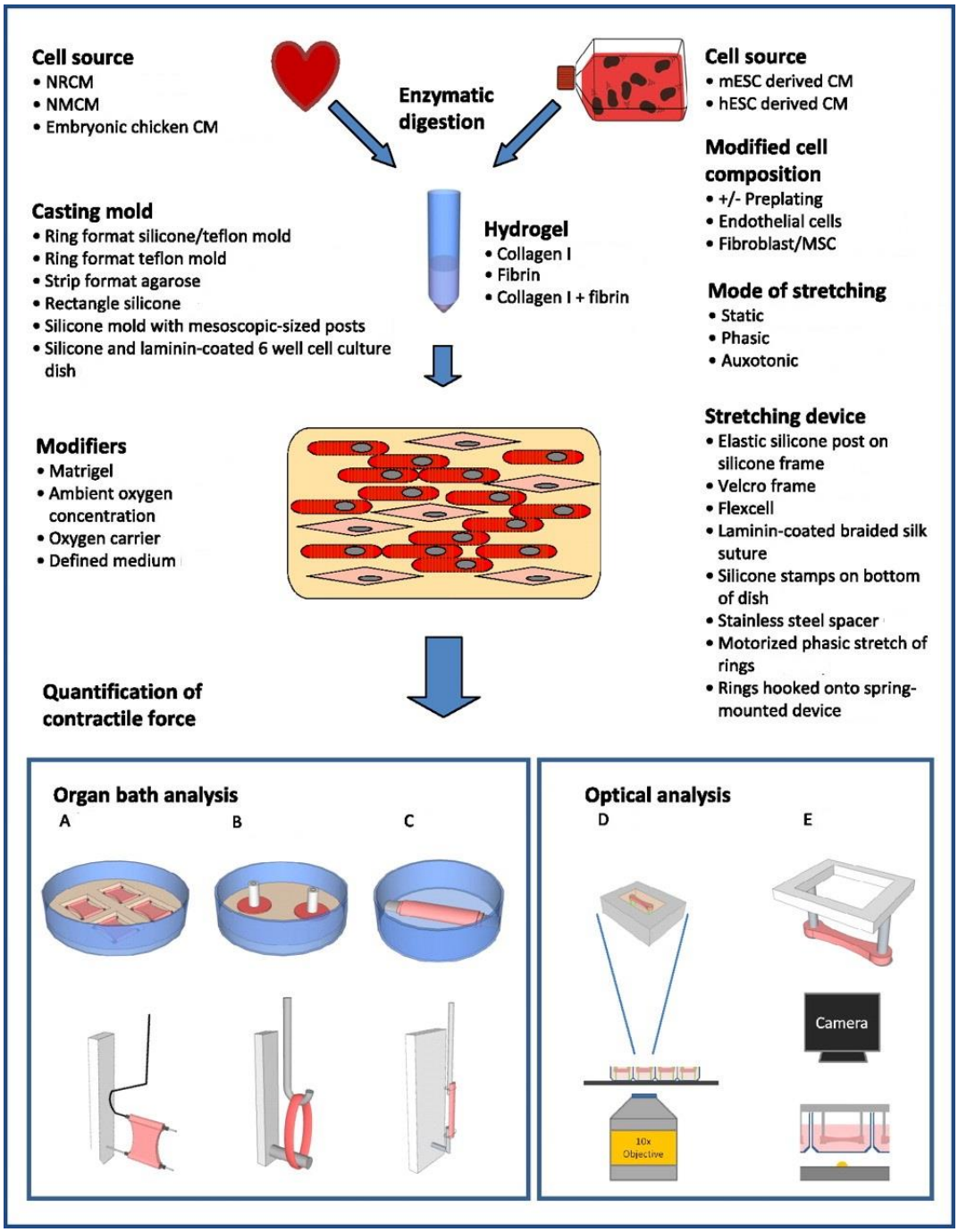

Figure 6. Different hydrogel- based cardiac tissue engineering approaches. [Illustration credit: (Eschenhagen, Eder et al. 2012)]

Besides the cell sources of the engineered cardiac tissues, a crucial component of cardiac 3D structures is the matrix which has been exhaustively described by Hirt and colleagues (Hirt, Hansen et al. 2014).

1.5.1. Prefabricated matrix

One of the tissue engineering approach has been seeding prefabricated porous solid matrices with cardiac cells. Several materials have been tested, including alginate (Leor, Aboulafia-Etzion et al. 2000), collagens (Radisic, Park et al. 2004), and gelatin sponges (Li, Jia et al. 1999), polyglycolic acid (Carrier, Papadaki et al. 1999), poly-l-lactic acid/polyglycolic acid composites (Lesman, Habib et al. 2010), and poly (glycerol sebacate) (Marsano, Maidhof et al. 2010). An advantage of this technique is the facility to engineer any desired 3D form and manipulate constructs in culture. It has been shown that a more natural environment, characterized by collagen sponge and chronic electric pacing, provides a better environment for the cells than the artificial polymers, allowing improved structure and function of the tissue (Radisic, Park et al. 2004).

1.5.2. Decellularized tissue

A second approach takes advantage of the natural environment attempting to produce an artificial heart by repopulating a decellularized whole heart with cardiac cells (Ott, Matthiesen et al. 2008). Decellularization is a procedure that almost completely eliminates cells from the tissue but leaves connective tissue architecture of blood vessels intact. This allows perfusion of the decellularized matrix but makes repopulation with cardiac cells difficult (Tong, Li et al. 2019).

1.5.3. Cell sheets

Cardiomyocytes tend to detach from the substrate as an approximately intact monolayer if they are cultured for extended periods on standard plastic dishes. Starting from this principle, Shimizu et al. developed temperature-sensitive coating materials that allow cell monolayers to detach as intact monolayers by leaving the culture dish at room temperature (Shimizu, Yamato et al. 2002). The stacking of several cell sheets generates 3D tissues that beat and develop force. Similar approaches have been developed before to engineer blood vessels (L'Heureux, Paquet et al. 1998). This scaffold-free technology is flexible and convenient for

transplantation, making it suitable for therapeutic cardiac repair (Kubo, Shioyama et al. 2013).

1.5.4. Hydrogel-based Technique

During the 1980s, the hydrogel method has been developed as an advanced culture method for fibroblasts and skeletal muscle cells and allowed the first successful engineered cardiac tissue generation (Vandenburgh, Karlisch et al. 1988, Eschenhagen, Fink et al. 1997). This matrix-based approach is composed by three fundamental elements:

- solutions of gelling natural products, such as collagen I, Matrigel, fibrin, or mixtures of them, which entraps cells in a 3D space during gelling;
- casting molds, in which engineered tissue takes the 3D form;
- anchoring constructs, allowing the growing tissue to fix and to develop mechanical tension between two or more anchor points.

Considerable aspects of this technique are that the naturally occurring hydrogels stimulate cells to form intercellular connections due to the free spreading and that the cells compress the gel, reduce the water content, leading to a reduction of size by several-folds. In the different hydrogel approaches, the macroscopic shape of the final construct is defined by the casting molds and the method on which the developing tissue is fixed to the anchoring constructs.

The latter is crucial because good cardiac tissue development occurs only in constructs growing under continuous mechanical load (Fink, Ergun et al. 2000, Bian, Liau et al. 2009). Specifically, anchoring applies a continuous mechanical strain on the growing tissue and induces orientation of cells parallel to the force lines. The hydrogels also appear to prevent cell death due to loss of cell-cell contacts, a process termed anoikis, typical of isolated cells (Karoubi, Ormiston et al. 2009, Munoz, Zhou et al. 2010). In the absence of mechanical strain, cells degenerate and do not form a beating tissue. Some evidence indicates that presence of fibroblasts

and endothelial cells in the hydrogel matrix may support tissue development (Naito, Melnychenko et al. 2006, Caspi, Lesman et al. 2007, Radisic, Park et al. 2008).

Engineered tissues made by hydrogel technology generally display lower mechanical stability compared to scaffold-based techniques, but this methodology is easily miniaturized and automated and allows standardized force measurements. Therefore, it is well-suited for in vitro testing.

1.5.5. Fibrin-based engineered heart tissue (EHT)

In 2010 Eschenhagen et al. published a study aimed at miniaturizing tissues made with the hydrogel method, fitting them in multi-well plate and promoting an automated evaluation of generated forces. The first fundamental improvement they made was substituting collagen I with fibrinogen, which is converted in fibrin by thrombin. Fibrin polymer presents, due to its nonlinear elasticity, a higher elastic modulus under shear stress and softness compared to other filamentous biopolymers (Janmey, Winer et al. 2009). Moreover, in vitro polymerization of fibrin results in a gel that is very similar to in vivo fibrin polymer. Fibrinogen is also easy to purify from different species, fully biodegradable by fibrinolytic enzyme and is able to covalently bind growth factors. These features make fibrin an interesting compound for tissue engineering applications. On the other hand, fibrin gels need constantly soaking in aprotinin-added medium to avoid proteolytic degradation.

The second important improvement that they introduced was producing anchoring constructs made of silicone and Teflon spacer for the generation of casting molds, both adaptable to a 24 well dish. The silicone racks contained four pairs of posts between which growing tissue can be anchored. Teflon spacers allow the production of molds using agarose.

Finally, they set up an automated video optical recording system that can also keep EHTs in the optimal condition of temperature and gases. Video optical analysis can be performed with a customized software based on figure recognition of the contracting muscle strip at top and bottom ends in a fully automated manner. Based on post geometry (diameter, length), elastic modulus of the silicone type used and

delta of post distance (post deflection), they were able to calculate values for frequency, average force, fractional shortening, contraction – and relaxation time of the engineered tissue (Hansen, Eder et al. 2010).

1.6. Recent advances in engineered cardiac tissues

Since the introduction of the first engineered heart tissue, more than two decades ago, the recent possibility of developing spheroids, organoids, and heart-on-a-chip models based on iPSCs derived cardiomyocytes incorporating the latest available technologies and materials, has extended the role of in vitro cardiac engineering to study cardiac development, homeostasis, regeneration, and diseases. The major limitation is, however, the very low degree of maturation of hiPSC-derived engineered cardiac tissues and efforts have been made to overcome this issue. Chronic mechanical stimulus induced by stretching or electrical stimulation has been shown to play key roles in inducing further maturation of cells and engineered tissues {Lu, 2021 #4213} {Tsui, 2021 #4212}{Hirt, 2014 #3644} {Abilez, 2018 #4176}{Ruan, 2016 #4215}. Recently, Bouchard and collaborators developed a protocol to easily generate cardiac tissues with electrophysiological activity, cell structure, and mechanical activity closer to those seen in the adult myocardium by subjecting the engineered tissues to electrically-induced biomimetic cues, applied at an increasing intensity {Ronaldson-Bouchard, 2019 #4211}. While the protocol still does not fully recapitulate the electromechanical properties of human adult myocardium, physical conditioning was necessary for modeling physiological responses to drugs and pathological hypertrophy. On the other hand, improvements of cardiomyocyte differentiation have been also achieved with several mechanical exogenous stimulation without electrical stimulation, including: an elastic support that provides resistance against each contraction{Boudou, 2012 #4216}{Hansen, 2010 #3932}, deformable elastic suspensions {Godier-Furnemont, 2015 #4217}{Zimmermann, 2006 #3401}, and mechanical stretching devices {Abilez, 2018 #4176}. For instance, Jackman et al. developed a system using laser-cut porous polymer frames to generate dynamic, free-floating culture conditions for engineering “cardiobundles”, 3-dimensional cylindrical tissues made from neonatal

rat cardiomyocytes or human pluripotent stem cell-derived cardiomyocytes (hPSC-CMs) embedded in fibrin-based hydrogel. In contrast to traditional static culture of hydrogel-based engineered heart tissues, this method relies on the application of free-floating dynamic culture conditions that lead to upregulation of mTORC1 signaling and robust structural and functional improvements associated with increased cardiomyocyte density, hypertrophy, and maturation {Jackman, 2016 #4218}.

A wide variety of tissue models have been designed in various geometries and formats over the past two decades {Weinberger, 2017 #4219}. Examples introduced in recent years include intensity-trained, hanging two-post mini EHT systems {Ronaldson-Bouchard, 2018 #4177}, cardiac biowires {Zhao, 2019 #4221}, microwires {Thavandiran, 2013 #4222}, patches {Zhang, 2013 #4223}, ring-shaped EHTs {Goldfracht, 2020 #4224}, and chamber-forming ventricle models {MacQueen, 2018 #4225}. With the advance of technologies such as 3D printing and laser-cut biomaterials, the design of engineered tissues has changed leading to systems where the microenvironmental architecture of the tissue may be finely controlled {Huebsch, 2016 #4226}{Gao, 2017 #4227}{Borovjagin, 2017 #4228}. Recently, Jayne and collaborators have developed a microfluid platform for engineering cardiac microtissues using direct laser writing lithography and soft lithography which allows the generation of highly-controlled microenvironments {Jayne, 2021 #4229}.

1.7. The importance of 3D in investigating cardiomyocytes proliferation and differentiation

Cardiomyocyte 3D cultures have a lot of advantages when compared to 2D cultures. First, the degree of cardiac differentiation and maturation in 3D models made from neonatal rat cardiac cells is higher and characterized by the following: high degree of sarcomere structure; longitudinal orientation and alignment; formation of M-bands, rod-shaped cardiac myocytes; relatively normal ratio of sarcomeres; mitochondria and nuclei; high degree of binucleation; normal diastolic resting potential of approximately −90 mV; high abundance of sarcomeric and sarcoplasmic

proteins; relatively normal action potential shape; and qualitatively normal physiological and pharmacological responses—such as Frank–Starling-behaviour, force–frequency relationship, and reaction to calcium, isoprenaline, and carbachol (Eschenhagen, Fink et al. 1997, Zimmermann 2002, Hansen, Eder et al. 2010, Tiburcy, Didie et al. 2011). Also, 3D cardiac constructs made from primary cardiac myocytes develop a primitive vascular network without (Zimmermann, Melnychenko et al. 2006), or with the addition of endothelial cells (Sekine, Shimizu et al. 2008, Stevens, Kreutziger et al. 2009). Moreover, fibrin-based Engineering Heart Tissues display benefits compared to the other 3D tissue techniques. Faster solidification of fibrin is associated with more homogeneous and reproducible cell distribution in the initial gel. Changing the format into strip also allowed miniaturization and automation in the 24-well format with minimal non-standardized handling. Video optical evaluation of contractile force supersedes the manual transfer and measurement of EHTs under non-standardized conditions and allows simply repeated measurements of large series. In summary, since the differentiation and the proliferation seem to be the two faces of the same coin, this methodology may be useful not only as a drug screening platform (Eder, Hansen et al. 2014) but also as a powerful tool to better understand cardiomyocytes biology.

2. AIMS OF THE THESIS

Cardiomyocytes in rodents retain the ability to proliferate only in a short window immediately after birth. Indeed, the response to injury during adulthood is the formation of a scar that can compromise cardiac function. Taking advantage of engineered heart tissues (EHTs), a model that was initially developed as a drug screening platform, we further “engineered” EHTs to investigate cardiomyocyte proliferation and maturation response to changes of mechanical loading and upon injury.

Aim1. To test the hypothesis that mechanical loading contributes to regulate cardiomyocytes proliferation and maturation in EHTs.

Mechanical loading plays a fundamental role in cardiomyocyte maturation, however, the mechanism with which cells may sense mechanical cues modulating maturation and proliferation is not fully understood. In our study we investigated the effect of mechanical loading on cardiomyocyte proliferation and maturation using a novel system based on EHT technology where mechanical can be modulated in a feasible and reproducible manner.

Aim2. To test the hypothesis that cryoinjury in mature EHTs, similarly to adult cardiac tissue, does not stimulate cardiomyocyte proliferation.

Myocardial infarction is characterized by necrosis and apoptosis followed by an extensive fibrosis as a result of the healing process. EHTs are composed of unpurified, native heart cells mix, including fibroblast and endothelial cells, organized in a 3D structure, with the potential to reproduce in vitro the response of an adult tissue to an ischemic injury. Using a custom-made model of cryoinjury in EHTs we evaluated the biochemical and proliferative response of cardiomyocytes and fibroblasts to develop a novel model aimed to study post-injury biology in a controlled manner.

3. MATERIALS AND METHODS

3.1. Neonatal rat cardiomyocytes isolation

Hearts from 10 to 15 neonatal Wistar rats (postnatal day 0 to 3) were minced and subjected to serial DNase/Trypsin digestion to release single cells. Cell fractions were collected in Fetal Calf Serum (FCS) (Thermo Fisher 26140-079) and kept on ice. Collected cells were centrifuged, filtered using 100 µm cell strainer and resuspended in culture medium consisting of DMEM (Biochrom F0415), heat inactivated 10% Fetal Calf Serum (Thermo Fisher 26140-079), 1% penicillin/streptomycin (Thermo Fisher 15140-122) and 1% L-Glutamine (200 mM Gibco).

3.2. Generation of fibrin-based EHTs

To generate fibrin-based EHTs a reconstitution mixture was prepared on ice as follow: (final concentration): $4.1\text{^}10^6$ cells/mL, 5 mg/mL bovine fibrinogen (Sigma F8630), DMEM 2X (20% DMEM 10x, 20% heat inactivated horse serum [Thermo Fisher 26050-088], 1% penicillin/streptomycin [Thermo Fisher 15140-122]). Casting molds were prepared by adding 1.5 mL 2% agarose in PBS (Invitrogen 15510-027) per well in 24-well culture dishes and placing Teflon spacers inside. After agarose jellification, the spacers were removed (LxWxD 12 x 3 x 4 mm) and silicone post racks were placed onto the dishes with pairs of posts reaching into each casting mold. For each EHT 100 µL reconstitution mix was mixed briefly with 3 µL thrombin (100 U/mL, Sigma Aldrich T7513) and pipetted into the agarose slot. For fibrinogen polymerization, the constructs were placed in a humidified cell culture incubator at 37°C, 7% CO_2 for 2 hours. To ease removal of the constructs from agarose casting molds, cell culture medium (300 µL) was then added in each well. Racks were transferred to new 24-well cell culture dishes. EHTs were maintained in 37°C, 7% CO_2 humidified cell culture incubator. Media was changed on Mondays, Wednesdays and Fridays. EHT medium consisted of DMEM (Biochrom F0415),

10% horse serum (Thermo Fisher 26050-088), 1% penicillin/streptomycin (Thermo Fisher 15140-122), insulin (10 µg/mL, Sigma-Aldrich I9278), and aprotinin (33 µg/mL, Sigma Aldrich A1153). EHTs were visually expected every day and are considered mature approximately 10 days after the development of coherent beating.

3.3. Immunohistochemistry and Immunofluorescent Analysis

EHTs were fixed with 4% paraformaldehyde for 24 hours and paraffin embedded**.** Four-µm thick tissue sections were de-waxed and rehydrated and processed for immunofluorescence or immunohistochemistry. Antigen retrieval was performed by boiling sections in 10 mM Tris base, 1 mM EDTA solution and 0.05% Tween 20 at pH 9.0 for 20 minutes and left at room temperature for 2 hours. Sections were rinsed three times in water and permeabilized 20 minutes in 0.25% Triton X-100 in PBS. For BrdU detection, DNA denaturation was performed by incubating section for 15 minutes in 0.1% Trypsin with 0.05% $CaCl_2$, then in 2M HCl for 30 minutes at room temperature and finally the reaction was stopped with 0.1 M of NaBorate solution. For EdU detection, slices were processed using the Click-IT EdU 594 Imaging kit (Life Technologies) to reveal EdU incorporation, according to the manufacturer's instructions, and counterstained with Hoechst 33342 (Life Technologies). EHT sections were stained overnight at 4°C with a combination of these antibody: anti-cardiac troponin I antibody (ab47003), anti-cardiac troponin T antibody (ab8295), anti-BrdU (ab6323), anti-phospho-Histone H3 (Ser10) antibody (06-570), anti- Ki67 antibody (ab15580) and anti-collagen I (ab34710). Cross-sectional area of EHT CMs was performed by immunohistochemistry using an anti- dystrophin antibody (ab15277) and VECTASTAIN ABC Kit (PK-6100) and ImmPACT DAB (SK-4105). Counterstaining was performed with hematoxylin. The minimum threshold for cross-sectional area was set at 40 μm^2 as previously described (Hirt, Sorensen et al. 2012), and all dystrophin positive cells per 3 section for each EHT were analyzed.

3.4. Gene expression analysis

Total RNA was isolated using TRIzol (Invitrogen). Mechanical sample homogenization was achieved using “Lysing Matrix D” (MPBio), for two 30 seconds cycles (6500 speed units) using a MagNA Lyser (Roche). Between cycles, samples were chilled in ice, and after homogenization, samples were always kept on ice unless stated otherwise. Supernatant was separated from tissue debris and phenol/chloroform extraction was performed. DNase/RNase free water was used to resuspend pellet and stored at -80°C. RNA concentration and quality was evaluated using Nanodrop 1000 Spectrophotometer (Thermo Fisher Scientific) and agarose gel electrophoresis. Reverse transcription was performed using the High-Capacity cDNA Reverse Transcription kit (Applied Biosystems) using random primers. Diluted cDNAs were used for quantitative assessment of RNA expression of selected genes using a BioRad CFX96 Touch™ Real-Time PCR Detection System. Results were normalized by the expression of housekeeping genes. TaqMan (Applied Biosystem) system was used to quantify levels of gene expression using TaqMan probes listed in table 1 and following manufacturer’s instruction. For each experimental condition, at least three biological replicates and two technical replicates were used. Fold change between control and treated samples was identified with $2^{-\Delta\Delta CT}$ method.

Name	Gene	TaqMan code
Alpha smooth muscle actin	Acta2	Rn01759928_g1
Alpha-actinin-1	Actn1	Rn00667357_m1
Chemokine (C-C motif) ligand 2	CCL2	Rn00580555_m1
Collagen type I	Col1a1	Rn01463848_m1
Fibronectin	Fn1	Rn00569575_m1
Interleukin 1 Beta	Il1-β	Rn00580432_m1
Matrix metalloproteinase-12	Mmp12	Rn00588640_m1
Matrix metalloproteinase-2	Mmp2	Rn01538170_m1

ATPase Sarcoplasmic/Endoplasmic Reticulum Ca^{2+}	Atp2a2	Rn00568762_m1
Sodium-calcium exchanger	SLC8A1	Rn04338914_m1
TIMP metallopeptidase inhibitor 1	Timp1	Rn01430873_g1
Myosin heavy chain 6	Myh6	Rn00568304_m1
Myosin heavy chain 7	Myh7	Rn01488777_g1
Glyceraldehyde 3-phosphate dehydrogenase	GAPDH	Rn01775763_g1

3.5. Video optical recording and analysis

EHTs contraction was recorded with an Andor Neo sCMOS camera integrated in Nikon eclipse T1 using a Plan UW 1X objective that can perform live imaging using a dedicated humidified incubator at 37°C, 7% CO_2. Recording was performed for 10 seconds at 100 frames per second. For spontaneous beating measurements, EHTs were recorded in the moment of maximum frequency contraction (burst), intrinsic feature of rat cardiomyocytes. For stimulated contraction measurements, EHTs were electrical stimulated as previous describe (Hansen, Eder et al. 2010) at 4 Hz using a Hugo Sachs Elektronik Stimulator c type 224.

Based on post geometry, elastic modulus of Sylgard 184 (2.6 kPa) and delta of post distance (post deflection) force was calculated according to a published equation (Vandenburgh, Shansky et al. 2008). For a post of radius R and length L, cast from material with a known elastic modulus (E), the moment of inertia (I) is given by $I=\frac{1}{4}R^4$ and force based on post deflection δ by the formula:

$$F = \frac{3EI\delta}{L^3} = \frac{3\pi ER^4\delta}{4L^3} = \mu N$$

3.6. Mechanical unloading and increased afterload in EHTs

EHTs are 6 mm long engineered tissue anchored to 2 elastic silicone Sylgard 184 posts with a known Young modulus (2.6 kPa). The resistance offered by the posts allows linear cardiomyocyte orientation and leads to an increase in cell maturation, as previously described. Mechanical unloading was achieved either by physically detaching one of the EHT extremities using a blade (irreversible unloading) or by reducing the distance between the two posts using a bended steel wire (reversible unloading). Increased afterload was achieved by inserting a 36G metal needle inside each silicone post before casting of EHTs.

3.7. Adjustable mechanical loading system

A standard silicone post rack (EHT technology) was modified by introducing a 30G needle (meso-relle) on the side of each single silicone post. The needle was bent to form a hook near the anchoring area of the silicone post (Fig. 7). Needles can be moved up and down to fit in the well and match exactly the silicone post anchoring. The hook shape was selected among other shapes because of its ability to overcome the spontaneous reduction of EHT length which naturally occurs during development due to the presence of fibroblasts. The hook system allows a resting position where the loading is achieved by the resistance offered by the silicone post (standard loading); an unloading position where the convex side of the hook can be rotated against the posts thus reducing the distance between the two extremities of the EHTs; an increased afterload position where the concave side of the hook can be rotated around the post to increase loading.

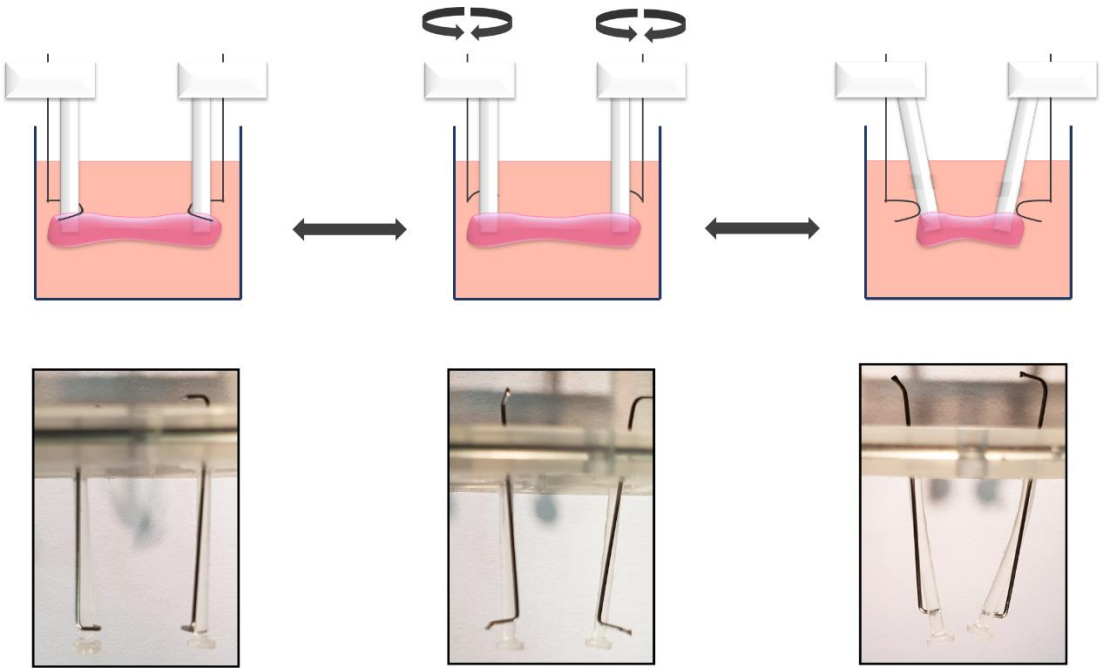

Figure 7. Schematic representation of the adjustable mechanical loading system. EHTs in the three possible custom configurations (top), and how needle displace silicone posts (bottom).

3.8. Cryoinjury

We built a custom-made system to deliver cryoinjury to the middle section of EHTs. Briefly, a 50 ml tube was connected through a copper pipe to a 23G or a 26G needle that was bent to facilitate the contact with the EHTs in a discrete fashion. The tube was filled with liquid nitrogen and the lid was used to direct the flow through the needle, thus creating a cryo-probe. The EHT was placed in contact with the needle, while the liquid nitrogen was flowing, for 1 or 4 seconds and a clear area of freezing could be observed. The removal of the plunger would determine a stop of the flow through the needle and a rise in temperature that allows to safely detach the EHT. After the procedure, EHTs were placed in complete medium to recover.

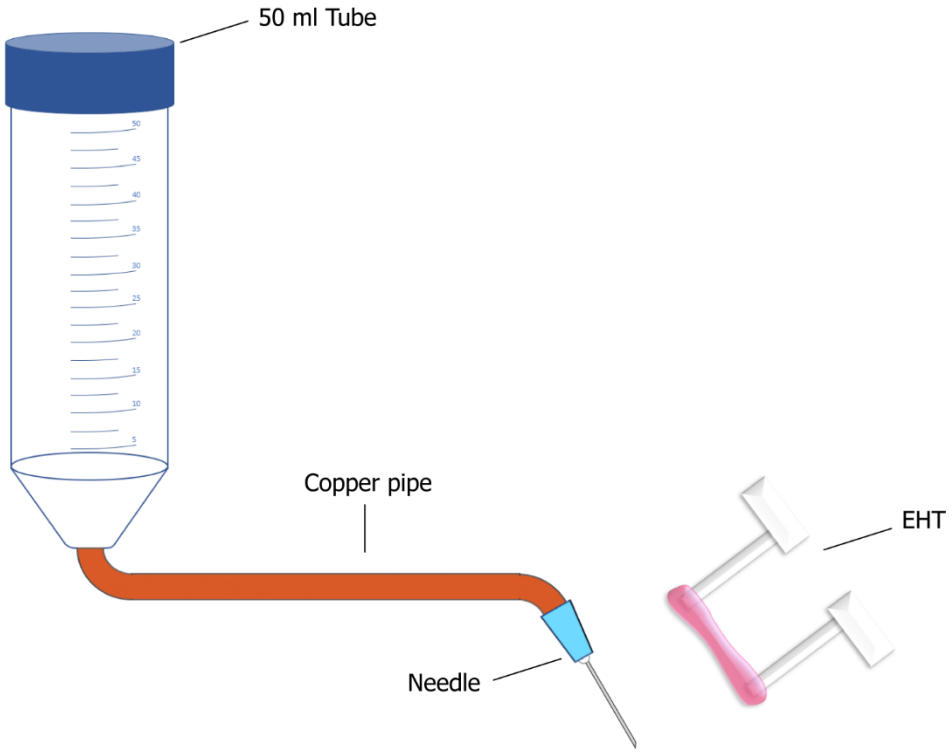

Figure 8. Schematic representation of cryoinjury. A 50mL tube was filled with liquid nitrogen. A needle was bent to facilitate the contact with EHTs.

3.9. MuDy video analysis

EHTs contraction was record as previously described and it was analyzed by MuDy software. The software analyses the tissue deformation required to identify the tissue motion from a sequence of two-dimensional images (B-mode). To this aim, a region of interest was manually drawn on the image in the frame corresponding to the initial, undeformed rest state. Tracking is performed by estimating the displacements (δx, δy) along the two Cartesian directions respectively, that minimize the square error E

$$E = \sum \left(\frac{\delta B}{\delta t} + \delta_x \frac{\delta B}{\delta x} + \delta_y \frac{\delta B}{\delta y} \right); (i)$$

of the advection equation for the brightness B of the ultrasound image. Time derivative indicates the difference between two consecutive frames and the spatial

derivatives are averaged between the same frames. The summation in (i) is computed over a square window centered at the interrogating points and the minimization of (i) leads to a linear system where the unknown are the frame-by-frame displacements δx, δy . The analysis is performed in three steps using a so-called coarse-to fine approach, reducing the window size from 32x32 to 16x16 to 8x8; the position of the interrogation point is continuously updated with the displacements integrated on the previous frames to end up with the tracking of the tissue points. The moving tissue, obtained from 2D tissue tracking, is eventually described by the coordinates of its moving points X (s1, s2, t), being the vector X=[X, Y]. The parametric coordinates s1 and s2 coincide with Cartesian coordinates at the undeformed (initial) condition and then identify the material points following the tissue motion during the deformation (Lagrangian, or material, coordinates). The 2D velocity vector of the tissue is defined at every point as the time derivative of the position vector V(s1 ,s2 ,t)=dX/dt. (Busato, Balconi et al. 2015).

3.10. Statistical analysis

All the results are expressed as mean ± standard deviation (SD) or standard error of the mean (SEM). Student's T-test, one-way ANOVA or two-way ANOVA tests were calculated using GraphPad Prism 6 (GraphPad Software, La Jolla California USA). Student's T-test was used to compare two groups, one-way ANOVA followed by Bonferroni's multiple comparison was used to compare multiple sample groups with one control, two-way ANOVA was used to compare multiple measurements of distinct sample groups. Statistical significance against control treatment was highlighted with "*" symbols as listed in the table below.

Statistical significance	Symbol
P > 0.05	None
P ≤ 0.05	*
P ≤ 0.01	**

$P \leq 0.001$	***

4. RESULTS

4.1. Cardiomyocyte DNA synthesis decreases during EHT development and is associated with an increase of binucleated cells

Regulation of mechanical load in bi-dimensional cultures of CMs can be achieved in different ways (Salameh, Wustmann et al. 2010, Rysa, Tokola et al. 2018, Kreutzer, Viehrig et al. 2019), however, the poor degree of CM maturation that can be reached in a culture dish together with the lack of a tridimensional structure represent a major limitation to performing mechanotransduction studies. In our research, we have taken advantage of engineered heart tissues (EHTs) which were initially developed as a drug screening platform (Hansen, Eder et al. 2010). EHTs are 3D cultures of unpurified cardiac cells that display many advantages when compared to 2D cultures, including a higher degree of maturation, possibility of long-term studies, low basal proliferation rate and contractile function analysis (Hansen, Eder et al. 2010, Hirt, Hansen et al. 2014). EHTs are cast in agarose molds and, by being anchored to two silicone posts, cardiomyocytes within the engineered tissue acquire a rod-shaped structure, a functional syncytium and develop a contractile phenotype that is linear and oriented along the major axis of the tissue. Because of this configuration, mechanical load on cardiomyocytes can be varied efficiently. In order to validate EHTs as a model to evaluate cardiomyocyte proliferation, we performed an initial study to determine the proliferative profile during EHTs development, which generally takes two weeks to be completed. We generated EHTs using neonatal rat heart cells and subjected them to a 48h pulse of BrdU at different time points between casting and 28 days post-casting. As shown in Fig.9A, we observed that after an initial increase in the percentage of $BrdU^+$ CMs early after EHT casting, CMs DNA synthesis progressively decreased becoming negligible at day 28 reaching a basal of 2% of $BrdU^+$ CMs. Interestingly, the decrease of $BrdU^+$ CMs was accompanied by a progressive increase of binucleated cardiomyocytes which goes

from 0% in the very early phase to almost 20% binucleated cells in the latest phase of development. During the early stage of EHT remodeling CMs beat independently due to the lack of functional syncytium thus the displacement of the silicone posts is not detectable. Approximately between day 8 and 10, CMs develop a functional syncytium leading to spontaneous and coherent beating of the whole EHT. Silicone post displacement can be measured determining the force of contraction. As expected, contractile force increases during tissue maturation reaching a plateau around day 22. Interestingly, the increase of binucleated CMs and the drop of DNA synthesis correspond to the beginning of a coherent and spontaneous contractile activity of EHTs, occurring around day 10, and suggesting that the increasing force of contraction required may represent the trigger to switch from a pro-proliferative state to a mature phenotype.

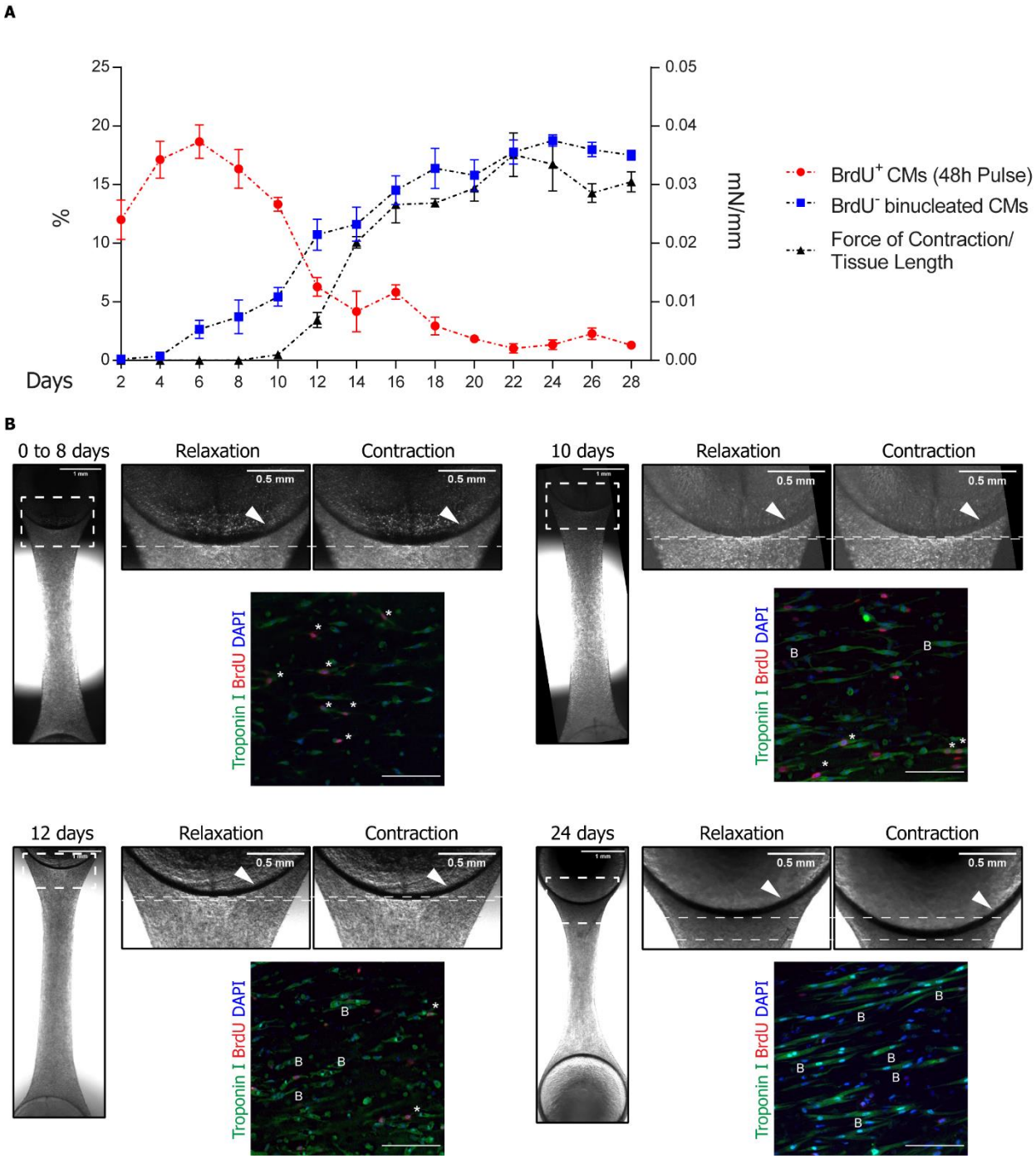

Figure 9. CM proliferation and maturation during EHT development. (A) rEHT were generated and subjected to 48h pulse of BrdU at different time points between casting and 28 days post-casting. Force of contraction was measured (black arrow) every other day and was standardized on the tissue length to overcome the tissue shortening that occurs in long term experiments. At each time point EHTs underwent histological analysis and frequency of BrdU positive CMs (red circle) and

binucleated CMs (blue square) was measured. **(B)** Representative images of EHTs at four progressive timepoints of their development showing maximum (contraction) and minimum (relaxation) displacement of silicone posts (white arrow) with the corresponding histological section stained for nuclei (Blue), troponin I (Green) and BrdU (Red)(Scale bar: 100µm). $BrdU^+$CMs and binucleated CMs are indicated respectively with white star (*) and white B.

4.2. Mechanical unloading in EHTs induces an increase in EdU^+ Cardiomyocytes

Cardiomyocytes in engineered tissue generate a force that counteracts the elastic resistance of silicone posts favoring cell maturation and proper orientation (Hansen, Eder et al. 2010). Indeed, it has been widely demonstrated that the construction of 3D self-assembly of a single cardiac muscle strand around microfabricated anchor points leads to an improvement of cardiac cell maturation (Stein, Mummery et al. 2020). We hypothesize that changes in mechanical load translate into remodeling of the sarcomeric cytoskeleton thus favoring cardiomyocytes proliferation. The mechanical load at which CMs are subjected may be modulated by modifying the physical and structural proprieties of the silicone posts (Hirt, Sorensen et al. 2012). To test the hypothesis that mechanical loading can regulate CM proliferation, we modified mature EHTs to perform irreversible and reversible unloading by detaching one extremity of the tissue from the post or by reducing the distance between the silicone posts with a metal wire. In this case (reversible unloading) contracting CMs are subjected only to the resistance offered by the fibrin matrix (Fig. 10A). In both cases mechanical unloading was performed for 72h supplementing the medium with EdU as marker of DNA synthesis. We detected 1.98 ± 0.12 % of EdU^+ CMs in the control EHTs which significantly increases to 6.85 ± 0.35% and 6.52 ± 0.74% EdU^+ CMs after irreversible and reversible unloading respectively suggesting that unloading induces DNA synthesis in CMs (Fig. 10B).

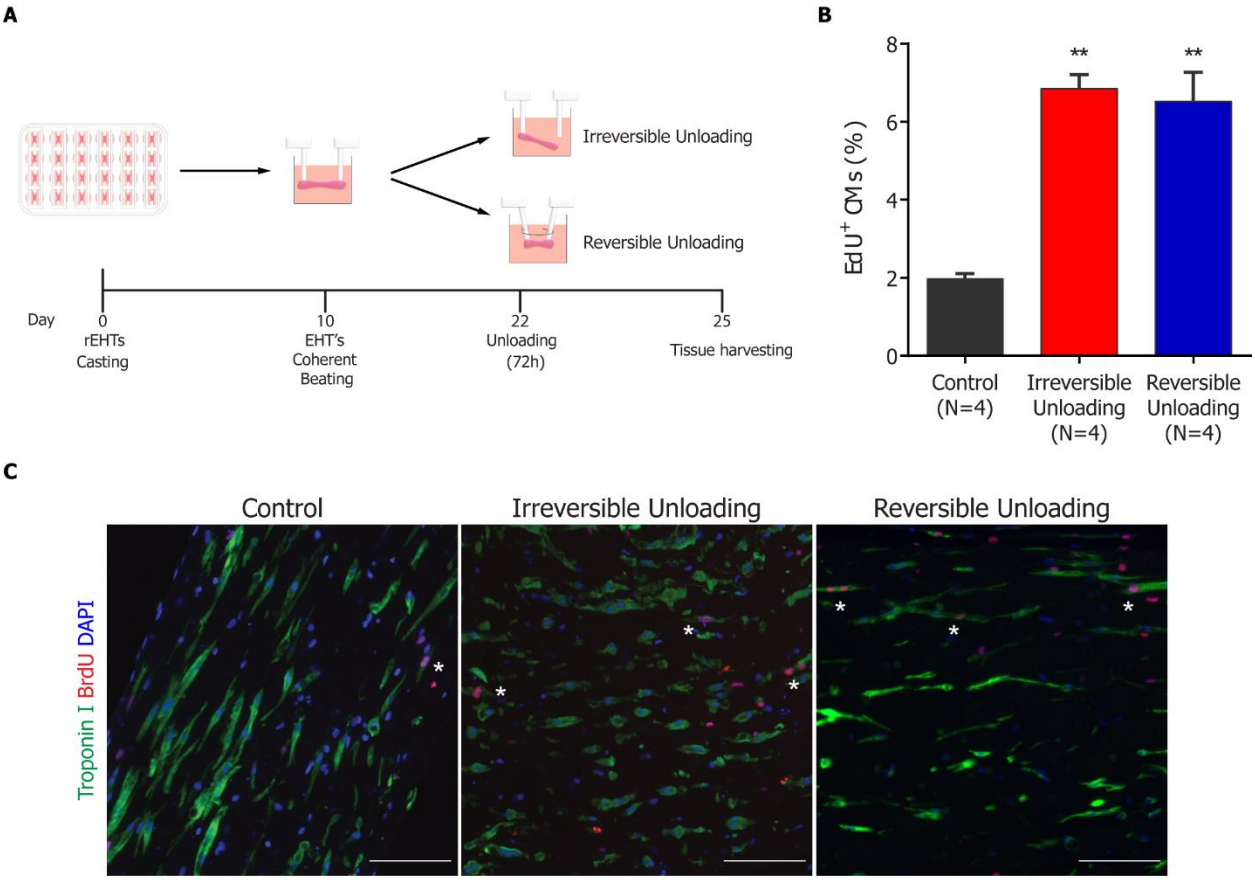

Figure 10. Mechanical unloading in EHTs induces a significant increase in EdU⁺ Cardiomyocytes. (A) Schematic representation of the experimental timeline and the methods used to induce mechanical unload. **(B)** Percentage of EdU⁺ CMs in the three groups (Data shown as mean ± SD). **(C)** Representative images of EHTs with merged immunofluorescence staining for nuclei (Blue), troponin I (Green) and EdU (Red)(Scale bar: 100µm). EdU⁺CMs are highlighted with white star.

4.3. EHT unloading reduces the expression of genes associated with mature cardiomyocyte phenotype

We next sought to test whether mechanical unloading was associated with a more immature gene expression profile. Increasing mechanical loading with chronic electrical stimulation (Lasher, Pahnke et al. 2012), (Hirt, Boeddinghaus et al. 2014) or with an increase of the young modulus of the anchoring supports (Hirt, Sorensen et al. 2012) leads to an improvement of cardiomyocytes maturation in EHTs. On the other hand, it is unclear whether the reduction of mechanical loading in mature

cardiomyocytes may be able to reverse the mature phenotype. We performed gene expression analysis of some known markers for cardiac maturation (Guo and Pu 2020) after irreversible unloading of mature EHTs and compared to the loaded control. Mechanical unloading was performed in mature EHTs and total RNA was isolated at 24 and 72 hours. As shown in Figure 11, the ratio between α- and β-myosin heavy chain (myh6/myh7) gene expression levels decrease significantly after 72 hours of unloading. The alpha isoform in rats is prevalent in adult cardiomyocytes while the beta isoform is associated to a more immature phenotype (McNally, Kraft et al. 1989). We also evaluated mRNA levels of α-actinin, SR Ca^{2+} ATPase 2 (SERCA2a) and Na^{+}/Ca^{2+} exchanger (NCX) at 24 and 72 hours from the unloading. mRNA levels of actinin, SERCA2a and NCX significantly decreased in the unloaded group after 24h compared to the control group (Fig. 11). We speculate that the small difference in mRNA levels of these markers between control and unloaded EHTs may be due to the already immature phenotype of the CM in the engineered tissue. The increase in CMs DNA synthesis together with the reduction of the expression of genes associated with CM maturation, suggests that mechanical unloading is associated to a more immature phenotype.

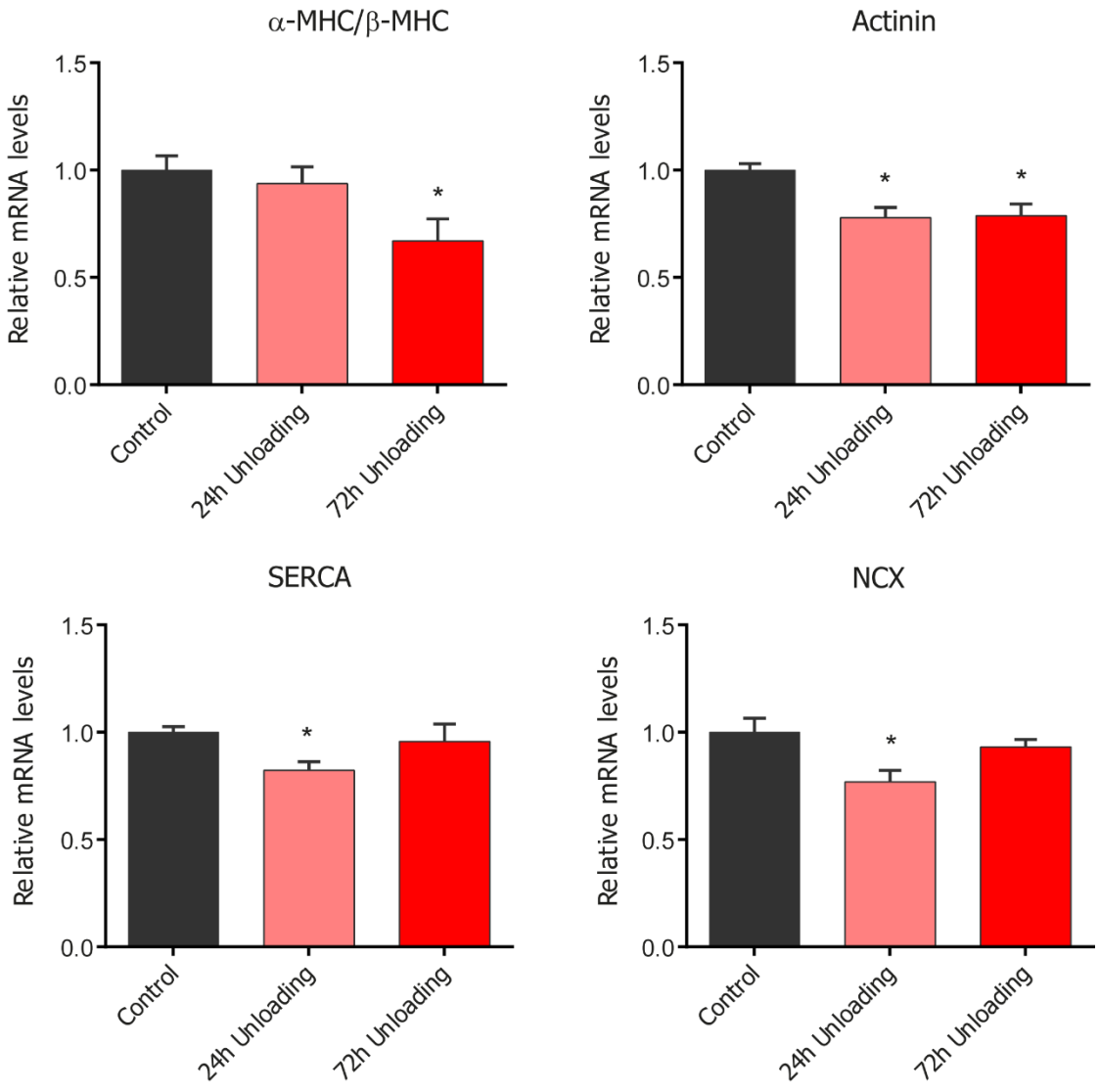

Figure 11. Quantitative RT PCR of EHTs after 24 and 72 hours of mechanical unloading. Relative mRNA levels α- and β-myosin heavy chain, α-actinin, $SRCa^{2+}$ ATPase 2 (SERCA2a) and Na^{+}/Ca^{2+} exchanger (NCX) over GAPDH in EHTs after mechanical unloading (n=4 per group). (Data shown as mean ± SEM).

4.4. Increasing afterload in EHTs leads to a trend toward reduced CMs DNA synthesis and a more organized sarcomeric structure.

Our data indicate that mechanical unloading in EHTs is associated to a significant increase of DNA synthesis in CMs and a more immature gene expression profile. We hypothesize that mechanical loading in our system may represent an important regulator of CMs proliferation/maturation thus we next sought to test whether an increase of loading in EHTs translates into reduced cardiomyocyte DNA synthesis and increased maturation. As shown in Figure 12A, a 36G metal needle was introduced inside every single silicone post to increase afterload. EHTs were randomized and cast to standard loading and increased afterload (IA) conditions. When EHTs reached maturation, both groups were furtherly randomized to 72 hours of unloading (standard loading and irreversible unloading, increased afterload and unload after IA) supplementing medium with EdU. As shown in Figure 12B, IA was associated to a trend toward reduced CMs DNA synthesis (p 0.1881). As shown before, unloading induced a significant increase in EdU+ CMs when compared to standard loading conditions. Interestingly, IA EHTs that were unloaded for 72 hours showed a further significant increase of EdU incorporation when compared to the unloading group. We speculate that IA may have increased the number of “mature” CMs when compared to standard loading and thus explaining the higher number of CMs incorporating EdU after unloading.

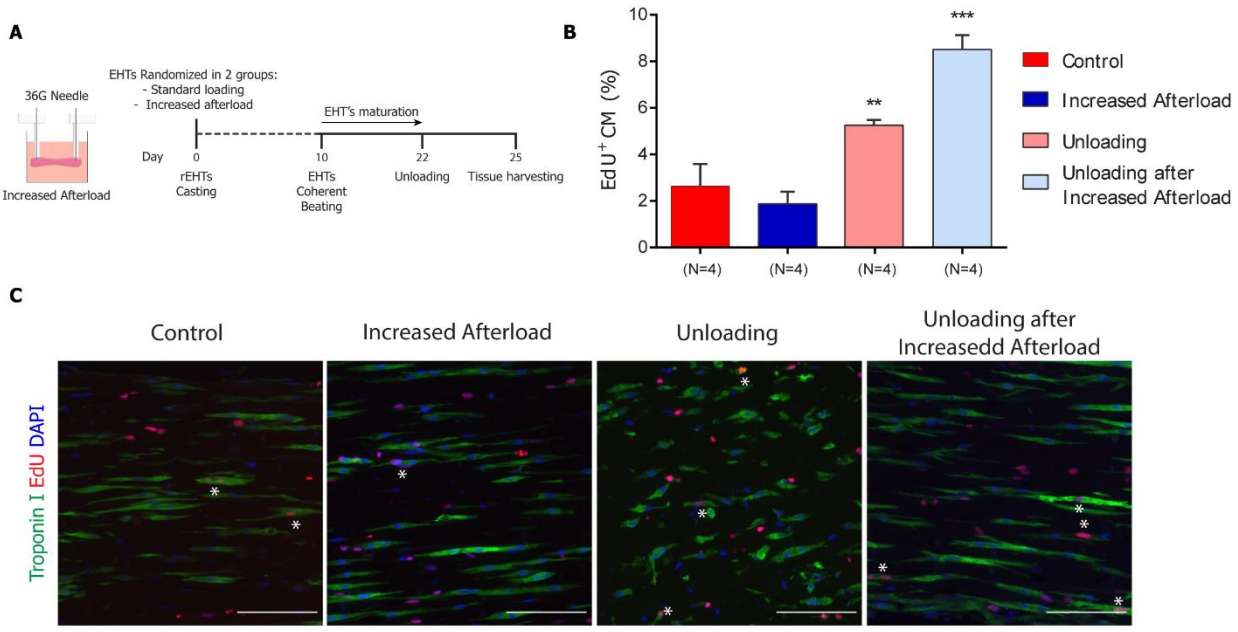

Figure 12. Increased Afterload (IA) in EHTs reduces CMS DNA synthesis. (A) Schematic representation of the experimental timeline and the modified silicone post with two 36G needles. **(B)** Percentage of EdU⁺CMs in EHTs in different experimental conditions (Data shown as mean ± SD). **(C)** Representative images of EHTs with merged immunofluorescence staining for nuclei (Blue), troponin I (Green) and EdU (Red) (Scale bar: 100µm). EdU⁺CMs are highlighted with white stars.

4.5. Mechanical loading in EHTs regulates CM proliferation and maturation.

In our first set of experiments, we modified EHTs to modulate mechanical loading using a custom-made procedure consisting of either cutting one of the extremities of the post, reducing the distance between the posts with a metal wire, or inserting a needle in the silicone posts. Although these procedures were effective in testing our hypothesis, this technique is time consuming, poorly reproducible and does not allow reversible adjustment of mechanical loading without damaging EHTs. Furthermore, the increase of mechanical loading was only possible at the casting of EHTs since the insertion of a needle in the post would have inevitably damaged the

EHT. For these reasons we developed a new simple and reproducible system that can be adjusted to subject EHTs to standard loading, unloading and increased afterload. We implemented the silicone posts by introducing a hook-shaped bent needle that can be rotated near the suspended tip of the silicone post (Fig. 13A). The hook can be kept in the resting position allowing standard loading; the concave side of the hook can be rotated around the post to increase the load; finally, the hook can produce unloading by rotating its convex side and reduce the distance between the two extremities of the EHTs. We performed an experiment where mature EHTs were subjected for 72 hours to unloading or increased afterload and compared to standard loading conditions. EdU was added to the medium to evaluate DNA synthesis in CMs. As expected, unloading induced a significant increase in EdU+ CMs when compared to control (1.4 ± 0.6% vs. 4.8 ± 0.9%). The increase of afterload for 72 hours did not significantly change the percentage of EdU+ CM when compared to standard loading (Fig. 13B). We next sought to evaluate whether the increase in CM DNA synthesis was translating in cellular division. We measured the percentage of CMs that were positive for known markers of cell proliferation, such as Phospho-Histone H3 (pH3) and Ki67. As shown in Figure 13C and D, unloading was associated to a significant increase of pH3+ CMs and Ki67+ CMs when compared to control (0.7 ± 0.7% vs. 2.5 ± 1.0 % and 0 ± 0 % vs. 1.0 ± 0.2%, respectively) suggesting that mechanical unloading stimulates CMs proliferation. As expected, the increase of loading for 72 hours did not produce any significant change in the rate of proliferating CMs when compared to control. In order to confirm that unloading induces cell division in CM, thus increasing the absolute number of CMs, we are currently quantifying the number of CMs in EHTs cross-sections at different timepoints. Furthermore, since EHTs are made using fibrin matrix that is remodeled during maturation, we investigated whether tissue remodeling occurring after unloading, where the distance between the post is reduced, may influence the mechanical load of the tissues inducing a re-establishment of a standard proliferative status. Mature rEHTs were subjected to mechanical unloading and a 48h pulse of EdU at different time points, from baseline to day 2, day 4 and day 6. After two days, as expected, the percentage of EdU^+ CMs significantly increased from 2.2 ± 0.5%

to 4.4± 1.2% as well as pH3^{+} CMs and Ki67^{+} CMs (respectively from 0.2 ± 0.2% and 0.4 ± 0.1% to 0.9 ± 0.4% and 0.9 ± 0.3%(Fig.13B). In the following time points we observed a progressive reduction of the three markers that at day 6 returned to the basal level suggesting that the biological effect of acute mechanical unloading is lost, possibly because of tissue remodeling.

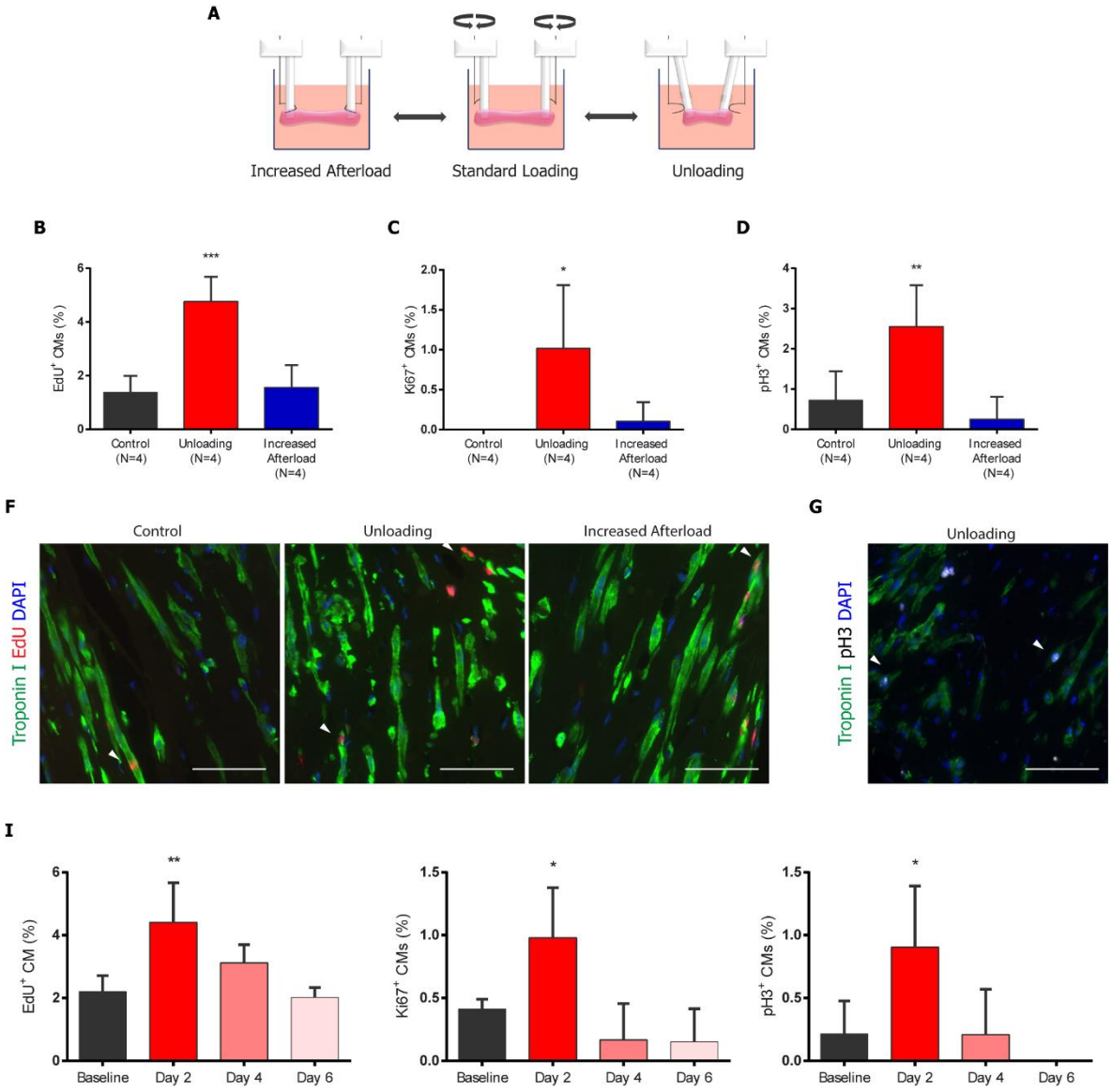

Figure 13. Mechanical unloading with hook-shaped modified posts induces cardiomyocytes proliferation. (A) Schematic representation of the system where silicone posts are modified with two 36G needles bent to form a hook-shape. Percentage of EdU^{+} CMs **(B)**, Ki67^{+}CMs **(C)**, pH3^{+}CMs **(D)** in EHTs after 72h of mechanical unloading or increased afterload (Data shown as mean ± SD).

Representative images with merged immunofluorescence staining for nuclei (Blue), troponin I (Green) and EdU (Red) **(F)** and pH3 (white) **(G)** of EHTs (Scale bar: 100µm). EdU^+CMs and $pH3^+$CMs are highlighted with white arrow. **(I)** Quantification of EdU^+ CMs, $Ki67^+$CMs and $pH3^+$CMs in EHTs 2, 4 and 6 days after unloading (n=4 per group).

In order to investigate whether a prolonged and sustained increase of afterload would translate into a significant reduction of CMs proliferation, mature EHTs were randomized to standard loading and increased afterload for 7 days. EHTs were video recorded to perform functional measurements and formalin fixed for histological analysis. The degree of sarcomeric structure organization may be quantified by measuring cross section of CMs, which is round in EHTs (Hirt, Sorensen et al. 2012). As shown in Figure 14A, CM cross-sectional area was significantly higher in the IA group when compared to control (75.5 ± 11.1 μm^2 vs. 57.7 ± 2.9 μm^2). Furthermore, CMs were more homogeneously distributed within the EHT section suggesting a higher degree of maturation (Fig. 14B) (Hirt, Sorensen et al. 2012). We also sought to evaluate whether this 31% increase in CMs cross-section would produce an increment of force of contraction. The hook was placed in resting position and the spontaneous beating was recorded for 10 seconds. Silicone post displacement was measured and used to calculate the force of contraction as shown before (Hansen, Eder et al. 2010). Sustained increased afterload produced a significant increase in the force of contraction when compared to control (0.1029 ± 0.0075 mN vs. 0.055 ± 0.0075) (Fig. 14C). As shown in Figure 14E, the average force of contraction generate by a single CM in the EHTs is significantly higher in the IA group indicating that the overall increase of force of contraction is due to an increase of sarcomeric strength of cardiomyocytes. Nevertheless, to evaluate the degree of sarcomeric organization after persistent increase afterload we are performing experiments using electron microscopy.

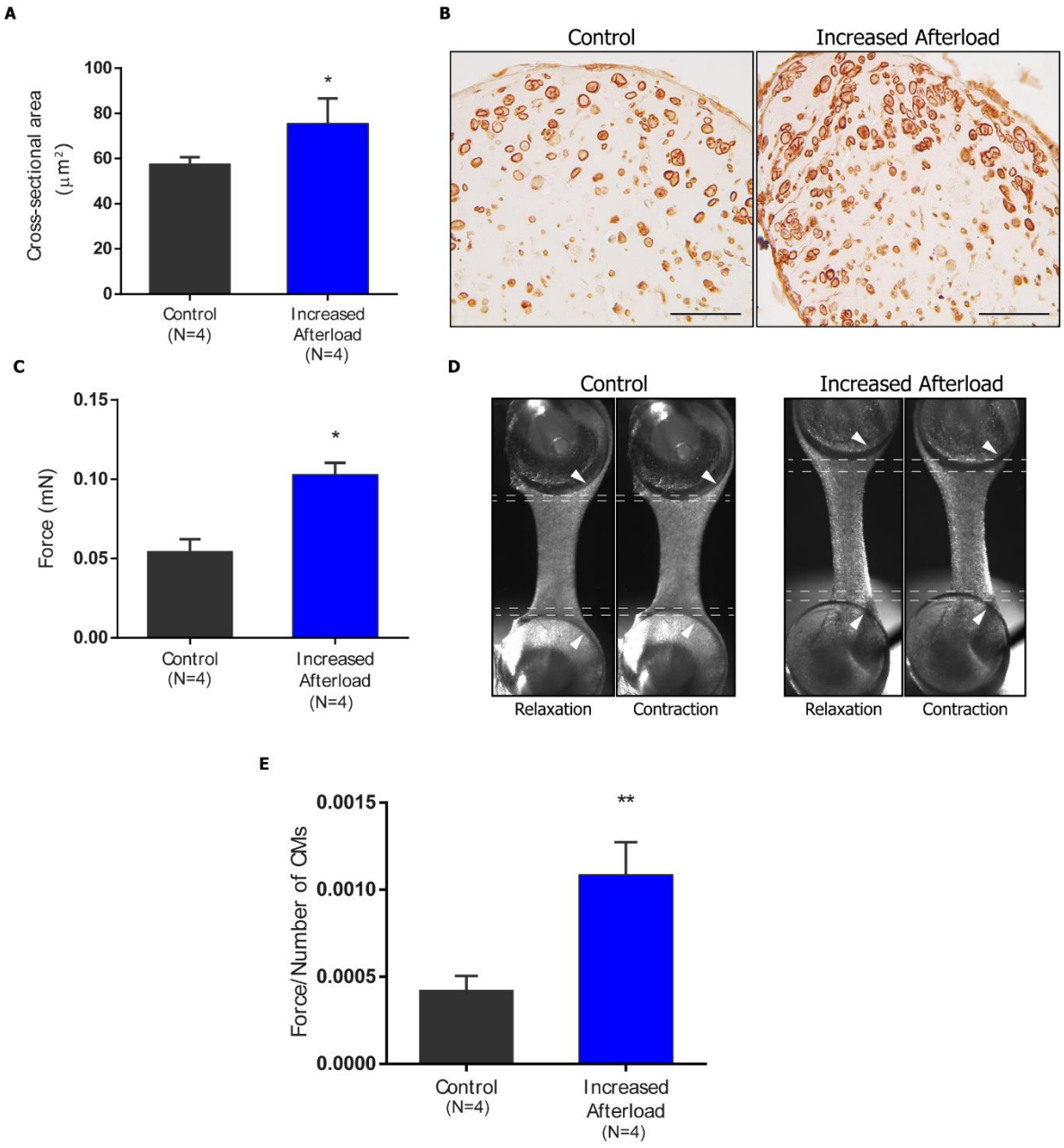

Figure 14. Sustained increased afterload leads to an increase in sarcomeric organization and improvement of contractile force. (A) EHT cross sectional area. **(B)** Representative images of dystrophin-stained cross-sections (Scale bar: 200µm). **(C)** Force generated by EHTs and calculated by measuring silicone posts displacement. **(D)** Representative images of post displacement (white arrow) **(E)** Force generated by the EHTs normalized to the number of total CMs in the cross-section. (Data shown as mean ± SD)

We also evaluated the proliferative profile of EHTs under IA condition by supplementing the medium with EdU 72h before tissue harvesting. As shown in

Figure 15A, EHTs in standard loading condition were characterized by 3.2 ± 0.8 % EdU$^+$CMs, 1.5 ± 0.4 % Ki67$^+$CMs and 1.0 ± 0.9 % pH3$^+$CMs. Interestingly, we observed that 7 days of IA lead to a significant increase of EdU$^+$CMs (4.6 ± 0.1%) but also to a significant decrease of Ki67$^+$CMs (0.6 ± 0.4%) and no significant change of pH3$^+$CMs. We speculate that the high rate of DNA synthesis in cardiomyocytes during mechanical overload may be related to and high increase of binucleation process. Indeed, the percentage of binucleated CMs in the IA group (15.0 ± 3.5%) is significantly higher when compared to the control group (7.4 ± 2.4 % of total CMs) (Fig. 15B). These results taken together suggest the pivotal role of mechanical loading in regulating cardiac maturation and proliferation and the robustness of the hook-shaped modified silicone post as a novel system to modulate it in EHTs.

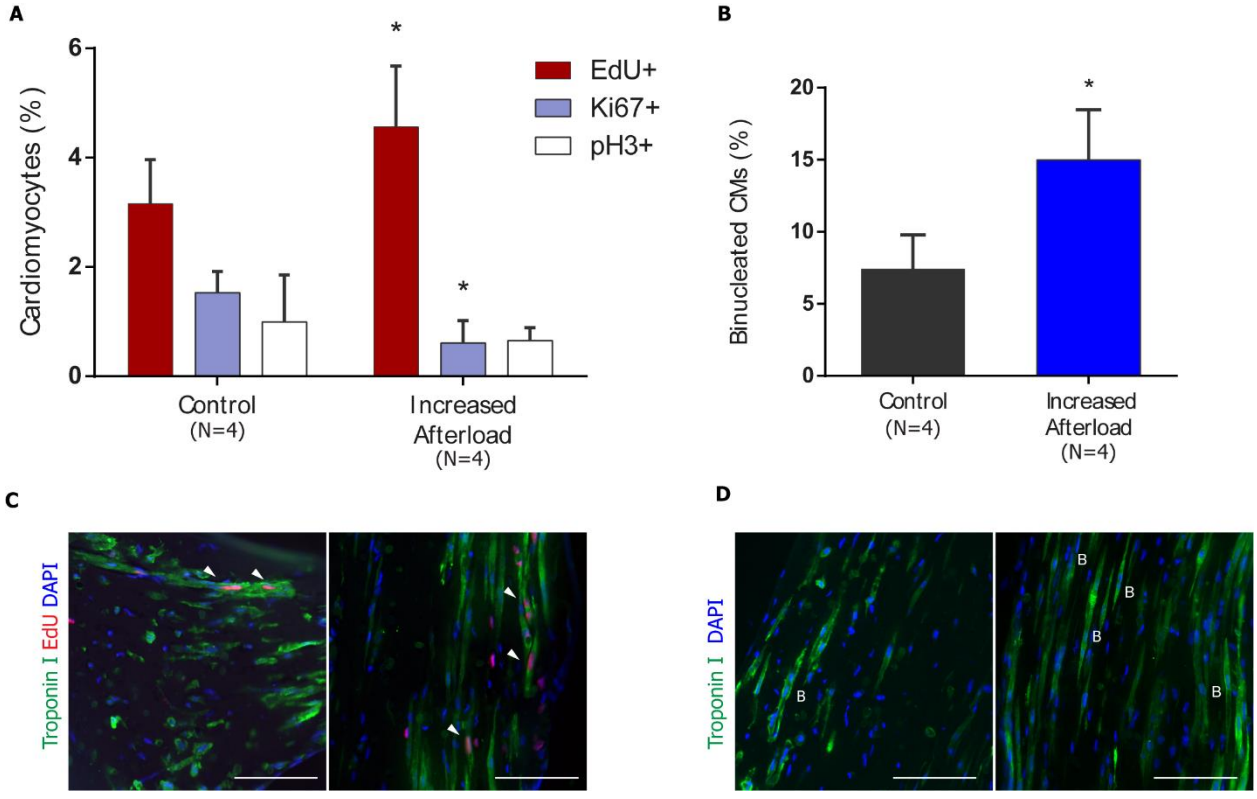

Figure 15. Sustained increased afterload increases CMs binucleation. (A) Quantification of EdU$^+$ CMs, Ki67$^+$CMs and pH3$^+$CMs in EHTs in standard loading and sustained increased afterload (7 days). EdU was added to the medium 72h before tissue harvesting. **(B)** Percentage of binucleated CMs. **(D)** Representative images with merged immunofluorescence staining for nuclei (Blue), troponin I (Green), EdU (Red) and pH3 (white) **(C)** and binucleated CMs **(D)**. (Scale bar: 100µm).

EdU^{+}CMs and binucleated CMs are highlighted with white arrow and white letter B respectively. (Data shown as mean ± SD)

4.6. Cryoinjury interrupts EHTs functional syncytium leading to loss of synchronous contraction

The lack of reliable in vitro tissue-like models to evaluate cardiac regeneration, in particular as a consequence of myocardial injury, represents a major limitation in performing high-throughput studies. Engineered heart tissues are made from unpurified, native heart cell mix, including fibroblast and endothelial cells, organized in an in vivo-like structure (Hansen, Eder et al. 2010, Stoehr, Hirt et al. 2016), recapitulating in part the tissue biology of the adult rodent heart, thus representing an exciting candidate to evaluate the effect of myocardial injury in a controlled manner. Indeed, although EHTs lack the presence of the immune system and an inflammatory infiltrate, major players in the cellular and molecular response after injury, this may be seen as an advantage when dissecting the specific role of CMs. Considering the technical challenge of inducing an infarct-like lesion in an in vitro system, where ischemic stimuli are difficult to apply to a selected area of the EHT, we used cryoinjury to deliver a discrete and reproducible lesion in the middle section of EHTs. As reported previously, the cryoinjury model generates in vivo a necrotic wound to the ventricle of consistent size and shape that resolves into a scar of uniform size, shape, and organization (Polizzotti, Ganapathy et al. 2016). The cryo-model also provides an extended injury border zone that exhibits classic markers of remodeling found in surviving cardiac tissue at the edge of a myocardial infarction (Strungs, Ongstad et al. 2013). We built a custom-made system to deliver cryoinjury to the middle section of EHTs (Fig. 8). Briefly, a 50 ml tube was connected to a 23G needle that was bent to facilitate the contact with the EHTs in a discrete fashion. The tube was filled with liquid nitrogen and the lid was used to direct the flow through the needle, thus creating a cryo-probe. The EHT was placed in contact with the needle, while the liquid nitrogen was flowing, for 4 seconds and a clear area of freezing could

be observed. The removal of the lid would determine a stop of the flow through the needle and a rise in temperature that allows to safely detach the EHT, a process that take an average of 10 seconds. After the procedure, EHTs were placed in complete medium to recover. In our first set of experiments, mature EHTs generated from rat neonatal cardiomyocytes, were randomized in 2 groups (n=6 per group) to receive injury or sham injury (4 seconds contact with the needle without liquid nitrogen).

As previously described, after maturation EHTs start to beat as a functional syncytium and rhythmically deflect the silicone posts. After cryoinjury, we observed a loss of coherent beating in the whole EHT characterized by two areas near each silicone post with contractile activity, which contract independently from each other, and the area between them with no contractile activity (Fig. 16B and D, Grey rectangle). In order to evaluate regional changes of contractile activity within the EHTs, we started a collaboration with Prof. G. Pedrizzetti from the Department of Engineering and Architecture, University of Trieste. We performed video analysis through the MuDy software (Busato, Balconi et al. 2015), a dedicated software utilized for analysis of ultrasound videos, which allows measurements of tissue deformation patterns such as contraction, dilatation, cross-plane, vertical strain, horizontal strain, vertical share, horizontal share, vertical displacement and horizontal displacement. The strain and displacement patterns describe the recorded phenomena analyzing the movement of the point that form the two-dimensional image with respect to two axes, horizontal and vertical. We selected a Region Of Interest (ROI), between the two silicone posts (Fig. 16, colored grids), and measured the vertical strain and displacement by tracking all the points included in the ROI. Subsequently, strain and displacement values were plotted in a graph versus time.

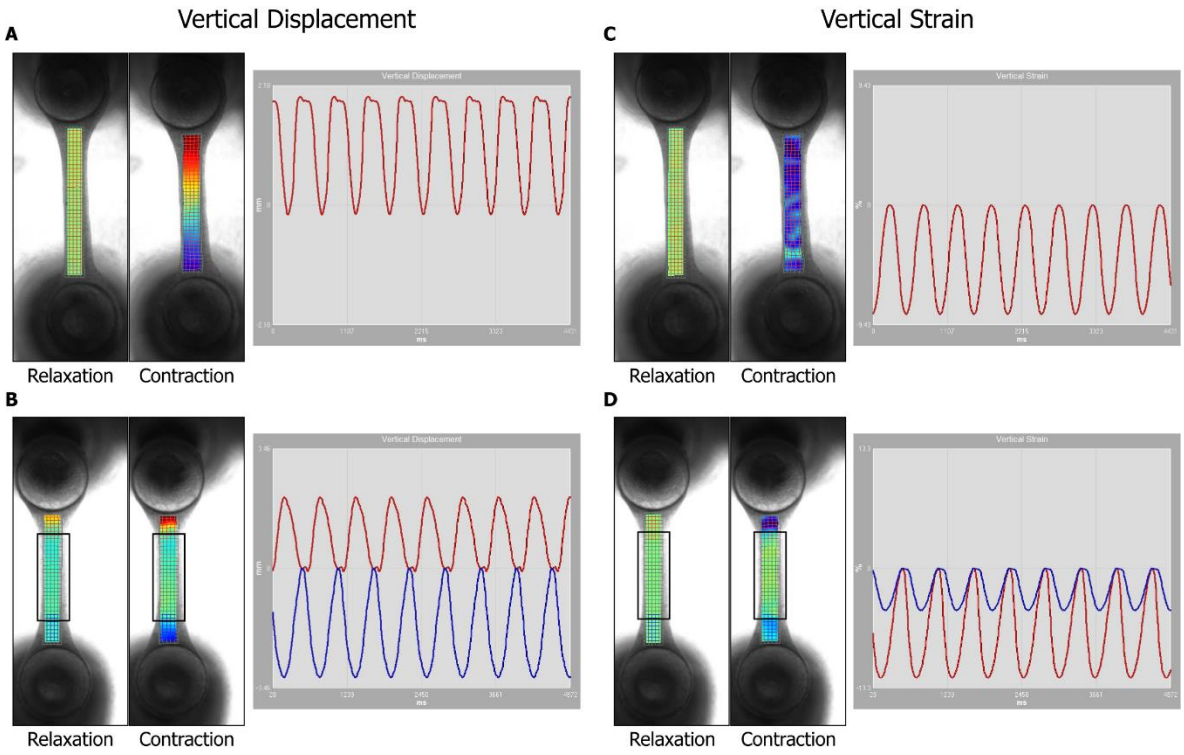

Figure 16. Cryoinjury interrupts the functional syncytium in EHTs. Vertical displacement is determined by the movement of every tracked points along the vertical axis and was measured before **(A)** and after **(B)** cryoinjury and represented as chromatic changes of the ROI and as graph representing changes over time. Vertical strain represents the force applied by every single region of EHT and was measured before **(C)** and after **(D)** cryoinjury and represented as chromatic changes of the ROI and as graph representing changes over time. Healthy EHTs display a coherent displacement and strain that is abolished (grey rectangle) after injury where two independent contractile areas are separated by the electrically and mechanically inert area.

MuDy software confirmed visual evidences showing two distinct regions of contraction with different values of vertical strain and vertical displacement over time compared to healthy EHTs, which exhibit a uniform contractile activity.

4.7. Cryoinjury leads to a reproducible 50% loss of force of contraction that does not recover over time

Although our initial results were promising, our goal was to develop a simple and reproducible model to deliver injury that can in part recapitulate the in vivo scenario

of myocardial infarction. The extent of injury delivered by our custom-made system can be modulated by either the duration of liquid nitrogen flow or by changing the dimension of the needle. We initially evaluated the effect of needle sizing by comparing a 23G needle and a 26G needle to an uninjured control (n=8 per group) and we used the force of contraction as readout. As shown before, cryoinjury was performed in the middle section of mature EHTs closing for 4 seconds the lid of the tube. We performed video analysis before and after 1 and 7 days from the cryoinjury on electrically stimulated (4 Hz) EHTs and recorded for 10 seconds. As shown in Figure 17A, 24h after injury, the force of contraction was significantly impaired for both groups when compared to sham EHTs and this reduction became substantial after 7 days where we observed a decrease from 0.1 to 0.03 mN (-70%) of force of contraction for the 26G needle group and a decrease from 0.09 to 0.04 mN (-55%) for the 23G needle group. Interestingly, our results suggest that a smaller needle may induce more damage to the engineered tissues, likely due to the longer time that is needed to exhausting flowing liquid nitrogen. As previously described, the time that occur from the opening of the lid and the return to not-freezing temperature of the needle takes around 10 seconds with the 23G needle, a period that may last for 14 to 16 seconds with the 26G needle (Data not shown). We decided to use the 23G needle for all our following experiments. We next evaluated the effect of cryo timing on the functional impairment of EHTs and thus we subjected mature rEHT to 23G needle cryoinjury for 1 and 4 seconds (Fig. 17B) and evaluated the force of contraction by video optical analysis. As expected, a longer cryoinjury corresponds to a more extensive impairment of the force of contraction. In particular, while 1 second was associated to reduction of 50% of force of contraction at day 7 (0.11 ± 0.03 mN vs. 0.05 ± 0.04 mN) 4 seconds injury leads to a 63% reduction (0.08 ± 0.02 mN vs. 0.03 ± 0.02 mN). Considering the results of this experiment, we decided that cryoinjury using a 23G needle for 1 second (23G1”) inducing a 50% loss of force of contraction at day 7 was the most appropriate for our studies. We have shown before that cardiomyocytes in EHTs retain a proliferative potential that may contribute to cardiac repair after injury and recover the force of contraction. To test this hypothesis, we subjected mature to 23G1” cryoinjury or sham injury (n=8 per group)

and evaluated the force of contraction at different timepoints. EHTs were video recorded at baseline, 24h and every 3 days after injury until day 11 (Fig. 17C). After video analysis, we observed that the force of contraction was reduced by 50% after cryoinjury and there was no recovery of contractile activity, suggesting that cardiac repair, if present, was not sufficient in our model to restore force of contraction, similarly to the adult mammalian cardiac tissue. This funding was confirmed performing MuDy software analysis of the horizontal strain profile of injured and control EHTs at day 1 and day 7 after cryoinjury (e.g., borderzone) thus evaluating tissue remodeling over time. As shown in Figure 17F, the horizontal strain value in the injured EHT fall to 0% (around 4% at the baseline) in the middle section where the cryoinjury is localized and does not recover at day 7, confirming the inability of the EHTs to regenerate the lost tissue.

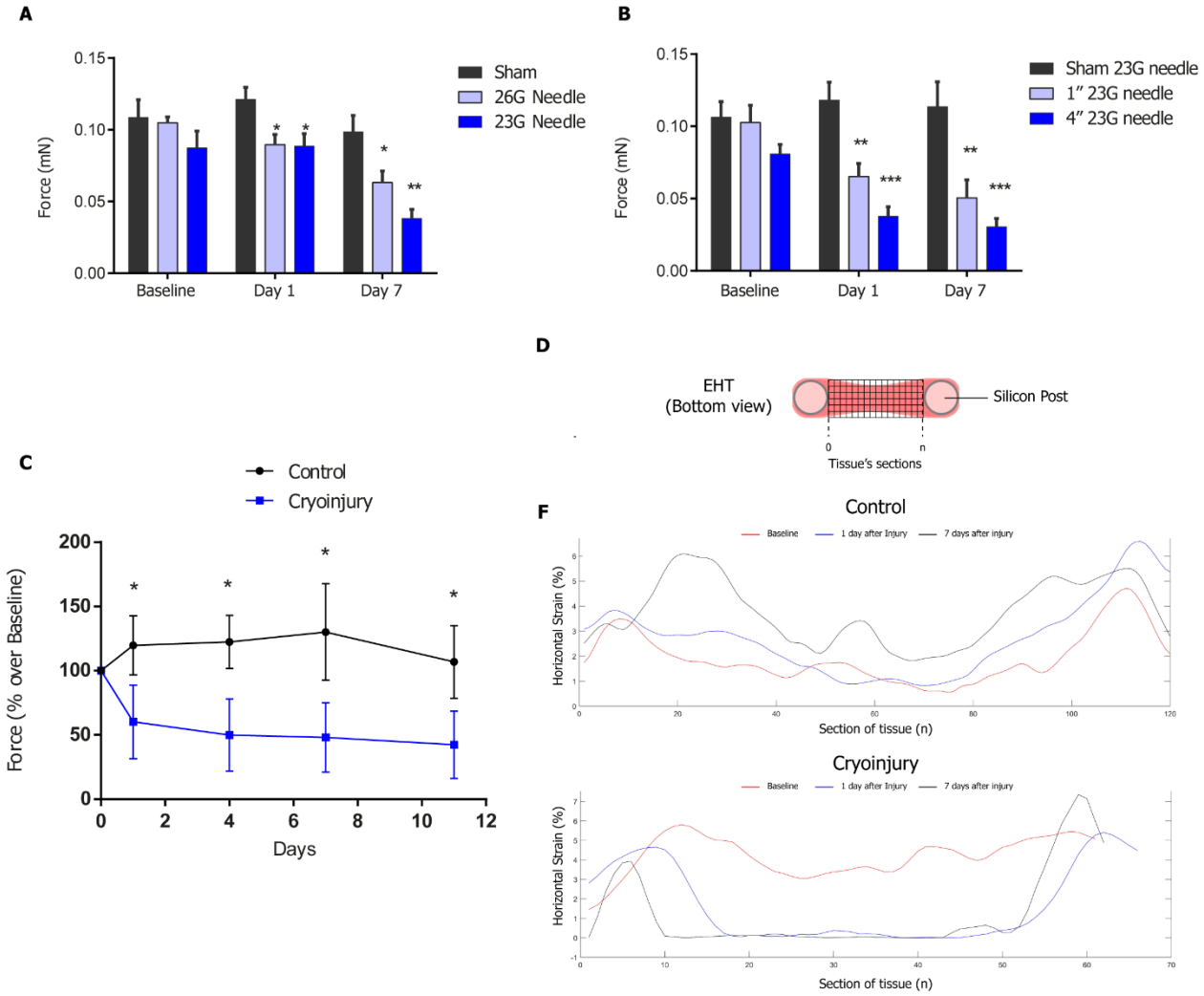

Figure 17. Cryoinjury induces a permanent damage in EHTs. **(A)** Cryoinjury with needles of different sizes induces a significant reduction of force of contraction. **(B)** Cryo-timing evaluation of force loss. **(C)** Force of contraction does not recover in injured EHTs over time. **(D)** Schematic representation of the region of interest analyzed with MuDy software. **(F)** Graph shows horizontal strain along the control EHT (Top) and injured EHT (Bottom) at baseline, day 1 and day 7. (Data shown as mean ± SD)

4.8. Cryoinjury-induced DNA synthesis in mature EHT CMs does not translate into an increase of proliferation

The proliferative potential of rodent cardiomyocytes is retained during a brief post-natal window and can produce an almost complete restitutio ad integrum after myocardial injury (Porrello, Mahmoud et al. 2011, Porrello and Olson 2014). This ability is inevitably lost in the rest of the life and myocardial loss is substituted by a scar (Soonpaa and Field 1998, Ahuja, Sdek et al. 2007, Walsh, Ponten et al. 2010). We have shown that cardiomyocytes in EHTs present a maturation profile that may resemble some aspect of rodents early postnatal life (Alkass, Panula et al. 2015), including progressive reduction of DNA synthesis and increase in binucleation. Cryoinjury has shown to induce an important CM proliferative response with tissue regeneration in human cardiac organoids (Voges, Mills et al. 2017). CMs were generated using human iPSC derived cardiomyocytes that are notoriously immature with features resembling fetal cardiomyocytes (Guo and Pu 2020) thus unsuitable to understanding the mechanism behind the lack of cardiac regeneration after MI in the adult. To test the hypothesis that mature EHTs can recapitulate in part the adult myocardium after injury we generated rEHTs as previously described and, upon maturation, we subjected them to a 48h pulse of EdU at different time points, from baseline to day 2, day 4 and day 6 after cryoinjury. We observed a significant increase of EdU^+CMs at day 4 and day 6 post injury when compared to baseline (1.6 ± 0.3% vs 4.9 ± 1.6 % vs. 5.4 ± 1.0 EdU^+CMs) (Fig. 18A). We also evaluated if DNA synthesis in CMs translated into CM proliferation. We evaluated the percentage of CMs that were positive for Ki67 and pH3 and we could not detect any significant difference at the different timepoints after injury suggesting that cryoinjury in mature rat EHTs induces DNA synthesis but not CM proliferation. Recent evidences have shown that the lack of proliferative response of cardiomyocytes after myocardial infarction is associated to DNA synthesis in CMs from the borderzone of infarcted myocardium leading to polyploidy and multinucleation but not cell division (Senyo, Steinhauser et al. 2013). Our data suggest that the degree of CM maturity in our

model and the response upon injury may represent a novel tool to investigate cardiomyocyte proliferation and biology in vitro.

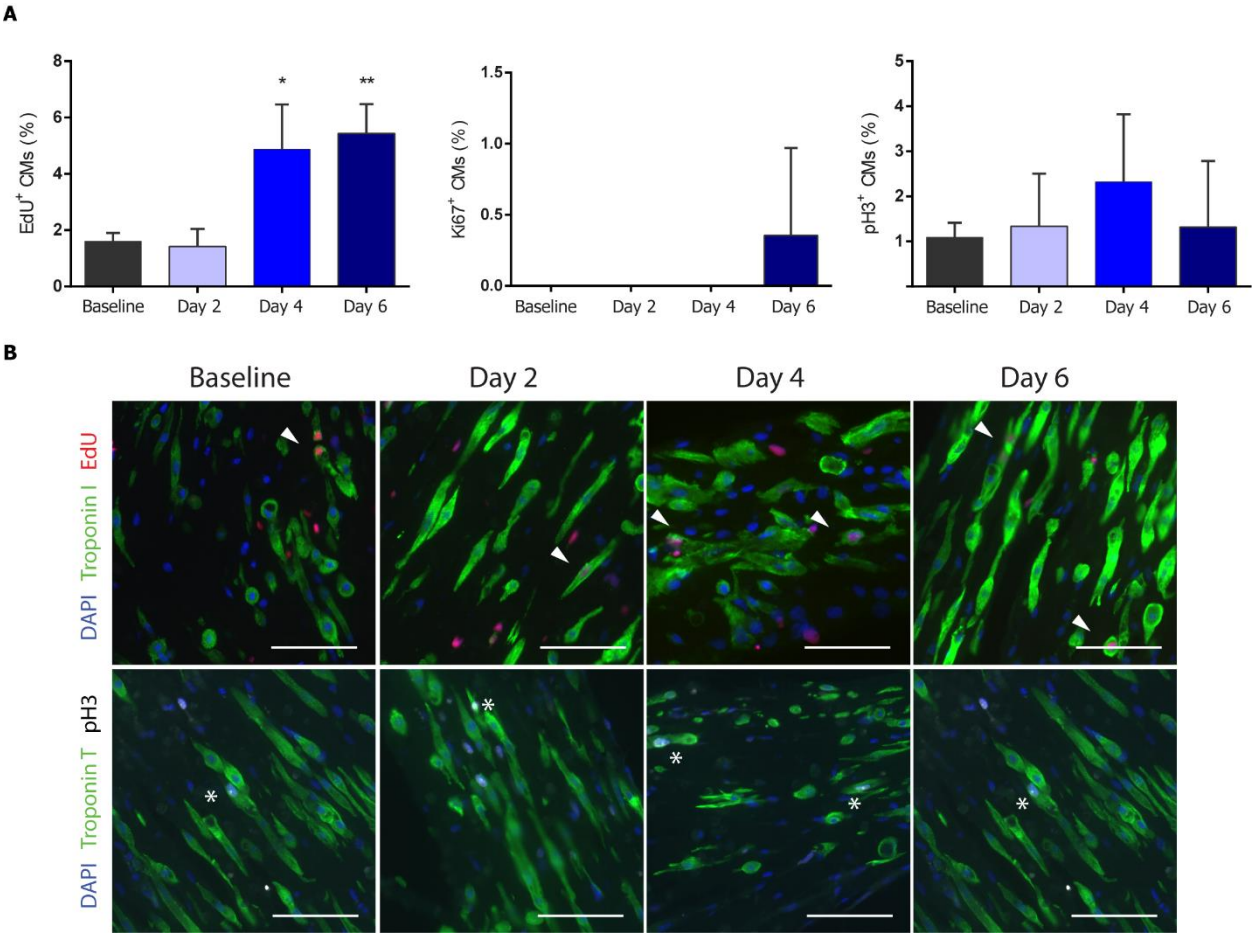

Figure 18. Cryoinjury induces CMs DNA synthesis without cell division. (A) Quantification of EdU⁺ CMs, Ki67⁺CMs and pH3⁺CMs in EHTs 2, 4 and 6 days after cryoinjury (n=4 per group). EdU was supplemented to the medium for a pulse of 48h, every timepoints represents the proliferative window of the previous 2 days (Data shown as mean ± SD). **(B)** Representative images with merged immunofluorescence staining for nuclei (Blue), troponin I (Green), EdU (Red) and pH3 (white) of EHTs (Scale bar: 100µm). EdU⁺CMs are highlighted with white arrows and pH3⁺CMs with white stars.

4.9. Cryoinjury in immature EHTs induced CMs proliferation

To confirm the hypothesis that the degree of maturation of EHTs is crucial for determining the proliferative response after cryoinjury, we performed cryoinjury in the first week after EHT casting and we evaluated markers of cardiomyocytes proliferation. We arbitrarily chose to perform cryoinjury the day after the onset of coherent beating which corresponded to day 5, when a functional syncytium has just formed and CM DNA synthesis was the highest (Figure 9A). As described before, we generated rEHTs and we delivered cryoinjury at day 6 and 18 after casting subjecting them to a 48h pulse of EdU. As shown in Figure 20 we observed a significant increase of EdU^+ CMs in both mature and immature EHTs when compared to their controls (6.3 ± 1.9% vs 10.1 ± 1.6 % and 2.1 ± 1.3 vs 6.02 ± 1.5 EdU^+CMs respectively for day 8 and day 20). As expected, the number of Ki67 and pH3 positive cardiomyocytes was not significant increased in mature EHT after cryoinjury. Interestingly, CMs increased DNA synthesis after cryoinjury in immature EHTs was associated to a significant increase of $Ki67^+$ and $pH3^+$ CMs (1.1 ± 0.3% and 1.3 ± 0.3% vs. 0.4 ± 0.1% and 0.3 ± 0.3% of their age-matched control (Fig. 20), indicating that the degree of cardiomyocyte maturation plays a crucial role in the proliferative response after cryoinjury.

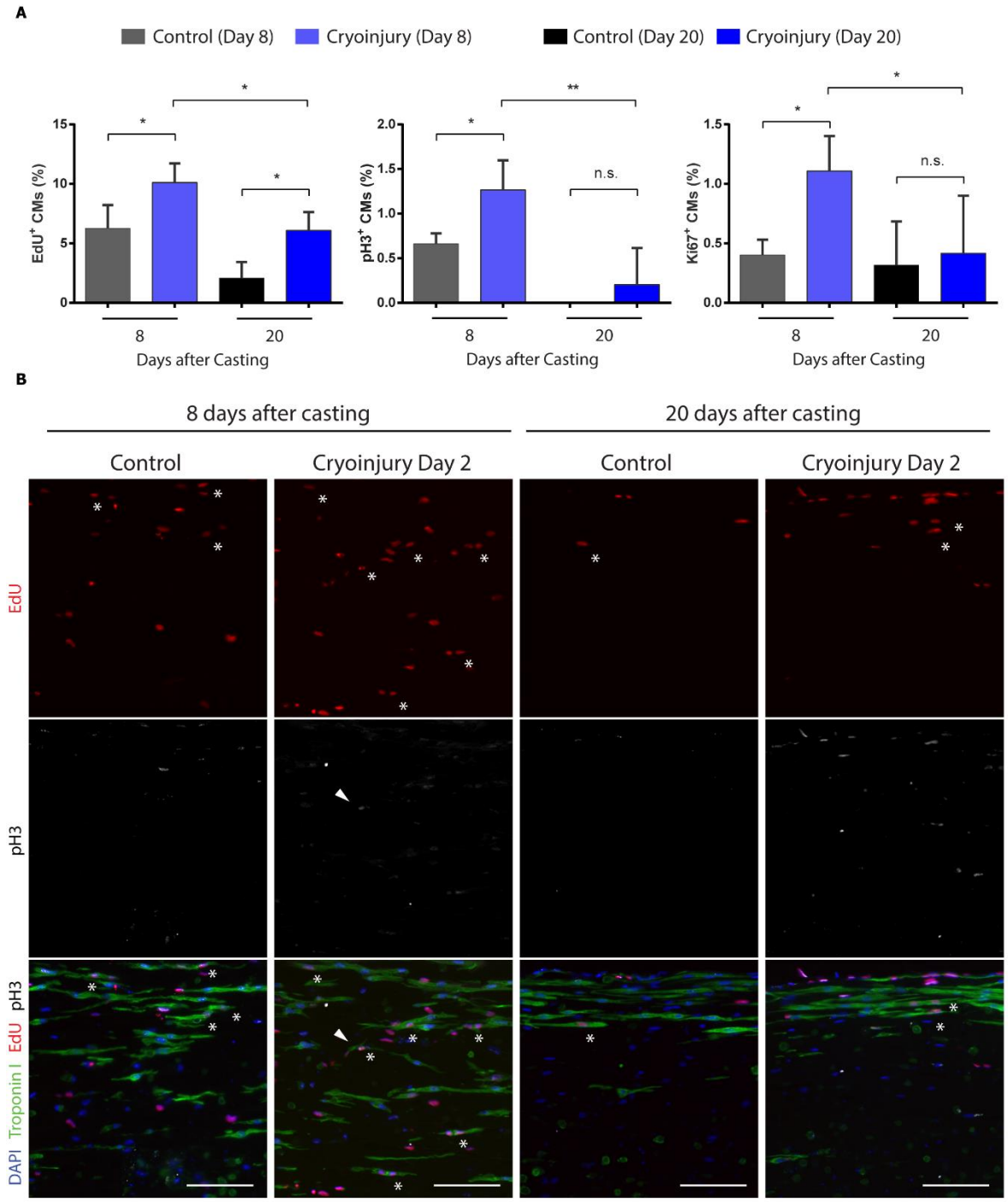

Figure 20. Cryoinjury induces CMs proliferation in immature EHTs. (A) Quantification of EdU^{+} CMs, Ki67^{+}CMs and pH3^{+}CMs after 2 days from cryoinjury performed in immature (1 day after coherent beating, day 6) and mature EHTs (18 days after casting) (n=4 per group). EdU was supplemented to the medium for a pulse of 48h, each timepoint represents the proliferative window of the previous 2 days (Data shown as mean ± SD). **(B)** Representative images with merged

immunofluorescence staining for nuclei (Blue), troponin I (Green), EdU (Red) and pH3 (white) of EHTs (Scale bar: 100µm). EdU^+CMs are highlighted with white arrows and $pH3^+$CMs with white stars.

4.10. Cryoinjury induces focal collagen deposition which decreases over time.

Cardiac fibroblasts are one of the most abundant cell populations represented in EHTs besides cardiomyocytes (Hirt, Sorensen et al. 2012). As previously discussed, fibroblasts have a pivotal role in modulating cardiac tissue response and outcome after myocardial infarction. Among all the functions that fibroblasts have, one of the most important is the formation of fibrotic tissue which is characterized by a sustained secretion of ECM, mostly collagen. Fibroblasts are activated by ischemia itself and by molecules released by dead cardiomyocytes to proliferate and then mature with anti-inflammatory and pro-fibrotic mediators released to promote the deposition of ECM (Humeres and Frangogiannis 2019). In order to further characterize the cellular and biochemical response of EHTs after injury, we subjected mature EHTs to cryoinjury and compared to uninjured control (N=4 per group). Tissues were harvested at different timepoint (baseline, day 2, day 4 and day 6 after injury) and immunofluorescence analysis for collagen I was performed. Quantification of collagen I positive areas indicates an increase of collagen deposition over time after injury which became significant at day 4 when compared to baseline (0.9 ± 0.4 vs. 0.3 ± 0.2 %) (Fig. 21 A) and returned to the pre-injury level at day 6 (Fig. 21A). Moreover, as shown in Figure 21C, we noticed that collagen areas were not homogeneously distributed among the tissue, nor were localized in specific areas and were independent from the site of the injury. Moreover, we confirmed by immunofluorescence analysis the presence of vimentin positive fibroblasts inside the areas of collagen accumulation (Fig. 21C). We speculate that fibroblast reaction to cryoinjury may be dependent from the microenvironment that surrounded them which is variable due to the random distribution of the cells that takes place during EHT's casting.

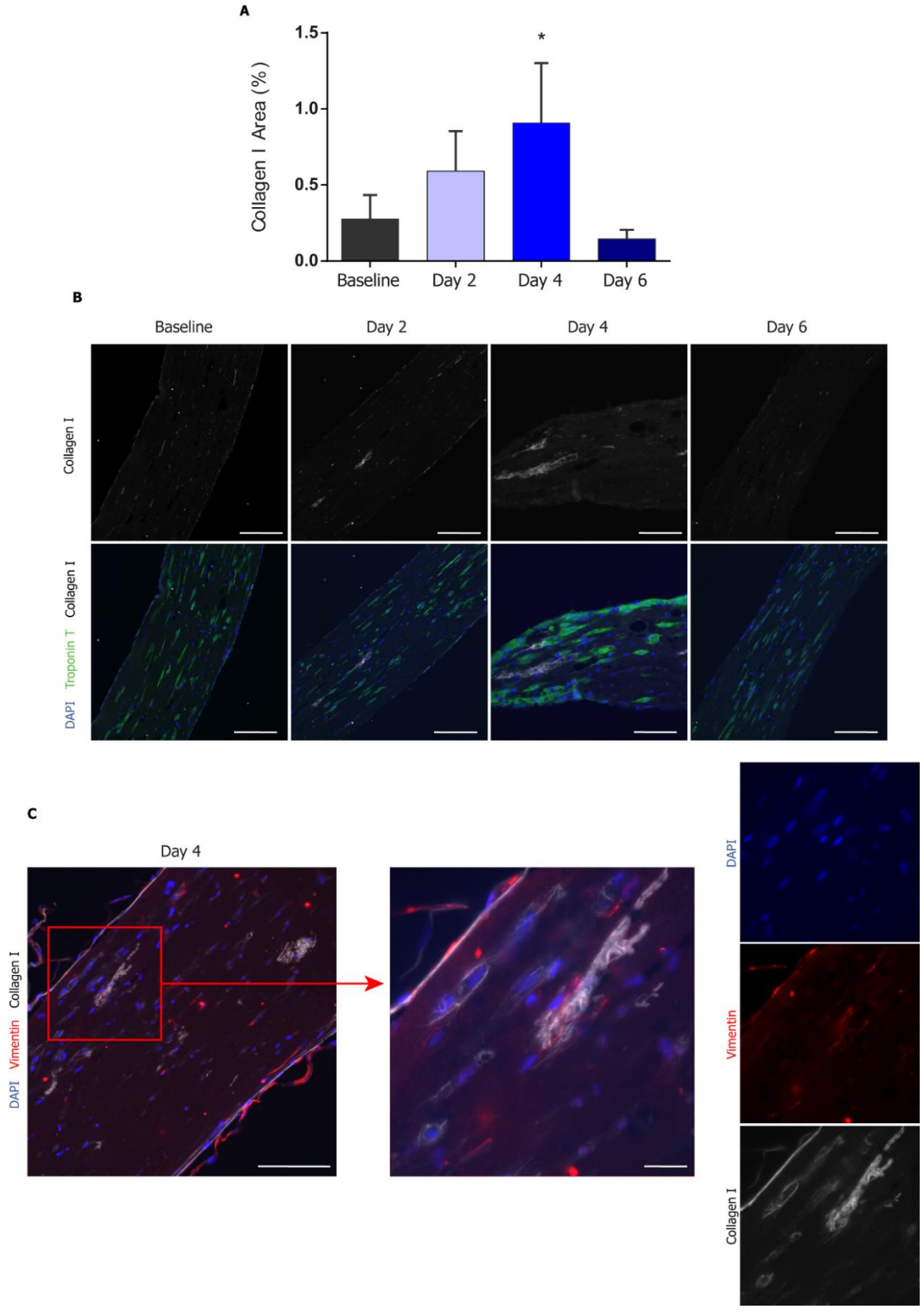
A
Collagen I Area (%)
1.5
1.0
0.5
0.0
*
Baseline
Day 2
Day 4
Day 6
B
Baseline
Day 2
Day 4
Day 6
Collagen I
DAPI Troponin T Collagen I
C
Day 4
DAPI Vimentin Collagen I
DAPI
Vimentin
Collagen I

Figure 21. Cryoinjury induces focal collagen deposition in EHTs. (A) Quantification of Collagen I area over total area (Data shown as mean ± SD). **(B)** Representative immunofluorescence images for collagen I. Nuclei (Blue), troponin I (Green), Collagen I (White) (Scale bar: 300µm).**(C)** On the left, representative image of a collagen accumulation (White) characterized by the presence of vimentin positive fibroblasts (Red) (Scale bar:300 µm). Higher magnification on the right (Scale bar:100 µm).

4.11. Cryoinjury stimulates a gene expression profile which resembles the activation of cardiac fibroblast after myocardial infarction

We next sought to investigate whether cryoinjury in EHTs modifies gene expression of resident cardiac fibroblasts. Cardiac fibroblasts upon MI secrete cytokines and chemokines such as IL-1 and CCL2 to recruit and activate leukocytes (Dewald, Zymek et al. 2005, Bujak, Dobaczewski et al. 2008). Subsequently, cytokine-stimulated fibroblasts secrete matrix metalloproteinases (MMPs), promoting extracellular matrix degradation and release of pro-inflammatory matrix fragments (Phatharajaree, Phrommintikul et al. 2007). In rats, MMP2 and MMP12 are two of the most relevant metalloproteinases involved in this process (Iyer, Patterson et al. 2015, DeLeon-Pennell, Meschiari et al. 2017). As a regulatory mechanism, fibroblasts start to express metalloproteases inhibitors such as Timp1. Moreover, fibroblasts migrate to the MI borderzone, proliferate and undergo myofibroblast differentiation, incorporating a-SMA into cytoskeletal stress fibers (Humeres and Frangogiannis 2019). At this stage myofibroblasts secrete extracellular matrix protein such as fibronectin (Fn1) and different types of collagen among which Collagen type 1 (Col1a1) is one of the most characteristic of fibrosis after MI (Moore-Morris, Cattaneo et al. 2018). To further investigate whether our model of cryoinjury may recapitulate in vivo fibroblast response to MI, we performed gene expression analysis measuring mRNA levels of the pivotal genes involved in this process. Mature rat EHTs were subjected to cryoinjury and harvested every day (N=4 per

group) for five timepoints in total. As shown in Figure 22, in the very first days after injury, we observed a sudden and significant increase of proinflammatory molecules like CCL2 (3.9-fold change) and IL-1β (2.3-fold change) when compared to control, suggesting that damage-associated molecular patterns (DAMPs) deriving from dying cells have stimulated fibroblasts to secrete cytokines and chemokines. Interestingly, CCl2 mRNA levels decreased over time returning to pre-injury levels at day 4, while IL-1β mRNA levels remain stable for all the subsequent timepoints. MMP2 and MMP12, early markers of matrix remodeling in vivo, significantly increased at day 2-3 post injury and decreased to baseline levels afterward. Simultaneously mRNA levels of the metalloproteinase inhibitor Timp1 increased significantly immediately after injury and gradually decreased in the following days to become significantly lower at day 5. We also observed a significant increase in the expression of α-SMA (Acta2), a marker of myofibroblast differentiation that corresponded to the acquisition of a secretory phenotype. As shown in Figure 22, both Collagen 1 and fibronectin significantly increased after injury and returned to pre-injury levels by day 4. Taken together, our data indicate that cryoinjury in EHTs is capable of activating cardiac fibroblasts, similarly to the adult myocardium. The lack of a sustained pro-fibrotic response in EHTs may be the consequence of the complete absence of the immune system which is fundamental in vivo for generating the scar.

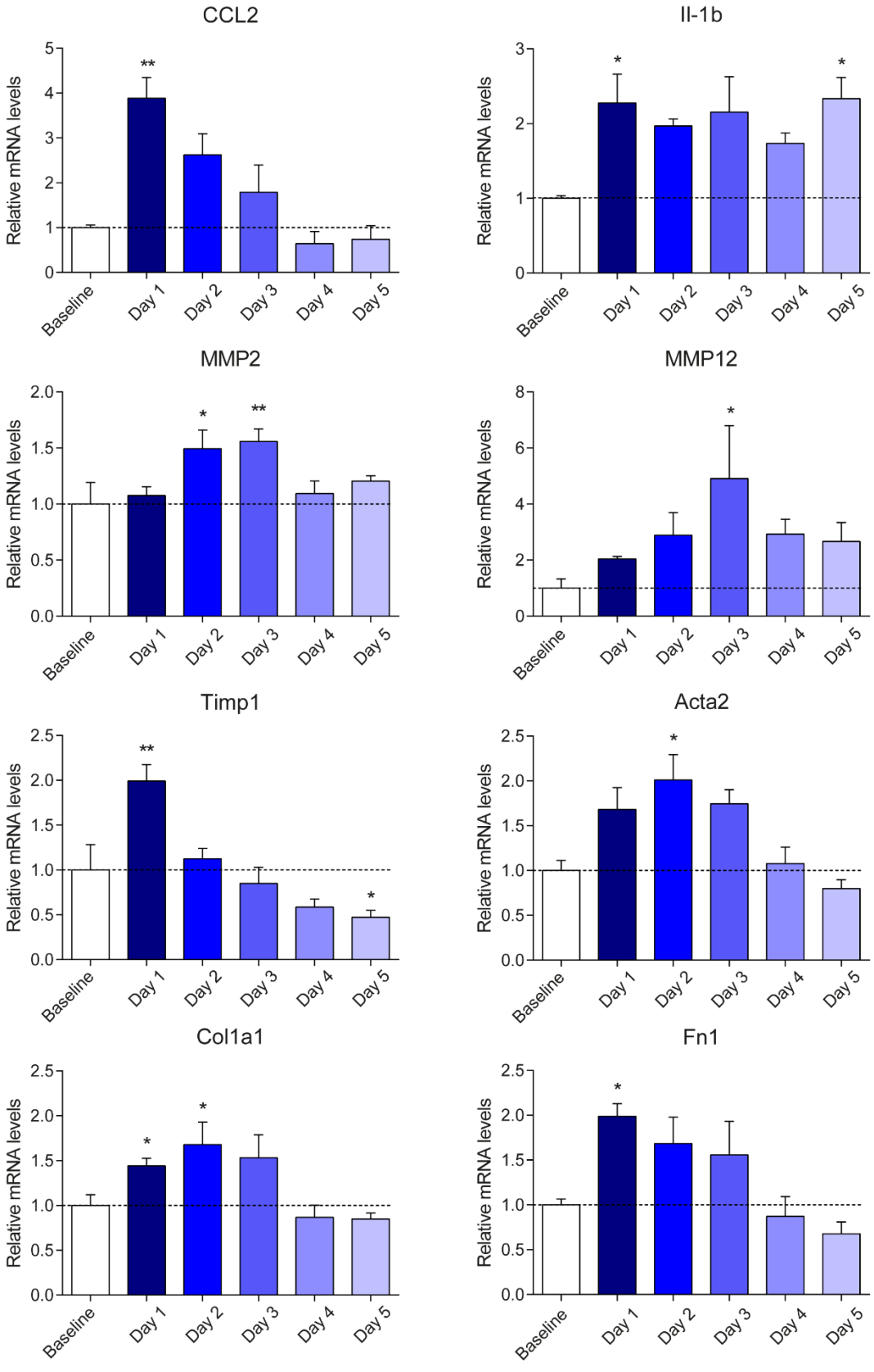
CCL2
Il-1b
MMP2
MMP12
Timp1
Acta2
Col1a1
Fn1
Relative mRNA levels
Baseline
Day 1
Day 2
Day 3
Day 4
Day 5

Figure 22. Gene expression analysis in EHTs after cryoinjury suggests resident fibroblasts activation. Relative mRNA levels of chemokine (C-C motif) ligand 2 (CCL2), interleukin 1 beta (IL-1β) metalloproteinases 2 and 12 (MMP2 and MMP12), metalloproteinase inhibitor 1 (Timp1), α-SMA (Acta2), Fibronectin (Fn1) and Collagen I (Col1a1) in EHTs at different timepoints after cryoinjury (Data shown as mean ± SEM).

4.12. Cryoinjury induces proliferation of fibroblasts localized at the injury border zone

Besides collagen deposition, another hallmark of an activated cardiac fibroblast is proliferation. Fibroblasts in the borderzone of the infarct increase in number and undergo to myofibroblast conversion promoting the formation of a mature scar (Weber, Sun et al. 2013). To evaluate whether cryoinjury stimulates proliferation of EHT resident fibroblasts, we first evaluated the number of EdU^+ fibroblasts at different timepoints after injury. Rat EHTs were generated as previously described and EdU was added to the medium with 48h pulse. Four EHTs per timepoint were fixed at the baseline and at day 2, 4, 6, 8 and 10 after injury and compared to the uninjured control. Immunofluorescence staining for EdU reveals a progressive increase of $Vimentin^+$ cells during the days following the injury starting with 5.4 % in the basal condition to reach 29.8% and 26.7% and at day 2 and 4 respectively (Fig. 23 A). After the fourth day, the number of EdU^+ fibroblasts was comparable to the basal level suggesting that the contribution of cryoinjury to cell division is prevalent in the first 96 hours after injury and is followed by a physiological proliferation turnover of non-cardiomyocytes cells in EHTs (Fig. 23A). Finally, as shown in Figure 23C, the majority of EdU^+ fibroblasts are localized at the borderzone, with a pattern that indicates a gradient towards the remote area, suggesting that this pro-proliferative cue may be due to paracrine factors derived from the injured part of the tissue.

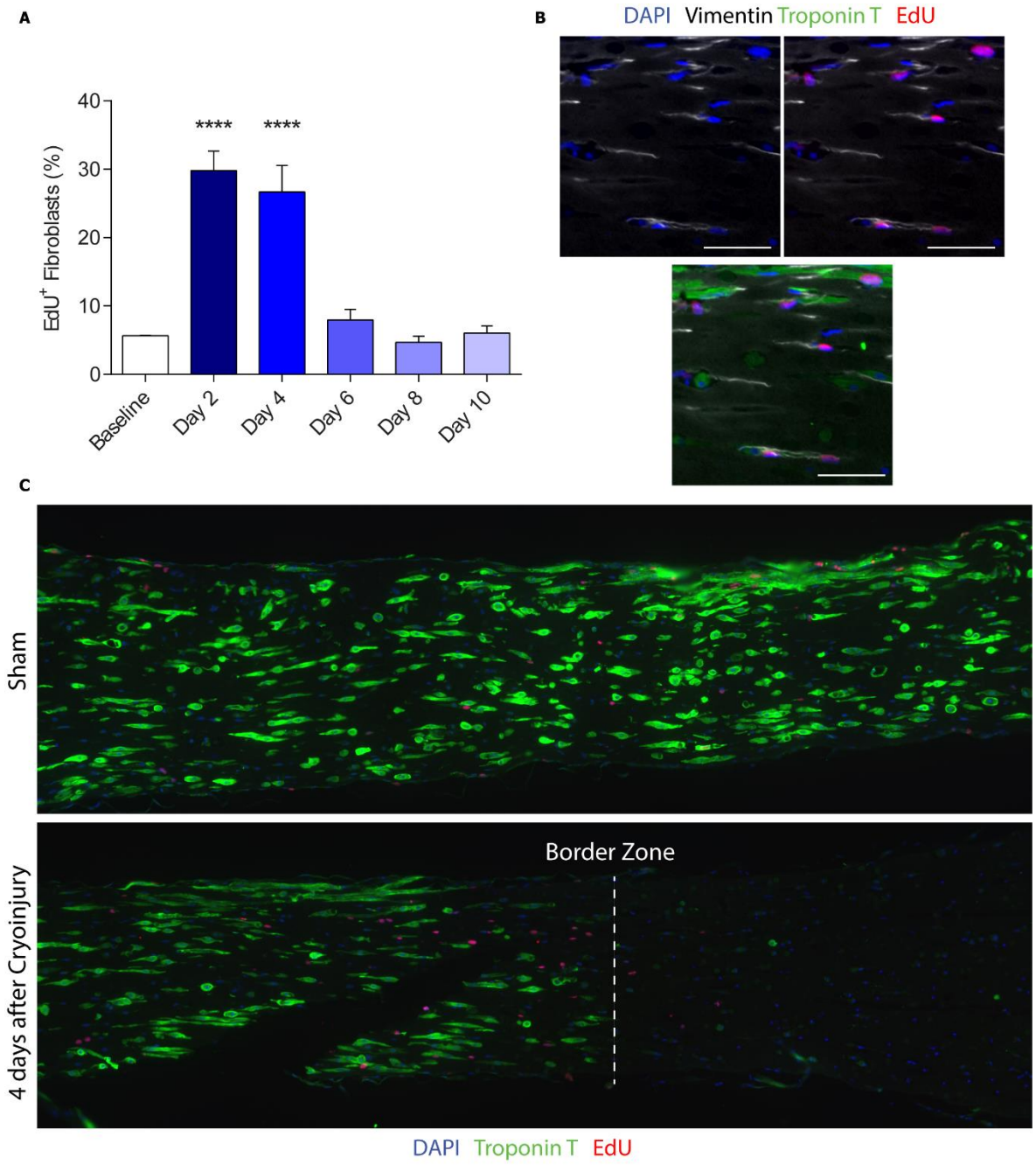

Figure 23. Cryoinjury induces proliferation of fibroblast in the first 4 days in EHTs. (A) Quantification of EdU^+/TnT^- cells in EHTs from 2 to 10 days after cryoinjury. EdU was supplemented to the medium starting from the 2 days before the injury until day 10 **(B)** Representative images of proliferative vimentin positive fibroblasts (white) at day 4 after injury (Scale bar: 50µm). **(C)** Representative images with merged immunofluorescence staining for nuclei (Blue), troponin I (Green), EdU (Red) and pH3 (white) of control EHT (top) and injured EHT (bottom). Dashed line highlights the borderzone. (Data shown as mean ± SD).

DISCUSSION

Myocardial infarction is one of the most severe acute pathologies of the cardiovascular system and the loss of cardiomyocytes that are replaced by scar tissue determines infarcts of different sizes which correlate to prognosis and outcome (Smith, Hamlin et al. 1992). As heart diseases are the leading cause of death of the 21st century, it is essential to understand the molecular and cellular mechanisms that are responsible for the poor regenerative capacity of the adult mammalian heart to develop therapies for the replacement or restoration of the damaged myocardium. Several strategies for cardiac repair have been proposed over the last two decades including stem cell-based therapies and implantation of new ex-vivo generated CMs from embryonic stem cell or induced pluripotent stem cells via direct cell-infusion or within engineered scaffolds (Chong, Yang et al. 2014, Weinberger, Breckwoldt et al. 2016). Both approaches are still not ideal and have generally provided only modest improvement in cardiac function due to lack of a substantial number of replaced CMs. Thus, new therapies able to stimulate cardiac regeneration are urgently needed. A key concept in regenerative medicine is that there is a strong correlation between regeneration and development. While it is well known and proved that lower vertebrates have an extraordinary ability to prompt cardiac regeneration (Poss, Wilson et al. 2002, Witman, Murtuza et al. 2011, Gamba, Harrison et al. 2014), in mice this regenerative ability is preserved exclusively in a time-window, from the fetal stage to 7 days post-natal life (Porrello, Mahmoud et al. 2011, Porrello and Olson 2014). Soon after birth such plasticity is, however, lost. A switch from a mononucleate to a binucleate phenotype occurs in cardiomyocytes. Binucleation is a feature of terminally differentiated cells, whereas mononucleate cells still retain the potential to undergo the normal cycle and thus proliferate. After a final round of acytokinetic mitosis (karyokinesis without cytokinesis), the majority of the cardiomyocytes become terminally binucleated (Soonpaa and Field 1998, Ahuja, Sdek et al. 2007, Walsh, Ponten et al. 2010).

Several postnatal regulatory events have been shown as putative causes for the phenotype switch of mammal CMs from the neonatal proliferative state to the adult post-mitotic state. A major post-natal event is the massive workload that the heart has to face in response to an increasing body weight; thus understanding the role of mechanotransduction in regulating the balance between CM proliferation and maturation may bring us to the identification of unknown mediators and new potential strategies to induce cardiac regeneration. Our work has indeed focused on developing a novel model to investigate, in a controlled and reproducible manner, the effect of mechanical loading on regulating those crucial post-natal events.

Mechanical cues in the animal hearts are scarcely manipulable due to the indivisible bond between coordinated mechanical contraction of the cardiomyocytes and a correct cardiac function. Thus, to investigate in depth the mechanism involved in the mechanotransduction in the heart, several in vitro models have been developed in the past two decades involving both animal cells and hiPSC derived cardiomyocytes. Among all the proposed model the common strategy that has been used is the one where cardiac cells are seeded on a substrate which can be stretched in different manner (Gwak, Bhang et al. 2008, Jungbauer, Gao et al. 2008). Unidirectional stretching is one of the leading methods due to the well-reported benefits of cardiomyocytes maturation and organization(Naruse, Yamada et al. 1998, Lee, Knight et al. 2011, Kamble, Vadivelu et al. 2018). To achieve this type of stretching, several approaches have been proposed among which electromechanical (Wan, Chung et al. 2011, Shao, Tan et al. 2013, Kreutzer, Viehrig et al. 2019) and pneumatic (Kreutzer, Ikonen et al. 2014, Tremblay, Chagnon-Lessard et al. 2014, Kamble, Vadivelu et al. 2018), substrate stretching are two of the major common methods. However, bidimensional cultures of cardiac cells remain extremely distant from adult cardiomyocytes in terms of cell maturation despite all the improvements that have been made to bring them as close as possible to in vivo environment. Moreover, current systems which investigate mechanotransduction by stretching the cells do not completely resemble the complexity characteristic of cardiomyocyte mechanobiology which is orchestrated not only by the interaction between integrins and ECM but also by the several interactions that take place at the intercalated disk.

The novelty of our approach has been to take advantage of a 3D cardiomyocyte culture model, initially developed as a drug screening platform called engineered heart tissues (EHTs) (Hansen, Eder et al. 2010), and to reaccustom it for investigating the putative role of mechanotransduction in cardiomyocyte proliferation. Cardiomyocyte 3D cultures have indeed a lot of advantages when compared to 2D cultures. First, the degree of cardiac differentiation and maturation in 3D models made from neonatal rat cardiac cells is higher and characterized by the following: high degree of sarcomere structure; longitudinal orientation and alignment; formation of M-bands, rod-shaped cardiac myocytes; relatively normal ratio of sarcomeres; mitochondria and nuclei; high degree of binucleation; normal diastolic resting potential of approximately −90 mV; high abundance of sarcomeric and sarcoplasmic proteins; relatively normal action potential shape; and qualitatively normal physiological and pharmacological responses—such as Frank–Starling behavior, force–frequency relationship, and reaction to calcium, isoprenaline, and carbachol (Eschenhagen, Fink et al. 1997, Zimmermann 2002, Hansen, Eder et al. 2010, Tiburcy, Didie et al. 2011). Also, 3D cardiac constructs made from primary cardiac myocytes develop a primitive vascular network without (Zimmermann, Melnychenko et al. 2006), or with the addition of endothelial cells (Sekine, Shimizu et al. 2008, Stevens, Kreutziger et al. 2009).

The first step of our work was to validate EHTs as an in vitro model that resembles cardiac biology of rodents after birth and evaluate the level of maturity reached by neonatal cardiomyocytes. We tested the robustness of EHTs as a model to investigate cardiac proliferation by evaluating the proliferative profile of EHTs cardiomyocytes during the maturation process. We observed that neonatal cardiomyocytes preserve their proliferative capacity in the first week of EHT development while the functional syncytium is not formed yet. As soon as cardiomyocytes start to beat coherently, the DNA synthesis progressively decreases and the number of binucleated cardiomyocytes increases suggesting that the sudden increase of mechanical loading may be the switch from a neonatal to a more mature phenotype. Therefore, our results are in line with the evidence shown in mice where the sudden increase of mechanical loading after birth leads to an

improvement of the contractile capacities of the cardiomyocytes, initially by hyperplasic growth and then by hypertrophic growth (Li, Wang et al. 1996), while on the other hand leads to an increasing mechanical stress and energetic demand for the sustainment of age-related physiological events (Lopaschuk and Jaswal 2010, Porrello, Mahmoud et al. 2011). Therefore, the interconnection between these events is detrimental for the maintenance of a proliferative state, thus promoting cardiomyocyte cell cycle arrest (Schmelter, Ateghang et al. 2006). While our initial results were promising in suggesting EHTs as a model to investigate CM proliferation and maturation, the process of "engineering" EHTs to test our hypothesis required a long series of custom-made adjustments to validate the model, test the reproducibility, optimize experimental conditions. We acknowledge that this technical time may have in part contributed to limit the amount of data that we have generated, with several experiments that are still ongoing to elucidate the mechanisms that regulate our finding. However, the development of a trustable and solid model was crucial for our hypothesis. We have indeed developed a novel model where mechanical loading can be easily modified and we took advantage of this system to evaluate the effect on cardiomyocyte biology, specifically in their ability to proliferate. We have shown how changes in mechanical loading may influence maturation and proliferation of CMs. Our system is based on modified silicone supports on which a hook-shaped 36G needle is placed near each silicone post which, with a simple rotation, can increase or decrease the loading. Specifically, we found that mechanical unloading may increase the ability of cardiomyocytes to proliferate, possibly by inducing the disassembly of the sarcomeric structure and regain a more immature phenotype. This is of particular interest since recent findings have highlighted a pro-proliferative response of human hearts subjected to a prolonged mechanical unloading obtained by left ventricular assist devices (LVADs)(Canseco, Kimura et al. 2015). On the other hand, increasing loading in EHTs is associated to a more mature phenotype as indicated by the increase in the force generated, the number of binucleated cardiomyocytes and the more complex sarcomeric structure. Our study reaffirms the importance of investigating the role of mechanotransduction in cardiomyocyte proliferation looking forward to putative

strategies to restore regeneration capability in adult heart. Because of the long time required to set up this model, our results are still missing the mechanisms that can explain our data, a crucial aspect to translate our findings into novel therapeutic opportunities. Although these data cannot be included at the time this thesis is written, to tackle this matter, we have already set up a series of experiments that are currently ongoing. In particular, considering the pivotal role of the Hippo and Wnt/β-catenin signaling pathways in cardiomyocyte proliferation, we are evaluating using specific reporters whether and how these pathways are involved in mechanical unloading-induced proliferation. At the same time, we have performed RNA sequencing on EHTs in the early phase of mechanical unloading and increased afterload to investigate expression variations of putative factors that may drive these processes. These data are currently being analyzed. The identification of these factors will be validated by specific experiments with loss and gain of function, in vitro and in vivo. Finally, we wish to highlight the robustness of EHTs as a model to elucidate this aspect of cardiac biology and the value of our novel hook system in modulating mechanical loading on engineered heart tissues.

With the idea of using EHTs to answer questions concerning myocardial biology in a controlled manner, we have also focused our work on developing an in vitro model of cardiac injury. Myocardial infarction is a multi-factorial cause of cardiac injury which leads to maladaptive cardiac remodeling driven by several types of cells. Fibroblasts are one of the master regulators involved in the wound healing together with immune system. Briefly, myocardial response to injury is characterized by a lack of cardiomyocyte proliferative response and by an activation of the fibroblasts which secrete cytokines and chemokines, proliferate and produce an over-deposition of ECM components. Recently proposed in vitro injury models take advantage of human iPSCs derived cardiomyocytes which allow a higher translatability of the findings at the expense of cell maturation and therefore to a reduced robustness of the model. Indeed, Voges and collaborators show how cryoinjury in human cardiac organoids leads to an injury that may be recovered due to the ability of cardiomyocyte to proliferate, a finding observed in the embryonic stage or immediately after birth in rodents but that is inevitably lost in adulthood

(Voges, Mills et al. 2017). Rat EHTs have the advantage of being an unpurified culture of cardiac cells including cardiomyocytes, fibroblasts, macrophages and endothelial cells. We set up a cryoinjury protocol performed with a custom-made system to deliver a discrete injury in EHTs. Our system is feasible and reproducible allowing the operator to induce different magnitudes of injury in a localized area of the engineered tissue. We established that cryoinjury produces a localized and reproducible injury in EHTs, leading to a selective loss of contractile activity accompanied by electrical isolation. The possibility of extending the in vitro study at a functional level (myocardial contractility i.e.) represents a major advantage to translate the results into an in vivo system. We have performed EHTs functional analysis using the MuDy Software that allows the evaluation of contractility parameters like displacement and strain in different regions simultaneously. The current configuration of the software used for EHTs analysis is based on figure recognition of the contracting muscle strip at top and bottom ends, which then extrapolates functional values, including frequency, average force, fractional shortening, contraction – and relaxation time (Hansen, Eder et al. 2010). Therefore, this software has the limitation of determining the contractile parameters as a function of the whole EHT. The advantage of the MuDy software is a more precise and discrete evaluation of contractility in different regions of the EHT, thus allowing the study of more fine changes, especially as a consequence of cardiac regeneration upon injury.

Similar to what has been shown in mice and rats after myocardial infarction, we show that cryoinjury induces DNA synthesis in CMs without a proper proliferative response. Indeed, injured EHTs do not recover the loss of contractile activity over time after cryoinjury. On the other hand, cryoinjury in EHTs at the early phase of their development with more immature CMs leads to a proliferative response suggesting EHTs as a novel model to investigate the biology of cardiac regeneration upon injury. Moreover, EHT fibroblast response to injury retraces the activation progression of cardiac fibroblast after MI characterized by increase of activation marker, increase of collagen deposition and proliferation. Our system is feasible and represents a robust novel model to investigate some critical aspects of myocardial

infarction biology avoiding confounding factors such as the immune system or circulating factors. We are performing experiments aimed at validating our novel system including testing whether the proliferative response is dependent on the timing when injury is induced during EHTs developments (similarly to what has been observed in rodents immediately after birth). Moreover, we are also validating the cryoinjury as a model to investigate pro-proliferative factors using the microRNA hsa-miR-199a-3p that has been shown to stimulate rodent CM entry into the cell cycle and cardiac regeneration after myocardial infarction (Eulalio, Mano et al. 2012). Finally, we are performing experiments to evaluate whether mechanical unloading is able to induce CM proliferation and functional recovery after cryoinjury. This novel finding may open new therapeutic avenues combining mechanical support circulatory devices that can support circulation while an infarcted heart is unloaded and stimulated to regenerate. The manuscript that describes our data that we have generated in collaboration with the department of engineering and architecture at the University of Trieste is currently in preparation.

To summarize, most of the efforts in this Ph.D. project have been directed to set up the EHT technology in our laboratory which is a time-consuming technique to master. Subsequently, several attempts have been made to accomplish both an efficient system to easily modulate mechanical loading and a reliable system to deliver cryoinjury. Unfortunately, the global situation that we have all faced in 2020 and is still ongoing has in part contributed to delay crucial experiments aimed at investigating the mechanism of our findings. The novelty of our results must be supported by the mechanistic data that we are confident will be provided by the ongoing experiments.

5. BIBLIOGRAPHY

Abilez, O. J., E. Tzatzalos, H. Yang, M. T. Zhao, G. Jung, A. M. Zollner, M. Tiburcy, J. Riegler, E. Matsa, P. Shukla, Y. Zhuge, T. Chour, V. C. Chen, P. W. Burridge, I. Karakikes, E. Kuhl, D. Bernstein, L. A. Couture, J. D. Gold, W. H. Zimmermann and J. C. Wu (2018). "Passive Stretch Induces Structural and Functional Maturation of Engineered Heart Muscle as Predicted by Computational Modeling." Stem Cells **36**(2): 265-277.

Ahuja, P., P. Sdek and W. R. MacLellan (2007). "Cardiac myocyte cell cycle control in development, disease, and regeneration." Physiol Rev **87**(2): 521-544.

Alkass, K., J. Panula, M. Westman, T. D. Wu, J. L. Guerquin-Kern and O. Bergmann (2015). "No Evidence for Cardiomyocyte Number Expansion in Preadolescent Mice." Cell **163**(4): 1026-1036.

Bassat, E., Y. E. Mutlak, A. Genzelinakh, I. Y. Shadrin, K. Baruch Umansky, O. Yifa, D. Kain, D. Rajchman, J. Leach, D. Riabov Bassat, Y. Udi, R. Sarig, I. Sagi, J. F. Martin, N. Bursac, S. Cohen and E. Tzahor (2017). "The extracellular matrix protein agrin promotes heart regeneration in mice." Nature **547**(7662): 179-184.

Becker, R. O., S. Chapin and R. Sherry (1974). "Regeneration of the ventricular myocardium in amphibians." Nature **248**(5444): 145-147.

Belkin, A. M., N. I. Zhidkova, F. Balzac, F. Altruda, D. Tomatis, A. Maier, G. Tarone, V. E. Koteliansky and K. Burridge (1996). "Beta 1D integrin displaces the beta 1A isoform in striated muscles: localization at junctional structures and signaling potential in nonmuscle cells." J Cell Biol **132**(1-2): 211-226.

Bian, W., B. Liau, N. Badie and N. Bursac (2009). "Mesoscopic hydrogel molding to control the 3D geometry of bioartificial muscle tissues." Nat Protoc **4**(10): 1522-1534.

Brancaccio, M., L. Fratta, A. Notte, E. Hirsch, R. Poulet, S. Guazzone, M. De Acetis, C. Vecchione, G. Marino, F. Altruda, L. Silengo, G. Tarone and G. Lembo (2003). "Melusin, a muscle-specific integrin beta1-interacting protein, is required to prevent cardiac failure in response to chronic pressure overload." Nat Med **9**(1): 68-75.

Bray, M. A., W. J. Adams, N. A. Geisse, A. W. Feinberg, S. P. Sheehy and K. K. Parker (2010). "Nuclear morphology and deformation in engineered cardiac myocytes and tissues." Biomaterials **31**(19): 5143-5150.

Brink, J. G. and J. Hassoulas (2009). "The first human heart transplant and further advances in cardiac transplantation at Groote Schuur Hospital and the University of Cape Town - with reference to : the operation. A human cardiac transplant : an interim report of a successful operation performed at Groote Schuur Hospital, Cape Town." Cardiovasc J Afr **20**(1): 31-35.

Bujak, M., M. Dobaczewski, K. Chatila, L. H. Mendoza, N. Li, A. Reddy and N. G. Frangogiannis (2008). "Interleukin-1 receptor type I signaling critically regulates infarct healing and cardiac remodeling." Am J Pathol **173**(1): 57-67.

Burridge, K. and M. Chrzanowska-Wodnicka (1996). "Focal adhesions, contractility, and signaling." Annu Rev Cell Dev Biol **12**: 463-518.

Busato, A., G. Balconi, V. Vismara, L. Bertele, G. Tonti and G. Pedrizzetti (2015). "Strain Analysis of Masseter Muscle by Ultrasound." J Biol Regul Homeost Agents **29**(3 Suppl 1): 74-81.

Buyandelger, B., C. Mansfield and R. Knoll (2014). "Mechano-signaling in heart failure." Pflugers Arch **466**(6): 1093-1099.

Canseco, D. C., W. Kimura, S. Garg, S. Mukherjee, S. Bhattacharya, S. Abdisalaam, S. Das, A. Asaithamby, P. P. Mammen and H. A. Sadek (2015). "Human ventricular unloading induces cardiomyocyte proliferation." J Am Coll Cardiol **65**(9): 892-900.

Carrier, R. L., M. Papadaki, M. Rupnick, F. J. Schoen, N. Bursac, R. Langer, L. E. Freed and G. Vunjak-Novakovic (1999). "Cardiac tissue engineering: cell seeding, cultivation parameters, and tissue construct characterization." Biotechnol Bioeng **64**(5): 580-589.

Caspi, O., A. Lesman, Y. Basevitch, A. Gepstein, G. Arbel, I. H. Habib, L. Gepstein and S. Levenberg (2007). "Tissue engineering of vascularized cardiac muscle from human embryonic stem cells." Circ Res **100**(2): 263-272.

Cassar, A., D. R. Holmes, Jr., C. S. Rihal and B. J. Gersh (2009). "Chronic coronary artery disease: diagnosis and management." Mayo Clin Proc **84**(12): 1130-1146.

Chen, C. S., M. Mrksich, S. Huang, G. M. Whitesides and D. E. Ingber (1997). "Geometric control of cell life and death." Science **276**(5317): 1425-1428.

Chen, C. S., J. Tan and J. Tien (2004). "Mechanotransduction at cell-matrix and cell-cell contacts." Annu Rev Biomed Eng **6**: 275-302.

Chong, J. J., X. Yang, C. W. Don, E. Minami, Y. W. Liu, J. J. Weyers, W. M. Mahoney, B. Van Biber, S. M. Cook, N. J. Palpant, J. A. Gantz, J. A. Fugate, V. Muskheli, G. M. Gough, K. W. Vogel, C. A. Astley, C. E. Hotchkiss, A. Baldessari, L. Pabon, H. Reinecke, E. A. Gill, V. Nelson, H. P. Kiem, M. A. Laflamme and C. E. Murry (2014). "Human embryonic-stem-cell-derived cardiomyocytes regenerate non-human primate hearts." Nature **510**(7504): 273-277.

Collaborators, G. B. D. C. o. D. (2018). "Global, regional, and national age-sex-specific mortality for 282 causes of death in 195 countries and territories, 1980-2017: a systematic analysis for the Global Burden of Disease Study 2017." Lancet **392**(10159): 1736-1788.

de Melker, A. A. and A. Sonnenberg (1999). "Integrins: alternative splicing as a mechanism to regulate ligand binding and integrin signaling events." Bioessays **21**(6): 499-509.

DeLeon-Pennell, K. Y., C. A. Meschiari, M. Jung and M. L. Lindsey (2017). "Matrix Metalloproteinases in Myocardial Infarction and Heart Failure." Prog Mol Biol Transl Sci **147**: 75-100.

Dewald, O., P. Zymek, K. Winkelmann, A. Koerting, G. Ren, T. Abou-Khamis, L. H. Michael, B. J. Rollins, M. L. Entman and N. G. Frangogiannis (2005). "CCL2/Monocyte Chemoattractant Protein-1 regulates inflammatory responses critical to healing myocardial infarcts." Circ Res **96**(8): 881-889.

Discher, D. E., D. J. Mooney and P. W. Zandstra (2009). "Growth factors, matrices, and forces combine and control stem cells." Science **324**(5935): 1673-1677.

Drenckhahn, J. D., Q. P. Schwarz, S. Gray, A. Laskowski, H. Kiriazis, Z. Ming, R. P. Harvey, X. J. Du, D. R. Thorburn and T. C. Cox (2008). "Compensatory growth of healthy cardiac cells in the presence of diseased cells restores tissue homeostasis during heart development." Dev Cell **15**(4): 521-533.

Dugaucquier, L., E. Feyen, L. Mateiu, T. A. M. Bruyns, G. W. De Keulenaer and V. F. M. Segers (2020). "The role of endothelial autocrine NRG1/ERBB4 signaling in cardiac remodeling." Am J Physiol Heart Circ Physiol **319**(2): H443-H455.

Eder, A., A. Hansen, J. Uebeler, T. Schulze, C. Neuber, S. Schaaf, L. Yuan, T. Christ, M. A. Vos and T. Eschenhagen (2014). "Effects of proarrhythmic drugs on relaxation time and beating pattern in rat engineered heart tissue." Basic Res Cardiol **109**(6): 436.

Eder, A., I. Vollert, A. Hansen and T. Eschenhagen (2016). "Human engineered heart tissue as a model system for drug testing." Adv Drug Deliv Rev **96**: 214-224.

Eschenhagen, T., A. Eder, I. Vollert and A. Hansen (2012). "Physiological aspects of cardiac tissue engineering." Am J Physiol Heart Circ Physiol **303**(2): H133-143.

Eschenhagen, T., C. Fink, U. Remmers, H. Scholz, J. Wattchow, J. Weil, W. Zimmermann, H. H. Dohmen, H. Schafer, N. Bishopric, T. Wakatsuki and E. L. Elson (1997). "Three-dimensional reconstitution of embryonic cardiomyocytes in a collagen matrix: a new heart muscle model system." FASEB J **11**(8): 683-694.

Eulalio, A., M. Mano, M. Dal Ferro, L. Zentilin, G. Sinagra, S. Zacchigna and M. Giacca (2012). "Functional screening identifies miRNAs inducing cardiac regeneration." Nature **492**(7429): 376-381.

Farhadian, F., F. Contard, A. Corbier, A. Barrieux, L. Rappaport and J. L. Samuel (1995). "Fibronectin expression during physiological and pathological cardiac growth." J Mol Cell Cardiol **27**(4): 981-990.

Fink, C., S. Ergun, D. Kralisch, U. Remmers, J. Weil and T. Eschenhagen (2000). "Chronic stretch of engineered heart tissue induces hypertrophy and functional improvement." FASEB J **14**(5): 669-679.

Fletcher, D. A. and R. D. Mullins (2010). "Cell mechanics and the cytoskeleton." Nature **463**(7280): 485-492.

Frank, D. and N. Frey (2011). "Cardiac Z-disc signaling network." J Biol Chem **286**(12): 9897-9904.

Frey, N. and E. N. Olson (2003). "Cardiac hypertrophy: the good, the bad, and the ugly." Annu Rev Physiol **65**: 45-79.

Gachet, Y., S. Tournier, J. B. Millar and J. S. Hyams (2001). "A MAP kinase-dependent actin checkpoint ensures proper spindle orientation in fission yeast." Nature **412**(6844): 352-355.

Gamba, L., M. Harrison and C. L. Lien (2014). "Cardiac regeneration in model organisms." Curr Treat Options Cardiovasc Med **16**(3): 288.

Gautel, M. (2011). "The sarcomeric cytoskeleton: who picks up the strain?" Curr Opin Cell Biol **23**(1): 39-46.

Gessert, S. and M. Kuhl (2010). "The multiple phases and faces of wnt signaling during cardiac differentiation and development." Circ Res **107**(2): 186-199.

Giacomelli, E., V. Meraviglia, G. Campostrini, A. Cochrane, X. Cao, R. W. J. van Helden, A. Krotenberg Garcia, M. Mircea, S. Kostidis, R. P. Davis, B. J. van Meer, C. R. Jost, A. J. Koster, H. Mei, D. G. Miguez, A. A. Mulder, M. Ledesma-Terron, G. Pompilio, L. Sala, D. C. F. Salvatori, R. C. Slieker, E. Sommariva, A. A. F. de Vries, M. Giera, S. Semrau, L. G. J. Tertoolen, V. V. Orlova, M. Bellin and C. L. Mummery (2020). "Human-iPSC-Derived Cardiac Stromal Cells Enhance Maturation in 3D Cardiac Microtissues and Reveal Non-cardiomyocyte Contributions to Heart Disease." Cell Stem Cell **26**(6): 862-879 e811.

Giacomelli, E., C. L. Mummery and M. Bellin (2017). "Human heart disease: lessons from human pluripotent stem cell-derived cardiomyocytes." Cell Mol Life Sci **74**(20): 3711-3739.

Goodenough, D. A. and D. L. Paul (2009). "Gap junctions." Cold Spring Harb Perspect Biol **1**(1): a002576.

Gopalan, S. M., C. Flaim, S. N. Bhatia, M. Hoshijima, R. Knoell, K. R. Chien, J. H. Omens and A. D. McCulloch (2003). "Anisotropic stretch-induced hypertrophy in neonatal ventricular myocytes micropatterned on deformable elastomers." Biotechnol Bioeng **81**(5): 578-587.

Guo, Y. and W. T. Pu (2020). "Cardiomyocyte Maturation: New Phase in Development." Circ Res **126**(8): 1086-1106.

Gwak, S. J., S. H. Bhang, I. K. Kim, S. S. Kim, S. W. Cho, O. Jeon, K. J. Yoo, A. J. Putnam and B. S. Kim (2008). "The effect of cyclic strain on embryonic stem cell-derived cardiomyocytes." Biomaterials **29**(7): 844-856.

Hansen, A., A. Eder, M. Bonstrup, M. Flato, M. Mewe, S. Schaaf, B. Aksehirlioglu, A. P. Schwoerer, J. Uebeler and T. Eschenhagen (2010). "Development of a drug screening platform based on engineered heart tissue." Circ Res **107**(1): 35-44.

Heineke, J., H. Ruetten, C. Willenbockel, S. C. Gross, M. Naguib, A. Schaefer, T. Kempf, D. Hilfiker-Kleiner, P. Caroni, T. Kraft, R. A. Kaiser, J. D. Molkentin, H. Drexler and K. C. Wollert (2005). "Attenuation of cardiac remodeling after myocardial infarction by muscle LIM protein-calcineurin signaling at the sarcomeric Z-disc." Proc Natl Acad Sci U S A **102**(5): 1655-1660.

Hilenski, L. L., X. H. Ma, N. Vinson, L. Terracio and T. K. Borg (1992). "The role of beta 1 integrin in spreading and myofibrillogenesis in neonatal rat cardiomyocytes in vitro." Cell Motil Cytoskeleton **21**(2): 87-100.

Hirt, M. N., J. Boeddinghaus, A. Mitchell, S. Schaaf, C. Bornchen, C. Muller, H. Schulz, N. Hubner, J. Stenzig, A. Stoehr, C. Neuber, A. Eder, P. K. Luther, A. Hansen and T. Eschenhagen (2014). "Functional improvement and maturation of rat and human engineered heart tissue by chronic electrical stimulation." J Mol Cell Cardiol **74**: 151-161.

Hirt, M. N., A. Hansen and T. Eschenhagen (2014). "Cardiac tissue engineering: state of the art." Circ Res **114**(2): 354-367.

Hirt, M. N., N. A. Sorensen, L. M. Bartholdt, J. Boeddinghaus, S. Schaaf, A. Eder, I. Vollert, A. Stohr, T. Schulze, A. Witten, M. Stoll, A. Hansen and T. Eschenhagen (2012). "Increased afterload induces pathological cardiac hypertrophy: a new in vitro model." Basic Res Cardiol **107**(6): 307.

Hornberger, L. K., S. Singhroy, T. Cavalle-Garrido, W. Tsang, F. Keeley and M. Rabinovitch (2000). "Synthesis of extracellular matrix and adhesion through beta(1) integrins are critical for fetal ventricular myocyte proliferation." Circ Res **87**(6): 508-515.

Humeres, C. and N. G. Frangogiannis (2019). "Fibroblasts in the Infarcted, Remodeling, and Failing Heart." JACC Basic Transl Sci **4**(3): 449-467.

Ibanez, B., G. Vilahur and J. J. Badimon (2007). "Plaque progression and regression in atherothrombosis." J Thromb Haemost **5 Suppl 1**: 292-299.

Ingber, D. E. (2006). "Cellular mechanotransduction: putting all the pieces together again." FASEB J **20**(7): 811-827.

Ingber, D. E. (2006). "Mechanical control of tissue morphogenesis during embryological development." Int J Dev Biol **50**(2-3): 255-266.

Itasaki, N., H. Nakamura, H. Sumida and M. Yasuda (1991). "Actin bundles on the right side in the caudal part of the heart tube play a role in dextro-looping in the embryonic chick heart." Anat Embryol (Berl) **183**(1): 29-39.

Iyer, R. P., N. L. Patterson, F. A. Zouein, Y. Ma, V. Dive, L. E. de Castro Bras and M. L. Lindsey (2015). "Early matrix metalloproteinase-12 inhibition worsens post-myocardial infarction cardiac dysfunction by delaying inflammation resolution." Int J Cardiol **185**: 198-208.

Janmey, P. A., J. P. Winer and J. W. Weisel (2009). "Fibrin gels and their clinical and bioengineering applications." J R Soc Interface **6**(30): 1-10.

Jungbauer, S., H. Gao, J. P. Spatz and R. Kemkemer (2008). "Two characteristic regimes in frequency-dependent dynamic reorientation of fibroblasts on cyclically stretched substrates." Biophys J **95**(7): 3470-3478.

Kamble, H., R. Vadivelu, M. Barton, M. J. A. Shiddiky and N. T. Nguyen (2018). "Pneumatically actuated cell-stretching array platform for engineering cell patterns in vitro." Lab Chip **18**(5): 765-774.

Karoubi, G., M. L. Ormiston, D. J. Stewart and D. W. Courtman (2009). "Single-cell hydrogel encapsulation for enhanced survival of human marrow stromal cells." Biomaterials **30**(29): 5445-5455.

Kelm, J. M., E. Ehler, L. K. Nielsen, S. Schlatter, J. C. Perriard and M. Fussenegger (2004). "Design of artificial myocardial microtissues." Tissue Eng **10**(1-2): 201-214.

Knoll, R., M. Hoshijima, H. M. Hoffman, V. Person, I. Lorenzen-Schmidt, M. L. Bang, T. Hayashi, N. Shiga, H. Yasukawa, W. Schaper, W. McKenna, M. Yokoyama, N. J. Schork, J. H. Omens, A. D. McCulloch, A. Kimura, C. C. Gregorio, W. Poller, J. Schaper, H. P. Schultheiss and K. R. Chien (2002). "The cardiac mechanical stretch sensor machinery involves a Z disc complex that is defective in a subset of human dilated cardiomyopathy." Cell **111**(7): 943-955.

Kresh, J. Y. and A. Chopra (2011). "Intercellular and extracellular mechanotransduction in cardiac myocytes." Pflugers Arch **462**(1): 75-87.

Kreutzer, J., L. Ikonen, J. Hirvonen, M. Pekkanen-Mattila, K. Aalto-Setala and P. Kallio (2014). "Pneumatic cell stretching system for cardiac differentiation and culture." Med Eng Phys **36**(4): 496-501.

Kreutzer, J., M. Viehrig, R. P. Polonen, F. Zhao, M. Ojala, K. Aalto-Setala and P. Kallio (2019). "Pneumatic unidirectional cell stretching device for mechanobiological studies of cardiomyocytes." Biomech Model Mechanobiol.

Kubo, H., T. Shioyama, M. Oura, A. Suzuki, T. Ogawa, H. Makino, S. Takeda, M. Kino-oka, T. Shimizu, T. Okano and S. Yamamori (2013). "Development of automated 3-dimensional tissue fabrication system Tissue Factory - Automated cell isolation from tissue for regenerative medicine." Conf Proc IEEE Eng Med Biol Soc **2013**: 358-361.

L'Heureux, N., S. Paquet, R. Labbe, L. Germain and F. A. Auger (1998). "A completely biological tissue-engineered human blood vessel." FASEB J **12**(1): 47-56.

Lasher, R. A., A. Q. Pahnke, J. M. Johnson, F. B. Sachse and R. W. Hitchcock (2012). "Electrical stimulation directs engineered cardiac tissue to an age-matched native phenotype." J Tissue Eng **3**(1): 2041731412455354.

Latacha, K. S., M. C. Remond, A. Ramasubramanian, A. Y. Chen, E. L. Elson and L. A. Taber (2005). "Role of actin polymerization in bending of the early heart tube." Dev Dyn **233**(4): 1272-1286.

Lazarides, E. (1980). "Intermediate filaments as mechanical integrators of cellular space." Nature **283**(5744): 249-256.

Lee, D. A., M. M. Knight, J. J. Campbell and D. L. Bader (2011). "Stem cell mechanobiology." J Cell Biochem **112**(1): 1-9.

Lee, Y. J. and P. C. Keng (2005). "Studying the effects of actin cytoskeletal destabilization on cell cycle by cofilin overexpression." Mol Biotechnol **31**(1): 1-10.

Leor, J., S. Aboulafia-Etzion, A. Dar, L. Shapiro, I. M. Barbash, A. Battler, Y. Granot and S. Cohen (2000). "Bioengineered cardiac grafts: A new approach to repair the infarcted myocardium?" Circulation **102**(19 Suppl 3): III56-61.

Lesman, A., M. Habib, O. Caspi, A. Gepstein, G. Arbel, S. Levenberg and L. Gepstein (2010). "Transplantation of a tissue-engineered human vascularized cardiac muscle." Tissue Eng Part A **16**(1): 115-125.

Li, F., X. Wang, J. M. Capasso and A. M. Gerdes (1996). "Rapid transition of cardiac myocytes from hyperplasia to hypertrophy during postnatal development." J Mol Cell Cardiol **28**(8): 1737-1746.

Li, J., E. Gao, A. Vite, R. Yi, L. Gomez, S. Goossens, F. van Roy and G. L. Radice (2015). "Alpha-catenins control cardiomyocyte proliferation by regulating Yap activity." Circ Res **116**(1): 70-79.

Li, R. K., Z. Q. Jia, R. D. Weisel, D. A. Mickle, A. Choi and T. M. Yau (1999). "Survival and function of bioengineered cardiac grafts." Circulation **100**(19 Suppl): II63-69.

Lien, W. H., O. Klezovitch, T. E. Fernandez, J. Delrow and V. Vasioukhin (2006). "alphaE-catenin controls cerebral cortical size by regulating the hedgehog signaling pathway." Science **311**(5767): 1609-1612.

Lin, Z., A. von Gise, P. Zhou, F. Gu, Q. Ma, J. Jiang, A. L. Yau, J. N. Buck, K. A. Gouin, P. R. van Gorp, B. Zhou, J. Chen, J. G. Seidman, D. Z. Wang and W. T. Pu (2014). "Cardiac-specific YAP activation improves cardiac function and survival in an experimental murine MI model." Circ Res **115**(3): 354-363.

Lopaschuk, G. D. and J. S. Jaswal (2010). "Energy metabolic phenotype of the cardiomyocyte during development, differentiation, and postnatal maturation." J Cardiovasc Pharmacol **56**(2): 130-140.

Lyon, R. C., F. Zanella, J. H. Omens and F. Sheikh (2015). "Mechanotransduction in cardiac hypertrophy and failure." Circ Res **116**(8): 1462-1476.

Marsano, A., R. Maidhof, L. Q. Wan, Y. Wang, J. Gao, N. Tandon and G. Vunjak-Novakovic (2010). "Scaffold stiffness affects the contractile function of three-dimensional engineered cardiac constructs." Biotechnol Prog **26**(5): 1382-1390.

McNally, E. M., R. Kraft, M. Bravo-Zehnder, D. A. Taylor and L. A. Leinwand (1989). "Full-length rat alpha and beta cardiac myosin heavy chain sequences. Comparisons suggest a molecular basis for functional differences." J Mol Biol **210**(3): 665-671.

Moore-Morris, T., P. Cattaneo, N. Guimaraes-Camboa, J. Bogomolovas, M. Cedenilla, I. Banerjee, M. Ricote, T. Kisseleva, L. Zhang, Y. Gu, N. D. Dalton, K. L. Peterson, J. Chen, M. Puceat and S. M. Evans (2018). "Infarct Fibroblasts Do Not Derive From Bone Marrow Lineages." Circ Res **122**(4): 583-590.

Morikawa, Y., T. Heallen, J. Leach, Y. Xiao and J. F. Martin (2017). "Dystrophin-glycoprotein complex sequesters Yap to inhibit cardiomyocyte proliferation." Nature **547**(7662): 227-231.

Moscona, A. A. (1959). "Tissues from dissociated cells." Sci Am **200**(5): 132-134 passim.

Munoz, J., Y. Zhou and H. W. Jarrett (2010). "LG4-5 domains of laminin-211 binds alpha-dystroglycan to allow myotube attachment and prevent anoikis." J Cell Physiol **222**(1): 111-119.

Naito, H., I. Melnychenko, M. Didie, K. Schneiderbanger, P. Schubert, S. Rosenkranz, T. Eschenhagen and W. H. Zimmermann (2006). "Optimizing engineered heart tissue for therapeutic applications as surrogate heart muscle." Circulation **114**(1 Suppl): I72-78.

Naruse, K., T. Yamada and M. Sokabe (1998). "Involvement of SA channels in orienting response of cultured endothelial cells to cyclic stretch." Am J Physiol **274**(5): H1532-1538.

Nelson, W. J. and R. Nusse (2004). "Convergence of Wnt, beta-catenin, and cadherin pathways." Science **303**(5663): 1483-1487.

Niessen, C. M., D. Leckband and A. S. Yap (2011). "Tissue organization by cadherin adhesion molecules: dynamic molecular and cellular mechanisms of morphogenetic regulation." Physiol Rev **91**(2): 691-731.

Ott, H. C., T. S. Matthiesen, S. K. Goh, L. D. Black, S. M. Kren, T. I. Netoff and D. A. Taylor (2008). "Perfusion-decellularized matrix: using nature's platform to engineer a bioartificial heart." Nat Med **14**(2): 213-221.

Passier, R., V. Orlova and C. Mummery (2016). "Complex Tissue and Disease Modeling using hiPSCs." Cell Stem Cell **18**(3): 309-321.

Peters, N. S., N. J. Severs, S. M. Rothery, C. Lincoln, M. H. Yacoub and C. R. Green (1994). "Spatiotemporal relation between gap junctions and fascia adherens junctions during postnatal development of human ventricular myocardium." Circulation **90**(2): 713-725.

Phatharajaree, W., A. Phrommintikul and N. Chattipakorn (2007). "Matrix metalloproteinases and myocardial infarction." Can J Cardiol **23**(9): 727-733.

Polizzotti, B. D., B. Ganapathy, B. J. Haubner, J. M. Penninger and B. Kuhn (2016). "A cryoinjury model in neonatal mice for cardiac translational and regeneration research." Nat Protoc **11**(3): 542-552.

Porrello, E. R., A. I. Mahmoud, E. Simpson, J. A. Hill, J. A. Richardson, E. N. Olson and H. A. Sadek (2011). "Transient regenerative potential of the neonatal mouse heart." Science **331**(6020): 1078-1080.

Porrello, E. R. and E. N. Olson (2014). "A neonatal blueprint for cardiac regeneration." Stem Cell Res **13**(3 Pt B): 556-570.

Poss, K. D., L. G. Wilson and M. T. Keating (2002). "Heart regeneration in zebrafish." Science **298**(5601): 2188-2190.

Price, R. L., M. Nakagawa, L. Terracio and T. K. Borg (1992). "Ultrastructural localization of laminin on in vivo embryonic, neonatal, and adult rat cardiac myocytes and in early rat embryos raised in whole-embryo culture." J Histochem Cytochem **40**(9): 1373-1381.

Puchner, E. M., A. Alexandrovich, A. L. Kho, U. Hensen, L. V. Schafer, B. Brandmeier, F. Grater, H. Grubmuller, H. E. Gaub and M. Gautel (2008). "Mechanoenzymatics of titin kinase." Proc Natl Acad Sci U S A **105**(36): 13385-13390.

Radisic, M., H. Park, T. P. Martens, J. E. Salazar-Lazaro, W. Geng, Y. Wang, R. Langer, L. E. Freed and G. Vunjak-Novakovic (2008). "Pre-treatment of synthetic elastomeric scaffolds by cardiac fibroblasts improves engineered heart tissue." J Biomed Mater Res A **86**(3): 713-724.

Radisic, M., H. Park, H. Shing, T. Consi, F. J. Schoen, R. Langer, L. E. Freed and G. Vunjak-Novakovic (2004). "Functional assembly of engineered myocardium by electrical stimulation of cardiac myocytes cultured on scaffolds." Proc Natl Acad Sci U S A **101**(52): 18129-18134.

Reshetnikova, G., R. Barkan, B. Popov, N. Nikolsky and L. S. Chang (2000). "Disruption of the actin cytoskeleton leads to inhibition of mitogen-induced cyclin E expression, Cdk2 phosphorylation, and nuclear accumulation of the retinoblastoma protein-related p107 protein." Exp Cell Res **259**(1): 35-53.

Ronaldson-Bouchard, K., S. P. Ma, K. Yeager, T. Chen, L. Song, D. Sirabella, K. Morikawa, D. Teles, M. Yazawa and G. Vunjak-Novakovic (2018). "Advanced maturation of human cardiac tissue grown from pluripotent stem cells." Nature **556**(7700): 239-243.

Ross, R. S. and T. K. Borg (2001). "Integrins and the myocardium." Circ Res **88**(11): 1112-1119.

Rybakova, I. N., K. J. Amann and J. M. Ervasti (1996). "A new model for the interaction of dystrophin with F-actin." J Cell Biol **135**(3): 661-672.

Rysa, J., H. Tokola and H. Ruskoaho (2018). "Mechanical stretch induced transcriptomic profiles in cardiac myocytes." Sci Rep **8**(1): 4733.

Salameh, A., A. Wustmann, S. Karl, K. Blanke, D. Apel, D. Rojas-Gomez, H. Franke, F. W. Mohr, J. Janousek and S. Dhein (2010). "Cyclic mechanical stretch induces cardiomyocyte orientation and polarization of the gap junction protein connexin43." Circ Res **106**(10): 1592-1602.

Samarel, A. M. (2005). "Costameres, focal adhesions, and cardiomyocyte mechanotransduction." Am J Physiol Heart Circ Physiol **289**(6): H2291-2301.

Samuel, J. L., F. Farhadian, A. Sabri, F. Marotte, V. Robert and L. Rappaport (1994). "Expression of fibronectin during rat fetal and postnatal development: an in situ hybridisation and immunohistochemical study." Cardiovasc Res **28**(11): 1653-1661.

Schlegelmilch, K., M. Mohseni, O. Kirak, J. Pruszak, J. R. Rodriguez, D. Zhou, B. T. Kreger, V. Vasioukhin, J. Avruch, T. R. Brummelkamp and F. D. Camargo (2011). "Yap1 acts downstream of alpha-catenin to control epidermal proliferation." Cell **144**(5): 782-795.

Schmelter, M., B. Ateghang, S. Helmig, M. Wartenberg and H. Sauer (2006). "Embryonic stem cells utilize reactive oxygen species as transducers of mechanical strain-induced cardiovascular differentiation." FASEB J **20**(8): 1182-1184.

Schwartz, M. A. and M. H. Ginsberg (2002). "Networks and crosstalk: integrin signalling spreads." Nat Cell Biol **4**(4): E65-68.

Schwartz, M. A., M. D. Schaller and M. H. Ginsberg (1995). "Integrins: emerging paradigms of signal transduction." Annu Rev Cell Dev Biol **11**: 549-599.

Sekine, H., T. Shimizu, K. Hobo, S. Sekiya, J. Yang, M. Yamato, H. Kurosawa, E. Kobayashi and T. Okano (2008). "Endothelial cell coculture within tissue-engineered cardiomyocyte sheets enhances neovascularization and improves cardiac function of ischemic hearts." Circulation **118**(14 Suppl): S145-152.

Senyo, S. E., M. L. Steinhauser, C. L. Pizzimenti, V. K. Yang, L. Cai, M. Wang, T. D. Wu, J. L. Guerquin-Kern, C. P. Lechene and R. T. Lee (2013). "Mammalian heart renewal by pre-existing cardiomyocytes." Nature **493**(7432): 433-436.

Shao, Y., X. Tan, R. Novitski, M. Muqaddam, P. List, L. Williamson, J. Fu and A. P. Liu (2013). "Uniaxial cell stretching device for live-cell imaging of mechanosensitive cellular functions." Rev Sci Instrum **84**(11): 114304.

Sheehy, S. P., S. Huang and K. K. Parker (2009). "Time-warped comparison of gene expression in adaptive and maladaptive cardiac hypertrophy." Circ Cardiovasc Genet **2**(2): 116-124.

Sheikh, F., R. S. Ross and J. Chen (2009). "Cell-cell connection to cardiac disease." Trends Cardiovasc Med **19**(6): 182-190.

Shimizu, T., M. Yamato, Y. Isoi, T. Akutsu, T. Setomaru, K. Abe, A. Kikuchi, M. Umezu and T. Okano (2002). "Fabrication of pulsatile cardiac tissue grafts using a novel 3-dimensional cell sheet manipulation technique and temperature-responsive cell culture surfaces." Circ Res **90**(3): e40.

Simpson, D. G., M. L. Decker, W. A. Clark and R. S. Decker (1993). "Contractile activity and cell-cell contact regulate myofibrillar organization in cultured cardiac myocytes." J Cell Biol **123**(2): 323-336.

Simpson, D. G., M. Majeski, T. K. Borg and L. Terracio (1999). "Regulation of cardiac myocyte protein turnover and myofibrillar structure in vitro by specific directions of stretch." Circ Res **85**(10): e59-69.

Singhvi, R., A. Kumar, G. P. Lopez, G. N. Stephanopoulos, D. I. Wang, G. M. Whitesides and D. E. Ingber (1994). "Engineering cell shape and function." Science **264**(5159): 696-698.

Smith, B. A., R. L. Hamlin, R. L. Bartels, R. G. Evans, T. E. Kirby, M. G. MacVicar and S. E. Weisbrode (1992). "Myocardial infarction size and scar dimensions: the influence of activity." Heart Lung **21**(5): 440-447.

Soonpaa, M. H. and L. J. Field (1998). "Survey of studies examining mammalian cardiomyocyte DNA synthesis." Circ Res **83**(1): 15-26.

Soonpaa, M. H., K. K. Kim, L. Pajak, M. Franklin and L. J. Field (1996). "Cardiomyocyte DNA synthesis and binucleation during murine development." Am J Physiol **271**(5 Pt 2): H2183-2189.

Spector, I., N. R. Shochet, Y. Kashman and A. Groweiss (1983). "Latrunculins: novel marine toxins that disrupt microfilament organization in cultured cells." Science **219**(4584): 493-495.

Spudich, J. A. (2001). "The myosin swinging cross-bridge model." Nat Rev Mol Cell Biol **2**(5): 387-392.

Stein, J. M., C. L. Mummery and M. Bellin (2020). "Engineered models of the human heart: directions and challenges." Stem Cell Reports.

Stevens, K. R., K. L. Kreutziger, S. K. Dupras, F. S. Korte, M. Regnier, V. Muskheli, M. B. Nourse, K. Bendixen, H. Reinecke and C. E. Murry (2009). "Physiological function and transplantation of scaffold-free and vascularized human cardiac muscle tissue." Proc Natl Acad Sci U S A **106**(39): 16568-16573.

Stoehr, A., M. N. Hirt, A. Hansen, M. Seiffert, L. Conradi, J. Uebeler, F. P. Limbourg and T. Eschenhagen (2016). "Spontaneous Formation of Extensive Vessel-Like Structures in Murine Engineered Heart Tissue." Tissue Eng Part A **22**(3-4): 326-335.

Stoehr, a., C. Neuber, C. Baldauf, I. Vollert, F. W. Friedrich, F. Flenner, L. Carrier, a. Eder, S. Schaaf, M. N. Hirt, B. Aksehirlioglu, C. W. Tong, a. Moretti, T. Eschenhagen and a. Hansen (2014). "Automated analysis of contractile force and Ca2+ transients in engineered heart tissue." AJP: Heart and Circulatory Physiology **306**: H1353-H1363.

Strungs, E. G., E. L. Ongstad, M. P. O'Quinn, J. A. Palatinus, L. J. Jourdan and R. G. Gourdie (2013). "Cryoinjury models of the adult and neonatal mouse heart for studies of scarring and regeneration." Methods Mol Biol **1037**: 343-353.

Taber, L. A., I. E. Lin and E. B. Clark (1995). "Mechanics of cardiac looping." Dev Dyn **203**(1): 42-50.

Tangney, J. R., J. S. Chuang, M. S. Janssen, A. Krishnamurthy, P. Liao, M. Hoshijima, X. Wu, G. A. Meininger, M. Muthuchamy, A. Zemljic-Harpf, R. S. Ross, L. R. Frank, A. D. McCulloch and J. H. Omens (2013). "Novel role for vinculin in ventricular myocyte mechanics and dysfunction." Biophys J **104**(7): 1623-1633.

Terracio, L., K. Rubin, D. Gullberg, E. Balog, W. Carver, R. Jyring and T. K. Borg (1991). "Expression of collagen binding integrins during cardiac development and hypertrophy." Circ Res **68**(3): 734-744.

Thery, M. and M. Bornens (2006). "Cell shape and cell division." Curr Opin Cell Biol **18**(6): 648-657.

Thomas, H., J. Diamond, A. Vieco, S. Chaudhuri, E. Shinnar, S. Cromer, P. Perel, G. A. Mensah, J. Narula, C. O. Johnson, G. A. Roth and A. E. Moran (2018). "Global Atlas of Cardiovascular Disease 2000-2016: The Path to Prevention and Control." Glob Heart **13**(3): 143-163.

Tiburcy, M., M. Didie, O. Boy, P. Christalla, S. Doker, H. Naito, B. C. Karikkineth, a. El-Armouche, M. Grimm, M. Nose, T. Eschenhagen, a. Zieseniss, D. M. Katschinski, N. Hamdani, W. a. Linke, X. Yin, M. Mayr and W.-H. Zimmermann (2011). "Terminal Differentiation, Advanced Organotypic Maturation, and Modeling of Hypertrophic Growth in Engineered Heart Tissue." Circulation Research **109**: 1105-1114.

Tong, C., C. Li, B. Xie, M. Li, X. Li, Z. Qi and J. Xia (2019). "Generation of bioartificial hearts using decellularized scaffolds and mixed cells." Biomed Eng Online **18**(1): 71.

Townsend, N., M. Nichols, P. Scarborough and M. Rayner (2015). "Cardiovascular disease in Europe — epidemiological update 2015." 2696-2705.

Tremblay, D., S. Chagnon-Lessard, M. Mirzaei, A. E. Pelling and M. Godin (2014). "A microscale anisotropic biaxial cell stretching device for applications in mechanobiology." Biotechnol Lett **36**(3): 657-665.

Uygur, A. and R. T. Lee (2016). "Mechanisms of Cardiac Regeneration." Dev Cell **36**(4): 362-374.

van der Flier, A., A. C. Gaspar, S. Thorsteinsdottir, C. Baudoin, E. Groeneveld, C. L. Mummery and A. Sonnenberg (1997). "Spatial and temporal expression of the beta1D integrin during mouse development." Dev Dyn **210**(4): 472-486.

Vandenburgh, H., J. Shansky, F. Benesch-Lee, V. Barbata, J. Reid, L. Thorrez, R. Valentini and G. Crawford (2008). "Drug-screening platform based on the contractility of tissue-engineered muscle." Muscle Nerve **37**(4): 438-447.

Vandenburgh, H. H., P. Karlisch and L. Farr (1988). "Maintenance of highly contractile tissue-cultured avian skeletal myotubes in collagen gel." In Vitro Cell Dev Biol **24**(3): 166-174.

Voges, H. K., R. J. Mills, D. A. Elliott, R. G. Parton, E. R. Porrello and J. E. Hudson (2017). "Development of a human cardiac organoid injury model reveals innate regenerative potential." Development **144**(6): 1118-1127.

Walsh, S., A. Ponten, B. K. Fleischmann and S. Jovinge (2010). "Cardiomyocyte cell cycle control and growth estimation in vivo--an analysis based on cardiomyocyte nuclei." Cardiovasc Res **86**(3): 365-373.

Wan, C. R., S. Chung and R. D. Kamm (2011). "Differentiation of embryonic stem cells into cardiomyocytes in a compliant microfluidic system." Ann Biomed Eng **39**(6): 1840-1847.

Wang, X., F. Li, S. E. Campbell and A. M. Gerdes (1999). "Chronic pressure overload cardiac hypertrophy and failure in guinea pigs: II. Cytoskeletal remodeling." J Mol Cell Cardiol **31**(2): 319-331.

Weber, K. T., Y. Sun, S. K. Bhattacharya, R. A. Ahokas and I. C. Gerling (2013). "Myofibroblast-mediated mechanisms of pathological remodelling of the heart." Nat Rev Cardiol **10**(1): 15-26.

Weinberger, F., K. Breckwoldt, S. Pecha, A. Kelly, B. Geertz, J. Starbatty, T. Yorgan, K. H. Cheng, K. Lessmann, T. Stolen, M. Scherrer-Crosbie, G. Smith, H. Reichenspurner, A. Hansen and T.

Eschenhagen (2016). "Cardiac repair in guinea pigs with human engineered heart tissue from induced pluripotent stem cells." Sci Transl Med **8**(363): 363ra148.

Witman, N., B. Murtuza, B. Davis, A. Arner and J. I. Morrison (2011). "Recapitulation of developmental cardiogenesis governs the morphological and functional regeneration of adult newt hearts following injury." Dev Biol **354**(1): 67-76.

Wozniak, M. A. and C. S. Chen (2009). "Mechanotransduction in development: a growing role for contractility." Nat Rev Mol Cell Biol **10**(1): 34-43.

Yeh, R. W. and A. S. Go (2010). "Rethinking the epidemiology of acute myocardial infarction: challenges and opportunities." Arch Intern Med **170**(9): 759-764.

Zhang, Y. S., J. Aleman, A. Arneri, S. Bersini, F. Piraino, S. R. Shin, M. R. Dokmeci and A. Khademhosseini (2015). "From cardiac tissue engineering to heart-on-a-chip: beating challenges." Biomed Mater **10**(3): 034006.

Zimmermann, W.-H. (2002). "Tissue Engineering of a Differentiated Cardiac Muscle Construct." Circulation Research **90**: 223-230.

Zimmermann, W.-H., I. Melnychenko, G. Wasmeier, M. Didié, H. Naito, U. Nixdorff, A. Hess, L. Budinsky, K. Brune, B. Michaelis, S. Dhein, A. Schwoerer, H. Ehmke and T. Eschenhagen (2006). "Engineered heart tissue grafts improve systolic and diastolic function in infarcted rat hearts." Nature Medicine **12**: 452-458.